NASA Technical Memorandum 106011

# Coupled Multi-Disciplinary Composites Behavior Simulation

Surendra N. Singhal
*Sverdrup Technology, Inc.*
*Lewis Research Center Group*
*Brook Park, Ohio*

and

Pappu L.N. Murthy and Christos C. Chamis
*National Aeronautics and Space Administration*
*Lewis Research Center*
*Cleveland, Ohio*

February 1993

NASA

## TABLE OF CONTENTS

# COUPLED MULTI-DISCIPLINARY COMPOSITES BEHAVIOR SIMULATION

Surendra N. Singhal
Sverdrup Technology, Inc.
Lewis Research Center Group
Brookpark, Ohio

Pappu L. N. Murthy and Christos C. Chamis
National Aeronautics and Space Administration
Lewis Research Center
Cleveland, Ohio

## ABSTRACT

The capabilities of the computer code CSTEM (Coupled Structural/Thermal/ Electro-Magnetic Analysis) are discussed and demonstrated. CSTEM computationally simulates the coupled response of layered multi-material composite structures subjected to simultaneous thermal, structural, vibration, acoustic, and electromagnetic loads and includes the effect of aggressive environments. The composite material behavior and structural response is determined at its various inherent scales: constituents (fiber/matrix), ply, laminate, and structural component. The thermal and mechanical properties of the constituents are considered to be nonlinearly dependent on various parameters such as temperature and moisture. The acoustic and electromagnetic properties also include dependence on vibration and electromagnetic wave frequencies, respectively. The simulation is based on a three dimensional finite element analysis in conjunction with composite mechanics and with structural tailoring codes, and with acoustic and electromagnetic analysis methods. An aircraft engine composite fan blade is selected as a typical structural component to demonstrate the CSTEM capabilities. Results of various coupled multi-disciplinary heat transfer, structural, vibration, acoustic, and electromagnetic analyses for temperature distribution, stress and displacement response, deformed shape, vibration frequencies, mode shapes, acoustic noise, and electromagnetic reflection from the fan blade are discussed for their coupled effects in hot and humid environments. Collectively, these results demonstrate the effectiveness of the CSTEM code in capturing the coupled effects on the various responses of composite structures subjected to simultaneous multiple real-life loads.

## INTRODUCTION

### Background Information

The recently increasing cooperation as well as competition among the nations of the world, fueled by far-reaching and faster communications, have led to a clear need for developing high speed transport systems. High speeds which are multiples of the speed of sound, bring about new demands on the material and structure of the aircrafts which must not only survive the elevated temperatures but also be environmentally acceptable and cost-effective. These demands can not be met with conventional materials and structural designs. Innovative new

materials and design concepts need to be developed. The various types of elevated temperature composite materials, which are already finding acceptance in the aircraft industry, must be exploited for an optimal mix of material resistance and structural response at all their scales. Single-discipline traditional analyses no longer suffice for high speed aircraft which is subjected to a multitude of loads and which is designed to fly safely and without unnecessary weight penalty. Designing with composite materials to account for coupling between multi-disciplinary loads in hostile environments is a real challenge that must be targeted with new and efficient approaches. These approaches rely on relatively inexpensive computational simulation to characterize the multi-disciplinary behavior of engine structural components and to aid in the selection of strategic experiments to verify and/or calibrate the simulation process.

Recognizing the need for developing coupled multi-disciplinary analysis methods/codes, a multi-faceted research program aimed at simulating coupled multi-disciplinary behavior of aircraft engine/frame structures made of advanced composite materials, was undertaken. The vast majority of the progress made at the NASA Lewis Research Center for simulating the characteristics and performance of elevated temperature composite materials and structures has been integrated in consistent, interactive, and compatible structural mechanics computational simulation computer codes (refs. 1, 2, and 3). Recently, a stand-alone multi-disciplinary simulation procedure/code, CSTEM (Coupled Structural/Thermal/ Electro-Magnetic Analysis/ Tailoring - ref. 4) was developed by integrating a special three dimensional finite element analysis method with several single-discipline (thermal, acoustic - ref. 5, electromagnetic - ref. 6) codes including those for integrated composite mechanics (ref. 7) and for structural tailoring (ref. 8).

**Objective of the Present Report**

The objective of the present report is to (1) summarize CSTEM's capabilities and applications versatility, (2) validate contractor-supplied demonstration cases, and (3) demonstrate the various code features for computational simulation of the coupled multi-disciplinary behavior of layered multi-material elevated temperature aircraft engine composite structures under simultaneous thermal, structural, acoustic, and electromagnetic loads in propulsion environments.

**Brief Description of CSTEM**

CSTEM (Coupled Structural/Thermal/Electro-Magnetic Analysis/Tailoring) is a general-purpose code for computationally simulating coupled multi-disciplinary heat transfer, structural, vibration, acoustic, and electromagnetic behavior of elevated temperature layered multi-material composite structures in aggressive environments. All the disciplines are coupled for nonlinear geometrical, material, loading, and environmental effects. For instance, the acoustic and electromagnetic responses can be computed for the updated structure geometry caused by large deformations due to structural loading. The structural response can be predicted at all the composite scales including constituents (fiber/matrix), ply, laminate, and structure. The coupling is mostly sequential because respective output from one discipline is used as input for the other disciplines.

A unique feature of CSTEM is its capability to simulate an aircraft under electromagnetic radiation (Figure 1). The simultaneous multi-disciplinary loads that CSTEM can analyze are shown for an aircraft engine in Figure 2.

CSTEM is based on a modular structure (Figure 3) accessed by the user through its executive module. The ICAN module simulates the composite mechanics depicted in Figure 4. The thermo-mechanical properties of the composites can be input at room temperature at the constituent scale. ICAN automatically computes material properties at all composite scales at elevated temperatures including the effect of environments. ICAN includes a resident material property data base for typical aerospace fiber and matrix materials. The user needs to specify only a code name of the desired material (rather than having to manually input all the properties) in the CSTEM input. CSTEM calls ICAN which automatically searches, selects, and updates the material properties from its data base. The data base is open-ended and can be easily augmented for other materials.

The CSTEM code offers a state-of-the-art stand-alone coupled multi-disciplinary analysis capability which is unique (inclusive of various complexities) and is not available in any commercial codes known to authors. The source code consists of approximately 76,000 FORTRAN statements. The contractor-supplied user's and demonstration manuals can be found in references 4 and 9, respectively. CSTEM is currently installed on NASA LeRC's CRAY-YMP system. Either VM or VAX can be used for processing input/output files.

## FEATURES

CSTEM can be run for individual analysis capability or for coupled analyses automatically using the same finite element mesh for all the analyses. This eliminates the need for transforming data from one, say thermal analysis results for a specific mesh to temperature input required by another mesh. More importantly, the effect of nonlinearities such as those due to geometry and material are automatically accounted for from one to another analysis. For example, (1) the analyses subsequent to the heat transfer analysis can be performed with the resultant nonlinear temperature distribution, (2) the analyses subsequent to structural analysis, such as vibration and acoustics, can be performed with the updated geometry, and stiffness, and (3) the effect of updated geometry of the structure due to large deformation is accounted for in computing the incidence angle for the electromagnetic exposure.

The thermo-mechanical properties in CSTEM are input automatically simply by inputting code names for the fiber and matrix of polymer-matrix composites. This feature is made possible by using the NASA in-house Integrated Composite Analyzer Code, ICAN within CSTEM. A second option is also available for inputting material properties at the ply scale. However, ply scale properties obtained from experiments for the various plies may not be consistent. Also, this option allows only temperature-dependence of the properties versus a general temperature/moisture/time/etc.-dependence of properties via ICAN. The acoustic properties are input directly for all types of materials. The electromagnetic properties are input through a separate data bank for all types of materials. The damping for acoustic noise

computations can be a nonlinear function of the vibration frequency. The electromagnetic properties can be nonlinear functions of both the temperature and the electromagnetic wave frequency.

Table 1 shows the various types of analyses available in CSTEM. The structural, vibration, acoustic, and electromagnetic analyses can be performed at user-specified steps of the transient heat transfer analysis. As can be seen in Table 1, CSTEM can also be used for the simultaneous tailoring of geometrical, material, loading, and environmental complexities. Sample demonstration cases for the tailoring capabilities of CSTEM are not included in this report.

**Mesh Generator**

CSTEM has a resident mesh generator that is capable of generating solids of revolution such as cylinders, cones, and general double curved surfaces of up to 360 degree rotation, with minimum input parameters needed to define the complicated geometries. In case of combined different types of solids of revolution/flat surfaces, duplicate nodes are automatically checked and only one of each coincident nodes is kept. The current version of CSTEM offers three types of isoparametric brick elements with 8, 16, and 20 nodes. Each element can be modelled as consisting of several layers for the composite material.

**Composite Mechanics**

As was already mentioned, CSTEM includes the Integrated Composite Analyzer (ICAN) module allowing automatic computation of the multi-scale composite properties of the virgin arbitrary combinations of multi-material layered composite configurations, as well as of the degraded configurations at various stages of the composite structure life-cycle. The room temperature fiber/matrix constituents properties for typical aircraft structure materials are automatically extracted from the ICAN resident data bank which can be augmented for properties of new materials. This feature results in a considerable saving of time required for searching and inputting the composite material property data. The ICAN module simulates the material behavior of polymer matrix composites. Simulation of metal matrix and ceramic matrix composite behavior requires appropriate modules specific for these composites.

**Heat Transfer Analysis**

CSTEM allows four types of heat transfer analyses: (1) linear steady state, (2) nonlinear steady state, (3) linear transient, and (4) nonlinear transient, all for conduction, convection, and radiation type heat transfer (Table 1). The thermal properties are computed and updated via the ICAN module. All types of thermal loads including prescribed temperatures, surface heat fluxes, convection, radiation, and internal heat generation are allowed. The output of the heat transfer analysis is the temperature distribution, defined at each node of the structure.

**Structural and Vibration Analysis**

CSTEM allows for three types of structural and vibration analyses: (1) static, (2) vibrations, and (3) buckling (Table 1), at the end of any heat transfer analysis step. All types of loads including displacements, forces, accelerations, centrifugal, and pressure are allowed. The pressure can vary across the element face. Several coordinate systems including global, skew, local, and material are allowed to provide maximum flexibility in inputting data for complex structures. For example, skew coordinate system allows input of skew boundary conditions. The vibration analysis outputs the free vibration frequencies and mode shapes. CSTEM accounts for environmental (temperature and moisture) and nonlinear geometric effects such as large deformation/centrifugal stiffening on the structural and vibration response. The pressure can be computed for either the original or the updated deformed geometry. Free vibration frequencies and mode shapes can be computed including the effect of updated geometry on the stiffness and mass matrices. Critical buckling loads can use updated stiffness for large deformation.

The structural and vibration analyses use the same finite element mesh that was used for the heat transfer analysis, thus minimizing the file transfer time and eliminating the errors incurred in transforming the temperatures from one discrete mesh to another.

**Acoustic Noise Analysis**

CSTEM allows two types of computations (Table 1) for the acoustic noise emitted from composite structures, due to (1) free vibration and (2) forced vibration induced by applying a force at a point of the structure to selectively excite the vibration modes of interest. CSTEM acoustic noise computations account for the effect of (1) updated geometry due to large deformation via (a) updated structure stiffness and mass and (b) updated geometry of the structure affecting the location and direction of the acoustic excitation force, (2) the effect of environments on thermal and mechanical properties via updated structure stiffness, and (3) the effect of natural vibration frequency on the modal loss factor (damping). A part of the structure can be masked from emitting the noise.

**Electromagnetic Analysis**

The electromagnetic analysis capability of CSTEM allows computations of reflection, absorption, and transmission of electromagnetic waves through composite structures. CSTEM offers three methods for computing electromagnetic response: (1) Waves, (2) Optics, and (3) Absorptivity (Table 1). All three methods are applicable for an electromagnetic wave impinging on a point of structure at a specific frequency, orientation, travel path, and polarization (fixed direction of electromagnetic wave propagation). The impingement location can be input specifically for user-selected element faces or all exposed faces may be analyzed at the same time. The boundary can be terminated in either the free space or in a short circuit. The first two methods use a data bank containing complex values of permittivity and permeability as functions of frequency and temperature. The third method uses a data bank containing the

fraction of the electromagnetic energy a material attenuates as a function of temperature, frequency, and polarization angle.

### Discipline Coupling

The coupling between the various disciplines due to geometrical, material, loading, and environmental complexities described above, allows many combinations of coupled multi-disciplinary analyses (Table 1), as will be demonstrated later for a fan blade. CSTEM includes several other advanced features such as two-way coupling of the updated geometry due to large deformation and the heat transfer analysis via multi-load increment analysis capability.

## COMPUTATIONAL PROCEDURE

The CSTEM computational procedure enables global multi-disciplinary as well as local structural analysis for layered multi-material composites. A schematic of the global multi-disciplinary analysis procedure is shown in Figure 5, including a block for local structural analysis. Figure 5 shows the major computational procedural modules in the order in which they are executed by the code. Specific steps can be omitted if the respective analysis is not desired, as discussed within each of the following steps.

### Step 1. Finite Element Model

The Finite Element Model Generator (FEMOGEN) is used to create the finite element model of the structure geometry, composite configuration, boundary conditions, and loads. CSTEM includes the resident module, FEMOGEN, to accomplish this task, independent of any commercial mesh-generation computer codes.

### Step 2. Composite Mechanics

The composite material properties can be input at the constituent (fiber/matrix) scale via ICAN module or can be defined directly at the structure scale, as shown in Figure 5. The material properties must be input via ICAN module if (1) the degradation in material resistance due to environments is to be included, and (2) local structural response at ply and constituent scales is desired.

Note that the finite element model, created in step 1 is at the structure scale but the material properties, if input via ICAN, are at the constituent scale. The left side of Figure 4 shows how the material properties are synthesized from the constituent scale to the laminate scale, via composite micro-mechanics and laminate theories. The constituent scale properties are updated for the effect of various parameters such as temperature, moisture, and time (bottom of Figure 4).

### Step 3. Heat Transfer Analysis

The Heat Transfer Analysis (HEATAN) module is used to compute the temperature distribution due to thermal loading via heat conduction, convection, and/or radiation heat transfer mechanisms. This step outputs temperatures at nodal points of the structure. This step is necessary unless the structure is subjected to a uniform temperature distribution throughout its surface. The Heat Transfer Analysis step may or may not be preceded by the Composite Mechanics step 2, depending on whether the thermal properties of the composite are available at the constituent or the structure scale and whether the environmental effects are to be included.

### Step 4(a). Global Structural Analysis

The Structural Analysis (STRAN) module computes global displacements at each nodal point and stress and strain at user-selected integration points of each layer in each element. The user-selected integration order determines the number and location of integration points. Step 4(a) can be bypassed if only acoustic and/or electromagnetic analyses are desired. However, for large deformation cases where the structure geometry and stiffness are updated, even for acoustic and/or electromagnetic analyses, the Global Structural Analysis step must be included.

The Structural Analysis step may or may not require the Composite Mechanics step 2, depending on whether the thermal and mechanical properties of the composite are available at the constituent or the structure scale and whether the environmental effects are to be included. Also, the Heat Transfer Analysis step 3 prior to the Global Structural Analysis step may or may not be needed, depending on whether the structure is subjected to thermal loads or a uniform temperature distribution throughout its surface.

### Step 4(b). Local Structural Analysis

The local structural analysis at the ply and constituent scales is performed via the ICAN module, as shown on the right hand side of Figure 4. The stresses are decomposed from the laminate scale to the constituent scale via the laminate theory and composite micro-mechanics. The local structural analysis can be performed at one or many nodal or integration points of the structure. Step 4(b) is not needed by the acoustic and/or electromagnetic analyses. The Global Structural Analysis step 4(a) must precede the Local Structural Analysis step 4(b). Also, the Composite Mechanics step 2 must be used in order to implement the Local Structural Analysis step 4(b).

### Step 5(a). Vibration Analysis

The Vibration Analysis (VIBRAN) module computes the vibration frequencies and mode shapes. This step is bypassed when either the vibration or the acoustic responses are not desired. Again, the Vibration Analysis step may or may not require the Composite Mechanics step 2, depending on whether the thermal and mechanical properties of the composite are available at the constituent or the structure scale and whether the environmental effects are to

be included. Also, the Heat Transfer Analysis step 3 may or may not be needed, depending on whether the structure is subjected to thermal loads or a uniform temperature distribution throughout its surface. Finally, the Global Structural Analysis Step 4(a) may or may not be skipped, depending on if the structure undergoes large deformation/geometric stiffening or not. The Local Structural Analysis step 4(b) is not needed for Vibration Analysis.

**Step 5(b). Acoustic Analysis**

The Acoustic Analysis (ACAN) module computes the acoustic noise power emitted by the structure. The acoustic analysis as such requires only the Finite Element Model step 1 and Vibration Analysis step 5(a). However, if the structure is subjected to thermal loads, the Heat Transfer Analysis step 3 must be included. But, hot structures with uniform temperature distribution can be analyzed for acoustic response without step 3. The Global Structural Analysis step 4(a) must be included if the effect of updated geometry, mass, and stiffness due to large deformation/geometric stiffening is to be included. Also, if the computation of the large deformation of the structure requires the material properties to be input at the constituent scale and/or if the environmental effects are present, then the Composite Mechanics step 2 must also be included. The Local Structural Analysis step 4(b) is bypassed for the Acoustic Analysis.

**Step 6. Electromagnetic Analysis**

The Electromagnetic Analysis (EMAN) module computes the reflection, absorption, and transmission coefficients for the electromagnetic exposure at the faces of the finite elements selected by the user. The electromagnetic analysis as such requires only the Finite Element Model step 1. However, if the structure is subjected to thermal loads, the Heat Transfer Analysis step 3 must be included. But, hot structures with uniform temperature distribution can be analyzed for electromagnetic response without step 3. The Global Structural Analysis step 4(a) must be included if the effect of updated geometry due to large deformation is to be included. Also, if the computation of the large deformation of the structure requires the material properties to be input at the constituent scale and/or if the environmental effects are present, then the Composite Mechanics step 2 must also be included. The Local Structural Analysis step 4(b) is bypassed for Electromagnetic Analysis. The Vibration Analysis step 5(a) and the Acoustic Analysis step 5(b) are also bypassed for the electromagnetic analysis.

**Step 7. Multi-Load Increment Analysis**

The Multi-Load Increment Analysis step is used for multi-directional coupling among all the participating disciplines by passing the updated geometry and updated material behavior back to any one or all analysis disciplines via a nonlinear iterative procedure. For example, the Heat Transfer Analysis step 3 can be performed after the structure geometry has been updated due to large deformation via the Global Structural Analysis step 4(a) of the first load increment analysis cycle. Any combinations of multi-disciplinary analysis steps can be used in any of the multiple load increments. The Multi-Load Increment Analysis thus provides a powerful two-way coupling among any of the participating disciplines.

## THEORETICAL BASIS

### Finite Element Analysis

The CSTEM computer code is based on the three dimensional finite element formulation, allowing coupled multi-disciplinary analysis. The nonlinear coupling among the participating analysis modules is handled via iterative solution techniques. The multi-block column solver type technique is used, allowing solution of very large problems.

### Composite Material Behavior

CSTEM draws upon the Integrated Composite Mechanics code, ICAN for characterizing material behavior at various composite scales, including the environmental effects. A nonlinear material characterization model (ref. 10) shown in Figure 6, is used at the matrix scale to simulate the degradation in material properties due to applied temperature, time, and environmental effects, etc. via an iterative approach, as shown on the left hand side of Figure 4. The ICAN module thus makes it possible to automatically compute the multi-scale composite properties of the virgin arbitrary combinations of layered multi-material composite configurations, as well as for the degraded configurations at various stages of the composite structure life-cycle.

### Heat Transfer Analysis

All three modes of heat transfer are included in the HEATAN module. (1) The Fourier's law of heat conduction is used for the heat transfer analysis. The rate of heat generated per unit volume is computed from the heat flow equilibrium in the interior of the body. (2) The heat convection is accounted for via the coefficient of convective heat transfer. (3) For radiation, the emissivity of the radiant and absorbing materials and the geometric view factors are considered. The nonlinear solution is obtained via the modified Newton-Raphson incremental iterative scheme for the heat flow equilibrium. The heat capacity effects are included as part of the rate of heat generated for the transient heat transfer analysis.

### Structural and Vibration Analysis

The Structural and Vibration Analysis is conducted using a special three dimensional displacement based finite element formulation. The stiffness of multi-layer elements is calculated using integration points located on the midplane of each ply within the element. The stiffness gradient controls the finite element model of a structure via the number of elements through the gradient and the number of numerical quadrature points within the element. The total composite stiffness including effects such as bending-twisting coupling, is computed by integrating local stiffnesses at each numerical integration point. The stress and strains are recovered at the same integration points. And, for the large deformation structural analysis, a unique incremental updated Lagrangian approach is used with iterative refinement. The free vibration frequencies and mode shapes can be calculated using (1) determinant search, or (2)

subspace iteration method.

### Local Stress Analysis

The local ply and constituent scale stresses (microstresses) at any point of the structure, are computed from the laminate scale stresses using laminate theory and composite micro-mechanics. The stress/strain results form the Global Structural Analysis module (step 4(a) in Figure 5) are integrated through the thickness of the structure at user-specified location, providing the loading which can be used for the computation of stresses at the ply and fiber/matrix scales.

### Acoustic Analysis

The acoustic noise is computed by first calculating radiation efficiencies of the structure for each natural vibration mode as a function of forced vibration frequency. the total sound power for each forced vibration frequency is then calculated by summing the contribution from each free vibration mode.

### Electromagnetic Analysis

The CSTEM electromagnetic analysis capability provides three methods: Waves, Optics, and Absorptivity. (1) The Waves method of electromagnetic analysis is based on determining the reflection and transmission properties of multi-layer plane impedance boundaries. The reflection and transmission coefficients are computed from complex impedance for given complex values of permittivity and permeability. (2) The Optics method is based on Maxwell's equations, Snell's Law and Fresnel formula to calculate reflection, refraction, and absorption coefficients for given values of permittivity and permeability. (3) The Absorptivity method is based on linear interpolation of absorptivity of layers for given absorptivity values. The first and second methods allow only temperature and frequency dependence whereas the third method allows temperature, frequency, as well as polarization angle dependence of electromagnetic properties.

## SAMPLE DEMONSTRATION CASES

The coupled multi-disciplinary analysis capabilities of the CSTEM code are demonstrated in two steps. First, the contractor-supplied demonstration cases were validated after the code was installed on NASA LeRC's CRAY-YMP system. This required some minor code and input modifications. Next, the code was demonstrated for several sample cases including the fan blade, exit nozzle segment, and combustor type structures with varying degree of coupling/complexity among various disciplines. The demonstration cases for the fan blade including various multi-disciplinary couplings are discussed here. Other structures will be presented elsewhere. The developer-contractor has validated the code for the various analysis capabilities including nonlinearities such as eigenvalue analysis on updated geometry. The validation was done with other computer codes. The results were also verified with

experimental data (Private communication with M. Hartle, General Electric Co., Cincinnati, Ohio).

**Validation of Contractor-Supplied Cases**

The CSTEM code was evaluated via contractor-supplied cases for demonstrating the code capabilities. These cases included various generic structures such as beam and plates and aircraft engine structural components such as fan blade, fan frame, exhaust duct, turbine blade, and turbine frame (Figure 7). Single and multi-disciplinary analyses were conducted for these engine structural components. The developer-contractor demonstrated only selected analysis capabilities for each structure (ref. 9). During the evaluation and validation of these cases at LeRC, new input files were created for demonstrating all available CSTEM analysis capabilities for all contractor-supplied structures. Table 2 shows the types of geometries and analyses that were conducted for each case. The results were verified with those provided by the contractor. Representative results for the contractor-supplied cases are documented in the demonstration manual (ref. 9). Some typical results, obtained as a part of the validation and not included in the contractor-supplied demonstration manual, are presented here. CSTEM results were post-processed via PATRAN (ref. 11) for graphical representation. Interface programs were developed for transferring results from CSTEM to PATRAN to expedite the process. The transient heat transfer capability is demonstrated for a turbine blade subjected to heat convection as shown in Figure 8. These results are for the temperature distribution at the tip of the leading edge. Results for the first vibration frequency and mode shape for a fan frame are shown in Figure 9. Results for acoustic noise emitted from the fan frame, subjected to a point vibratory acoustic load, are shown for various forcing frequencies in Figure 10. The noise level is shown in both, the commonly used decibels measure, as well as power in watts. Electromagnetic analysis sample case is for an exhaust duct subjected to electromagnetic waves, as shown in Figure at the top in Figure 11. The electromagnetic reflection from the duct's curved surface is also shown at the bottom in the same Figure 11, both in decibels and % power. Note that the decibels for the electromagnetic reflection are not the same as those commonly known for the acoustic noise. The zero electromagnetic reflection in decibels refers to a 100 % reflection of the incident electro-magnetic power. A perfect electromagnetic conductor will reflect all incident power, i.e., the reflection will be zero decibels. For reflection power less than 100 %, the decibel numbers (db) decrease as a logarithmic function of the square root of the power. For instance, the decibel value of -3 means about 50 % reduction in reflected power and the decibel value of -5 means about 70 % reduction in reflected power compared to the perfect conductor, and so on.

**Sample Cases - Fan Blade**

An aircraft engine fan blade with twist was simulated for a coupled multi-disciplinary thermal, structural, vibration, and acoustic response. Figure 12 shows a schematic of the fan blade with overall geometric dimensions. A summary of the various analysis disciplines, and coupling effects demonstrated for the fan blade, is provided in Table 3. All analysis capabilities were demonstrated for a metal and a multi-material layered composite blade, separately. While

this demonstrates CSTEM for all types of materials, isotropic and layered anisotropic, it also demonstrates advantages of using advanced composite materials. The thermal/structural/acoustic/electromagnetic loads, environmental conditions, boundary conditions, and the structure material for the metal fan blade are shown in Figure 13. These and the composite configuration for the composite fan blade are shown in Figure 14.

**Blade Structure, Material, and the Finite Element Model:** The blade consists of a twisted aerofoil shape with varying thickness along the span and the chord (Figures 12). The maximum span of the blade is 10.19 inches and the maximum chord is 3.43 inches. The thickness varies from 0.20 at the leading edge tip to 1.35 inches at the trailing edge tip. As noted above, the blade is analyzed for two materials; (1) metal - titanium, and (2) multi-material layered composite - 40 % thickness of titanium and 60 % thickness of six-layered T300/IMHS material with $(0/30/-30)_s$ ply orientations with 0.6 fiber volume ratio. T300 stands for graphite fibers and IMHS for intermediate modulus high strength epoxy matrix. The thermal and mechanical properties of T300 fibers and IMHS matrix at room temperature, retrieved from ICAN's module resident databank, are shown in Table 4. The finite element model, shown in Figure 15, consists of forty 20-noded (8 corner and 12 mid-sided) brick elements and 110 nodes.

**Thermal Loading/Heat Transfer Analysis:** For both the metal and composite fan blades, the root of the blade was held at a constant temperature of 200 °F and the blade surface was subjected to fluid flow at 300 °F. For the metal blade, an additional case with root at 500 °F and surface fluid flow at 1000 °F was also analyzed. The thermal material properties; thermal conductivity and coefficient of heat convection, were considered temperature-dependent via (a) direct input of temperature-dependent properties for the metal, and (b) ICAN for the composite. A nonlinear steady-state heat transfer analysis coupled with composite mechanics was conducted for both the metal and composite blades.

The heat transfer results, in terms of temperature contours, are shown for (1) the metal blade with root at 200 °F and surface fluid flow at 300 °F in Figure 16, (2) the metal blade with root at 500 °F and surface fluid flow at 1000 °F in Figure 17, and (3) the composite blade with root at 200 °F and surface fluid flow at 300 °F in Figures 18. The computed temperatures vary from 200 °F to 285 °F, 500 °F to 926 °F, and 200 °F to 275 °F for the three cases, respectively, as described above. A comparison of leading edge temperatures for the metal and composite blades subjected to the same thermal load, root at 200 °F and surface fluid flow at 300 °F, is shown in Figure 19.

**Thermo-mechanical Loading/Structural Analysis:** The root of the blade was fixed and a centrifugal loading of 1400 rpm was applied for both the metal and composite fan blades. The effect of propulsion environment was simulated for the following sample cases: (1) room temperature (70 °F) with no moisture absorption, (2) nonuniform temperature distribution as computed by the heat transfer analysis with no moisture absorption due to the thermal loading of 200 °F at the blade root and 300 °F for the surface fluid flow, (3) uniform temperature rise from 70 to 300 °F with no moisture absorption, and (4) nonuniform temperature distribution same as in case (2) combined with 2 % absorption of moisture in the composite, by weight.

Note that since the moisture absorption is not applicable for the metals, case (4) was demonstrated for the composite blade only. For the metal blade, cases (2) and (3) were repeated for blade root at 500 °F and surface fluid flow at 1000 °F. Cases (2) and (4) with nonuniform temperature distribution require coupled composite-mechanics/heat-transfer/structural analysis. A fifth case (5) was simulated for the effect of geometric stiffening at room temperature and no moisture. The thermal and mechanical properties; coefficient of thermal expansion, stiffness, and strength, were considered temperature-dependent via (a) direct input of temperature-dependent properties for the metal, and (2) ICAN for the composite fan blade. A static structural analysis was conducted for both materials.

The deformed shape of the blade rotating at 1400 RPM with nonuniform temperature distribution computed via coupled composite-mechanics/heat-transfer/structural analysis, with no moisture absorption and no effect of geometric stiffening, is shown for (1) the metal blade with root at 200 °F and surface fluid flow at 300 °F in Figure 20, (2) the metal blade with root at 500 °F and surface fluid flow at 1000 °F in Figure 21, and (3) the composite blade with root at 200 °F and surface fluid flow at 300 °F in Figures 22. A comparison of leading edge radial displacements for the metal and composite blades subjected to the same thermal load, root at 200 °F and surface fluid flow at 300 °F, is shown in Figure 23. Notice that the metal blade shows positive (i.e. increase in radius) leading edge radial displacements whereas the composite blade shows mostly negative (i.e. decrease in radius) leading edge radial displacements. This is also observed from deformed shapes in Figures 20 and 22.

The effects of various environmental conditions on structural response is shown for (1) the metal blade in Figure 24, and (2) the composite blade in Figure 25. Figure 24 shows leading edge radial displacements of the metal blade for (1) room temperature (70 °F) condition, (2) nonuniform temperature distribution of 200 °F to 285 °F, (3) uniform temperature distribution of 300 °F, (4) nonuniform temperature distribution of 500 °F to 926 °F, and (5) uniform temperature distribution of 1000 °F. As expected, the displacement increases with increasing temperature. Since moisture absorption is negligible for the metals, no such effect is shown. Figure 25 shows leading edge radial displacements of the composite blade for (1) room temperature (70 °F) condition, (2) nonuniform temperature distribution of 200 °F to 275 °F, (3) uniform temperature distribution of 300 °F, and (4) nonuniform temperature distribution of 200 °F to 275 °F with 2 % moisture by weight. Again, the displacement increases with increasing temperature as well as with increasing moisture absorption. Figures 24 and 25 show that the metal blade undergoes more radial deformation than does the composite blade. Though not presented herein, CSTEM outputs results for geometric stiffening effects on displacements and for global and local stresses at ply and fiber/matrix constituents scales.

**Free Vibration Analysis:** The root of the blade was fixed. Five vibration analysis cases similar to those described above for the "Structural Analysis", were simulated. Again, cases (2) and (4) with nonuniform temperature distribution computed via heat transfer analysis, require a coupled composite-mechanics/heat-transfer/vibration analysis. And, case (5) with geometric stiffening, requires a coupled composite-mechanics/structural/ vibration analysis to account for the effect of updated geometry due to geometric stiffening. The thermal and mechanical properties were similar to those described above for the "Structural Analysis". Three natural

vibration frequencies and their mode shapes were computed for all five cases for both materials.

The first three natural vibration frequencies for both the metal and composite blades with root at 200 °F and surface fluid flow at 300 °F, i.e. with nonuniform temperature distributions computed via heat transfer analysis and with no moisture absorption and no geometric stiffening, are shown in Figure 26. As expected, the composite blade exhibits higher vibration frequencies than does the metal blade. The corresponding mode shapes are shown in Figures 27 and 28 for the metal and composite blades, respectively.

The effects of various environmental conditions on vibration response is shown for (1) the metal blade in Figure 29, and (2) the composite blade in Figure 30. Figure 29 shows the fundamental vibration frequency of the metal blade for (1) room temperature (70 °F) condition, (2) nonuniform temperature distribution of 200 °F to 285 °F, (3) uniform temperature distribution of 300 °F, (4) nonuniform temperature distribution of 500 °F to 926 °F, and (5) uniform temperature distribution of 1000 °F. As expected, the vibration frequency decreases with increasing temperature as the material degrades. Since moisture absorption is negligible for the metals, no such effect is shown. Similarly, Figure 30 shows the fundamental vibration frequency of the composite blade for (1) room temperature (70 °F) condition, (2) nonuniform temperature distribution of 200 °F to 275 °F, (3) uniform temperature distribution of 300 °F, and (4) nonuniform temperature distribution of 200 °F to 275 °F and 2 % moisture by weight. Again, the vibration frequency decreases with increasing temperature as well as with increasing moisture absorption as the material degrades.

The effect of geometric stiffening on the fundamental vibration frequency is shown for (1) the metal blade in Figure 31, and (2) the composite blade in Figure 32. Geometric stiffening for these blades has negligible stiffness effect.

**Forced Vibration Excitation/Acoustic Analysis:** The root of the blade was fixed and sinusoidal forced vibrations of 10 lb amplitude were applied at the leading edge tip in the blade thickness direction, at several forcing frequencies ranging from 100 to 1000 cps. Again, five cases with thermo-mechanical properties as discussed above were simulated. Cases (1) and (3) with room temperature and uniform temperature distribution, respectively, require coupled composite-mechanics/vibration/acoustic analysis. Cases (2) and (4) with nonuniform temperature distribution computed via heat transfer analysis, require coupled composite-mechanics/heat-transfer/vibration/acoustic analysis, and case (5) with geometric stiffening, requires a coupled composite-mechanics/ structural/vibration/acoustic analysis. A special variation of case (2) with frequency-dependent modal loss damping factor was also run. This is just one of many special features of the computational simulation procedure demonstrated in the present report. The modal loss factors used for this evaluation are only estimates. The computational simulation of damping in composite materials is described in reference 12.

The acoustic noise emitted from the metal fan blade subjected to the thermal load, root at 200 °F and surface fluid flow at 300 °F, and the 10 lb sinusoidal acoustic load, is shown in Figure 33 for three different modal loss factors (damping). The noise level is shown in watts

as well as in decibels. To put the decibel values in perspective, the human whisper is at 50 decibels, a truck horn is at 110 decibels, and an airplane engine propeller is at 120 decibels. The acoustic noise emitted from the composite fan blade, under the same thermal and acoustic loads, is shown in Figure 34, also for three different modal loss factors. Increasing damping decreases the noise level. A comparison of the acoustic noise emitted from the metal and composite blades subjected to the same thermal load, root at 200 °F and surface fluid flow at 300 °F and the same 10 lb sinusoidal acoustic load, is shown in Figure 35. In the forcing frequency range of up to 200 cps, the noise is much less for the composite material than for metal.

The effect of vibration frequency dependent modal loss factors, is shown for (1) the metal blade in Figure 36, and (2) the composite blade in Figure 37. The modal loss factor decreases with the vibration frequency, as tabulated in Figures 36 and 37. The acoustic noise increases, only slightly, by accounting for frequency dependence of the modal loss factors both, for the metal and composite blades.

The significant observation is that the acoustic noise from the composite fan blade is negligible compared to that from the metal blade, Figure 35. The effect of frequency dependence of the modal loss factors is practically the same for the two blades, Figures 36 and 37.

The effects of various environmental conditions on the acoustic noise emitted from the metal blade, are shown in Figure 38 for (1) room temperature (70 °F) condition, (2) nonuniform temperature distribution of 200 °F to 285 °F, (3) uniform temperature distribution of 300 °F, (4) nonuniform temperature distribution of 500 °F to 926 °F, and (5) uniform temperature distribution of 1000 °F. The temperatures of up to 300 °F show negligible effect on the acoustic noise, whereas higher temperatures up to 1000 °F show a slight decrease in the noise level. Since moisture absorption is negligible for the metals, no such effect is shown. Similarly, the effects of various environmental conditions on the acoustic noise emitted from the composite blade, are shown in Figure 39 for (1) room temperature (70 °F) condition, (2) nonuniform temperature distribution of 200 °F to 275 °F, (3) uniform temperature distribution of 300 °F, and (4) nonuniform temperature distribution of 200 °F to 275 °F and 2 % moisture by weight. Higher temperature and added moisture show a slight increase in the noise level.

The acoustic noise decreases or increases depending on whether the forcing frequency is farther away from or closer to the natural vibration frequency, respectively. For the metallic fan blade, the noise decreased slightly with increasing temperature because the forcing frequency of 113 cps became farther away from the natural vibration frequency as the temperature increased (see Figures 29 and 38). On the other hand, for the composite blade, the noise increased slightly with increasing temperature because the forcing frequency of 119 cps became closer to the natural vibration frequency as the temperature increased (see Figures 30 and 39). This type of analysis provides important clues on what materials/designs will be less noisy at what forcing frequencies.

The effect of geometric stiffening on the acoustic noise emitted from the metal and composite blades at room temperature, is shown in Figures 40 and 41, respectively. The effect

of geometric stiffening is to decrease the acoustic noise as the forcing frequency moves away from the natural vibration frequency.

**Electromagnetic Exposure/Analysis:** The blade was subjected to electric and magnetic fields of forcing frequencies ranging from 1 Gcps to 20 Gcps, typical for radar detection of aeroplanes. The electromagnetic waves were directed to impinge on the front surface of the blade, i.e., at the T300/IMHS layer with zero degree orientation for the composite blade. The electromagnetic reflection was calculated using both the Waves and Optics methods for one case, i.e., with zero angle of incidence at room temperature. Identical results were obtained by both methods. All cases were simulated using the Optics method, which gives all the information that can be obtained from the Waves method as well as a layer-by-layer breakdown of electromagnetic response. Several cases were run to simulate the effect of electromagnetic material resistance, structure geometry, and incidence angle. The electromagnetic properties used for all the materials are estimates. In addition to titanium for metal and titanium + T300/IMHS for the composite blade, materials with relatively higher and lower electromagnetic conductivities were used to assess the effect of electromagnetic material resistance. The analysis was done for electromagnetic exposure of the entire surface of the blade for all cases. The analysis was, then, repeated for 30 degree angle of incidence, i.e., at 30 degrees from the through-the-thickness Z-axis (Figures 13 and 14). Further cases were run to assess the effect of uniform and nonuniform temperature distributions and updated structure geometry due to large structural deformation. Cases with room temperature and uniform temperature distribution require single discipline analysis for the metal blade and coupled composite mechanics-electromagnetic analysis for the composite case. Note that the composite mechanics was not used for the electromagnetic analysis the way it was used for the structural analysis. The electromagnetic analysis module computes the electromagnetic impedance/response layer-by-layer for the whole composite. And, cases with nonuniform temperature distribution require coupled heat-transfer/ electromagnetic analysis while cases with large structural deformation require coupling with structural analysis also.

The results of the electromagnetic analysis are shown in Figures 42 and 43 for electromagnetic reflection at the leading edge tip of the blade, for zero incidence angle for three different materials, and for the metal and composite blades, respectively. Notice that these Figures show a global and a local incidence angle. The global incidence angle is simply the angle with respect to the global through-the-thickness Z-axis (Figures 13 and 14), at which the waves impinge the blade. But, since the blade is twisted, the waves do not impinge normal to the blade surface at all points. The local incidence angle represents the angle between the local normal and the global normal, at any given point of the structure. The reflection from the material with the higher electromagnetic conductivity is higher, as expected.

Figures 44 and 45 show the electromagnetic reflection at four different locations of the metal and composite blades, respectively. The reflection is different at different locations, depending on the twist, i.e., the local incidence angle at that location. Figures 46 and 47 show the effect of non-zero global incidence angle, i.e. the effect of the direction of impingement, on the metal and composite blades, respectively. Notice that the reflection decreases with

increasing global incidence angle but increases with increasing local incidence angle. The significant observation is that the electromagnetic reflection from the composite blade is less than that from the metal blade which has higher electromagnetic conductivity. And, the amount of reflection at various structure locations for various impingement directions depends on the combined effect of the impingement direction (global incidence angle) and the blade twist (local incidence angle).

The effects of various environmental conditions on the electromagnetic reflection from the metal blade, are summarized in Figure 48 for (1) room temperature (70 °F) condition, (2) nonuniform temperature distribution of 200 °F to 285 °F, (3) uniform temperature distribution of 300 °F, (4) nonuniform temperature distribution of 500 °F to 926 °F, and (5) uniform temperature distribution of 1000 °F. Similarly, the effects of various environmental conditions on the electromagnetic reflection from the composite blade, are shown in Figure 49 for (1) room temperature (70 °F) condition, (2) nonuniform temperature distribution of 200 °F to 275 °F, and (3) uniform temperature distribution of 300 °F. An increase in temperature decreases the electromagnetic conductivity of the material, thus increasing the reflection. Negligible effects are observed in Figures 48 and 49 because the conductivity does not change significantly over the temperature ranges of the materials simulated for these sample cases. Other cases, not included here, were run with artificially high dependence of conductivity on temperature and the results showed significant differences in reflection. The effect of moisture on electromagnetic reflection can be simulated similar to temperature effects, by including the moisture degradation in electromagnetic properties.

The effect of deformation due to geometric stiffening on the electromagnetic reflection from the metal and composite blades at nonuniform temperature distribution of 200 °F to 285 °F for the metal blade and 200 °F to 275 °F for the composite blade, is shown in Figures 50 and 51, respectively. The effect of these is relatively small. However, if the geometry of the structure changes significantly due to large deformations, this could affect the local incidence angle and hence the amount of electromagnetic reflection significantly.

## GENERAL REMARKS

A stand-alone computational simulation procedure has been demonstrated for coupled response of an aircraft engine fan blade under multi-disciplinary thermal/ structural/vibration/acoustic/electromagnetic loading in propulsion environments. The procedure was developed via integrating the three dimensional finite element technique with in-house single-discipline codes coupled with acoustic analysis methods. The simulation procedure is of general-purpose in nature and can be used for designing/analyzing multi-material layered composite structures. The results, such as the decrease in acoustic noise levels by accounting for structural/acoustic coupling due to geometric stiffening, demonstrate the significance of coupled multi-disciplinary simulation of the blade. Results such as these can be generated via a single coupled multi-disciplinary code in a very short time. In an effort to satisfy the competing requirements imposed by individual discipline-specific behavior, many design variations/parameters will need to be considered. Multi-disciplinary computational simulation

is the approach that will provide a realistic assessment of the various competing design requirements of advanced composite materials/structures. Unlike experimental data generation that may be time consuming and costly, computational simulation is able to produce rapid reasonable results for specific designs.

The environmental effects described and discussed herein include temperature and moisture. Other environmental effects such as chemical interactions can be incorporated in the same way. The effect of chemical interaction on the degradation of material resistance can be simulated via the Integrated Composite Analyzer Code, ICAN, by adding respective terms in the nonlinear material characterization model, shown in Figure 6 (ref. 10). The modified form of the nonlinear material characterization model will consist of a product of nonlinear factors for each environmental effect. Such nonlinear multi-factor interaction models (MFIM) for factor such as cyclic effect have been implemented in metal matrix composite analysis codes. The effect of chemical interaction on changes in the geometry, if any, can be addressed in the finite element models by suitable changes in the dimensions. These effects can then be passed on to the multi-disciplinary analysis via the geometry update module.

## SUMMARY

A general-purpose computational simulation procedure is presented for coupled multi-disciplinary thermal, structural, vibration, acoustic, and electromagnetic analysis of elevated temperature composite structures in propulsion environments. All the disciplines are coupled for nonlinear geometrical, material, loading, and environmental effects. The procedure is embedded in a stand-alone state-of-the-art computer code, enabled by integrating the three dimensional finite element technique with in-house codes for integrated composite mechanics, thermal, and acoustic analysis methods. A nonlinear material characterization model is used to simulate the degradation in material properties due to applied temperature, time, and environmental effects. Sample cases exhibiting various combinations of coupled multi-disciplinary analysis of an aircraft engine fan blade, are presented. Results indicate lower temperatures, higher vibration frequencies, and substantially lower acoustic noise levels and lower electromagnetic reflection for the T300/IMHS composite versus that for titanium.

## REFERENCES

1. Chamis, C.C.: Integrated Analysis of Engine Structures. NASA TM–82713, 1981.

2. Chamis, C.C.; and Johns, R.H.: Computational Engine Structural Analysis. NASA TM–87231, 1986.

3. Chamis, C.C.: Computational Structural Mechanics for Engine Structures. NASA TM–102119, 1989.

4. Hartle, M.: CSTEM User's Manual. General Electric Company, Cincinnati, OH, 1990.

5. Hayes, P.E.: Determining Vibration, Radiation Efficiency, and Noise Characteristics of Structural Designs Using Analytical Techniques. Proceedings—Society of Automotive Engineers, VOL. P–106, SAE, Warrendale, PA, 1982, pp. 236–270.

6. Krueger, Jr., C.H.: A Computer Program for Determining the Reflection and Transmission Properties of Multilayer Plane Impedance Boundaries. Report AFAL–TR–67–191, Air Force Avionics Laboratory, Wright-Patterson Air Force Base, OH, Sept. 1967.

7. Murthy, P.L.N.; and Chamis, C.C.: Integrated Composite Analyzer (ICAN)—User's and Programmer's Manual, NASA TP–2515, 1986.

8. Structural Tailoring of Engine Blades (STAEBL). NASA CR–167949, Pratt & Whitney Aircraft Co., East Hartford, CT, 1982.

9. Hartle, M.: CSTEM Demonstration Manual. General Electric Company, Cincinnati, OH, 1990.

10. Chamis, C.C.: Simplified Composite Micro-Mechanics Equations for Hygral, Thermal, and Mechanical Properties. NASA TM–83320, 1987.

11. PATRAN Plus User Manual, July 1988.

12. Saravanos, D.A.; and Chamis, C.C.: Mechanics of Damping for Fiber Composite Laminates Including Hygrothermal Effects. AIAA J., vol. 28, no. 10, Oct. 1990, pp. 1813–1819.

# Table 1: CSTEM Analysis Capabilities

| ANALYSIS | FEATURES |
|---|---|
| Heat Transfer<br>* Steady State-Linear<br>* Steady State-Nonlinear<br>* Transient-Linear<br>* Transient-Nonlinear | - Conduction<br>- Convection<br>- Radiation |
| Structural and Vibration<br>* Static<br>* Structural Dynamics - Vibrations<br>* Buckling | - Coupled Integrated Composite Mechanics With ICAN<br>- Large Deformation<br>- Coupled With Heat Transfer |
| Acoustic<br>* Free Vibration<br>* Forced Vibration | - Coupled With Heat Transfer<br>- Coupled With Structural Behavior |
| Electromagnetic<br>* Waves<br>* Optics<br>* Absorptivity | - Large Deformation<br>- Coupled With Heat Transfer |
| Tailoring<br>* Cost, Weight<br>* Temperature<br>* Vibration Frequency<br>* Displacement / Stress<br>* Acoustic Noise<br>* Electromagnetic Radiation | - Constraints<br>- Design Variables |

Table 2: CSTEM Validation of Contractor-supplied Cases

| Structure | Analysis | | | |
|---|---|---|---|---|
| | Heat Transfer | Structural/ Vibration | Acoustic | Electro-Magnetic |
| Beam | ✓* | ✓ | ✓* | ✓* |
| Panel | ✓* | ✓ | ✓ | ✓* |
| Fan Blade | ✓* | ✓ | ✓* | ✓ |
| Fan Frame | ✓* | ✓ | ✓* | ✓ |
| Exhaust Duct | ✓ | ✓ | ✓* | ✓* |
| Turbine Frame | ✓ | ✓ | ✓* | ✓* |
| Turbine Blade | ✓* | ✓ | ✓* | ✓* |

✓ : Tested/ Demonstrated/ Validated

*: New Cases

Table 3: Sample Cases - Fan Blade

| Analysis Discipline | Loading | Coupled with |
|---|---|---|
| Heat Transfer<br>* Steady State - Nonlinear | - Prescribed Temperature<br>- Convection | ● Composite Mechanics |
| Structural<br>* Static | - Centrifugal Loading | ● Composite Mechanics<br>● Heat Transfer Analysis |
| Vibration<br>* Vibration Frequencies/ Mode Shapes | | ● Composite Mechanics<br>● Heat Transfer Analysis<br>● Structural Analysis via Geometric Stiffening |
| Acoustic<br>* Forced Excitation Noise | - Point Load | ● Composite Mechanics<br>● Heat Transfer Analysis<br>● Structural Analysis via Geometric Stiffening<br>● Vibration |
| Electromagnetic<br>* Optics | - Electromagnetic Exposure | ● Composite Mechanics<br>● Heat Transfer Analysis<br>● Structural Analysis via Geometric Stiffening<br>● Vibration |

## Table 4: Constituent (fiber/matrix) Material Properties of Fan Blade

| T300 Fiber | | IMHS Matrix | |
|---|---|---|---|
| Filament Equivalent Diameter | = 0.0003 inch | Weight Density | = 0.044 $lb/in^3$ |
| Weight Density | = 0.064 $lb/in^3$ | Elastic Modulus | = $0.5 \times 10^6$ psi |
| Modulus in Longitudinal Direction | = $32 \times 10^6$ psi | Poisson's Ratio | = 0.35 |
| Modulus in Transverse Direction | = $2 \times 10^6$ psi | Thermal Expansion Coefficient | = $36 \times 10^{-6}$ in /in - °F |
| In-plane Poisson's Ratio | = 0.2 | Heat Conductivity | = 1.25 Btu/hr-ft - °F |
| Out-of-plane Posson's Ratio | = 0.25 | Tensile Strength | = 15,000 psi |
| In-plane Shear Modulus | = $1.3 \times 10^6$ psi | Compressive Strength | = 35,000 psi |
| Out-of-plane Shear Modulus | = $0.7 \times 10^6$ psi | Shear Strength | = 13,000 psi |
| Thermal Expansion Coefficient in Longitudinal Direction | = $-0.55 \times 10^{-6}$ in /in - °F | Void Fraction | = 0.225 |
| Thermal Expansion Coefficient in Transverse Direction | = $5.6 \times 10^{-6}$ in /in - °F | Glass Transition Temp. | = 420 °F |
| Thermal Conductivity in Longitudinal Direction | = 48.3 Btu/hr-ft - °F | | |
| Thermal Conductivity in Transverse Direction | = 4.83 Btu/hr-ft - °F | | |
| Tensile Strength | = 35,000 psi | | |
| Compressive Strength | = 30,000 psi | | |

Conversion Factors for SI Units: 1 in = 0.0254 m; $1 lb/in^3 = 0.2714 \times 10^6 N/m^3$; 1 psi = $6.895 \times 10^3 N/m^2$

°F = 1.8 °C + 32; 1 Btu/hr-ft - °F = 1.73 watts/meter - °K

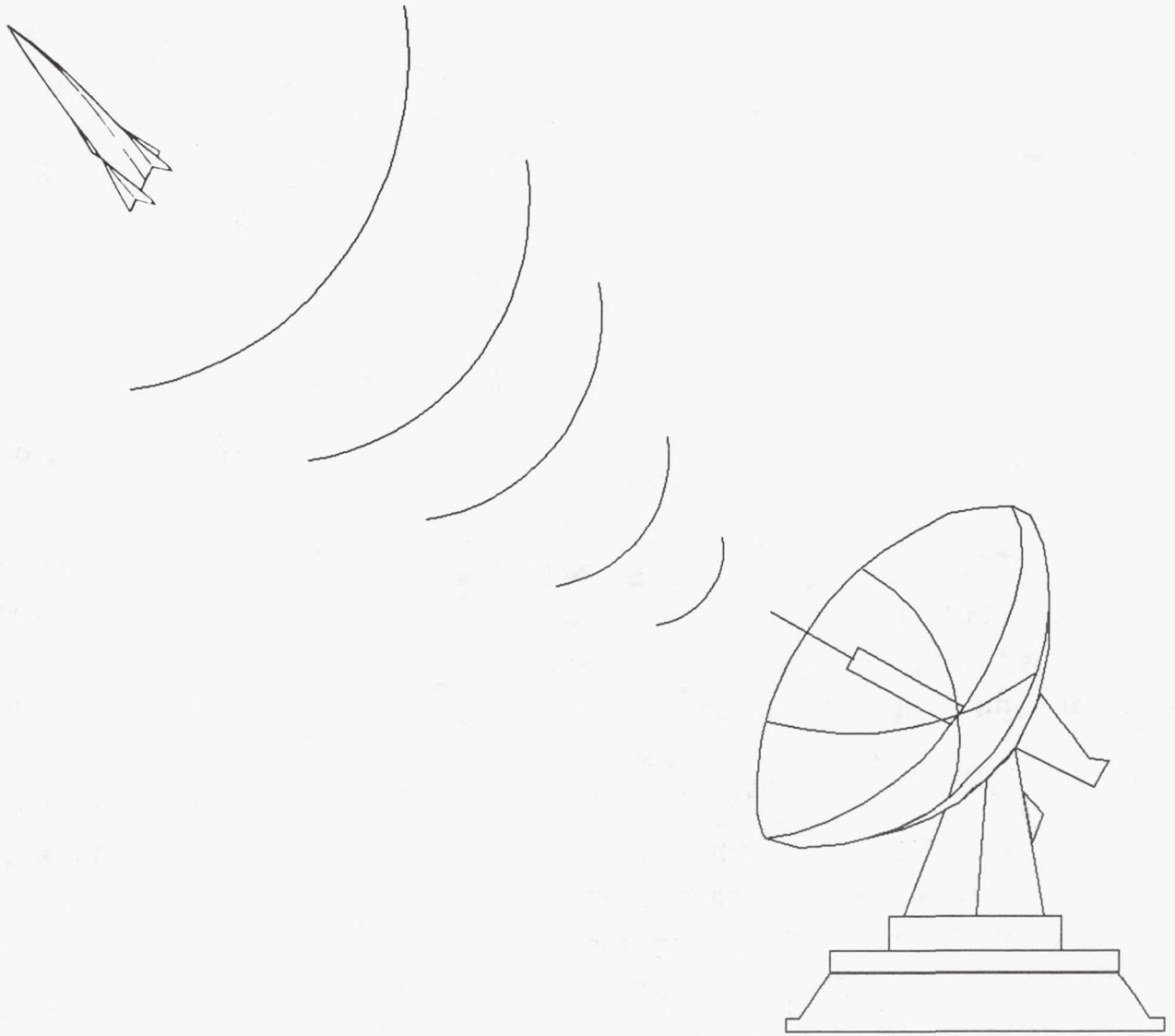

Figure 1: Aircraft under Electromagnetic Radiation

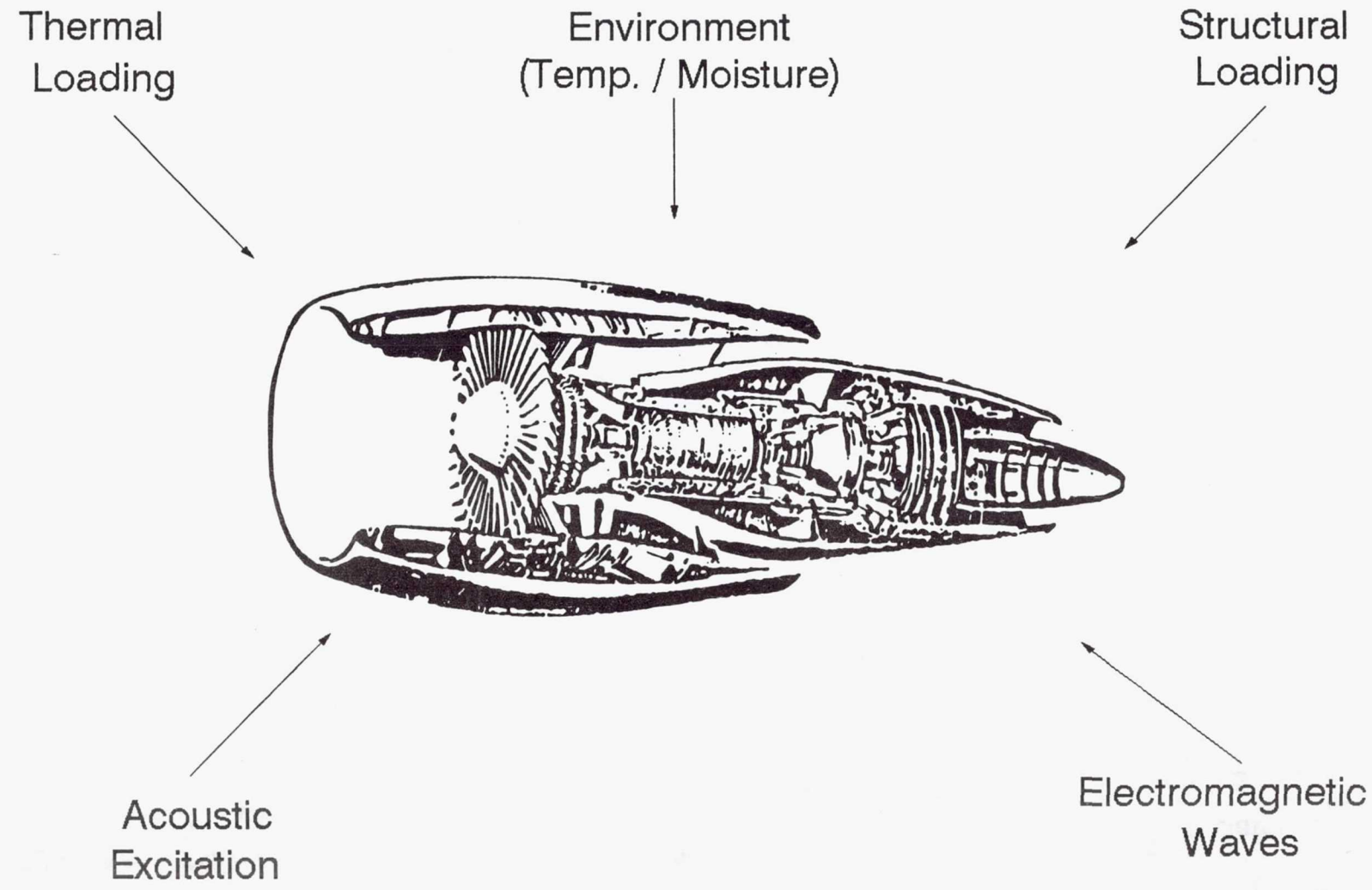


Figure 2: Simultaneous Multi-disciplinary Loadings for an Aircraft Engine

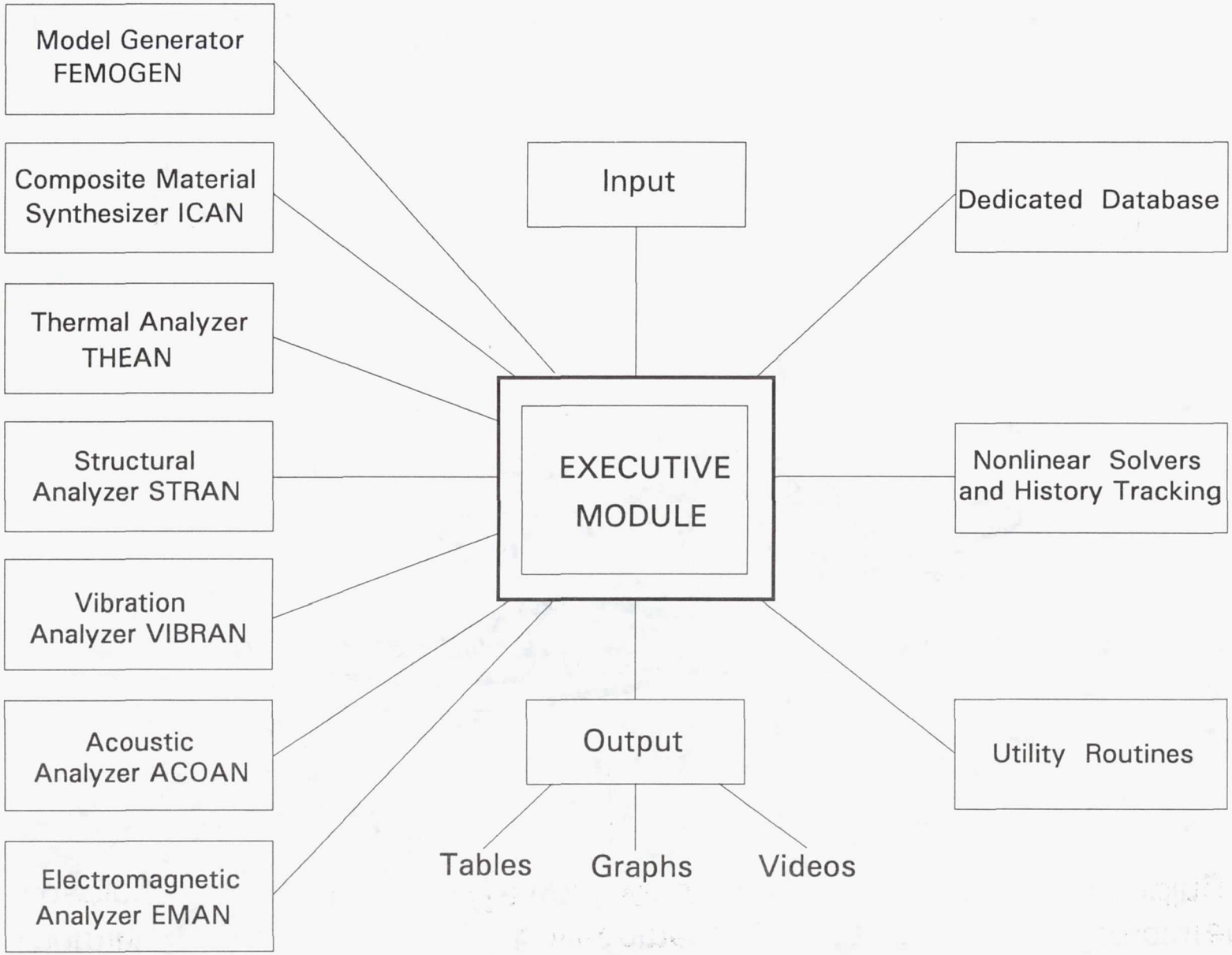


Figure 3: CSTEM Modular Structure

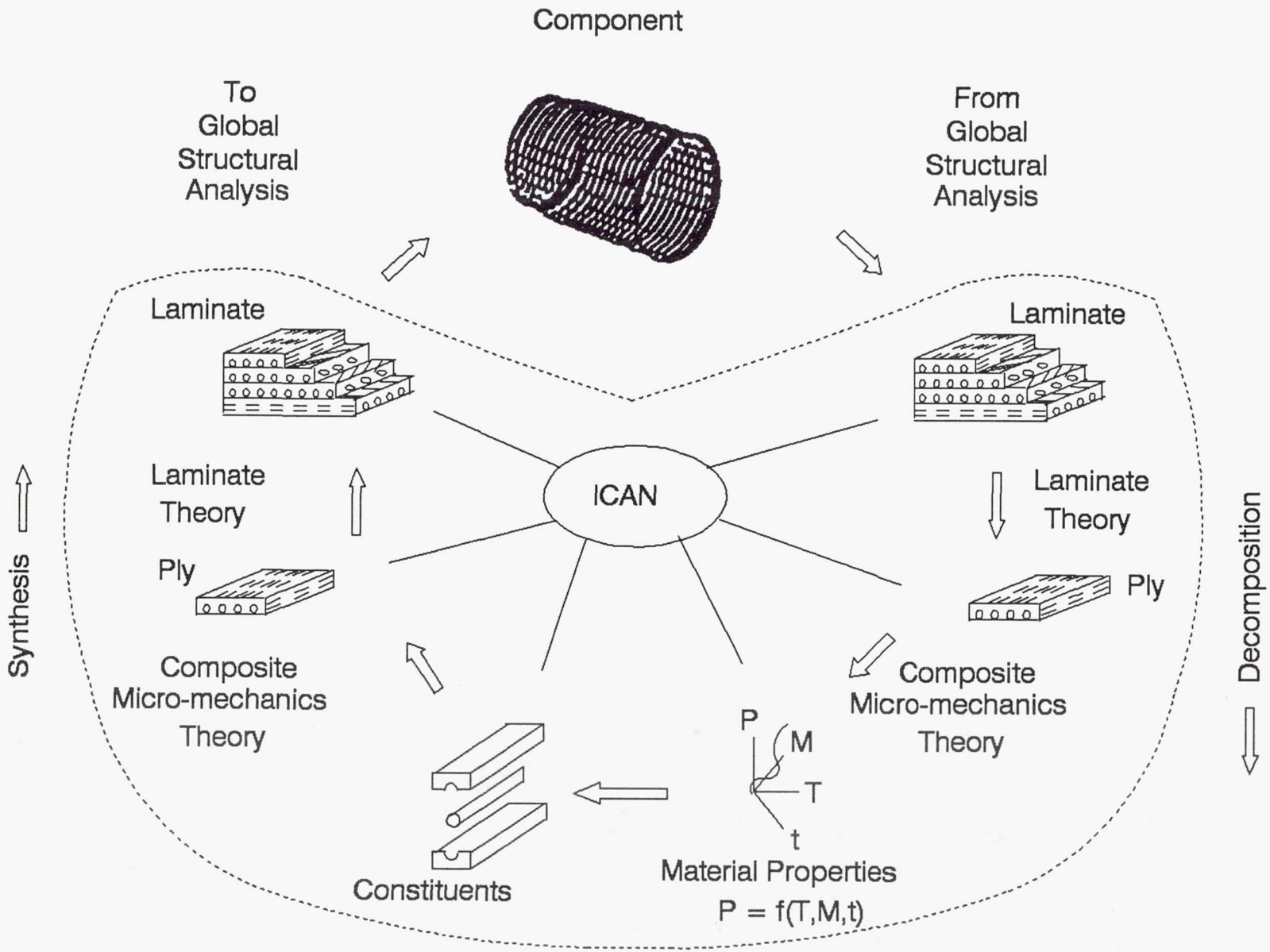


Figure 4: Integrated Composite Analysis (ICAN)

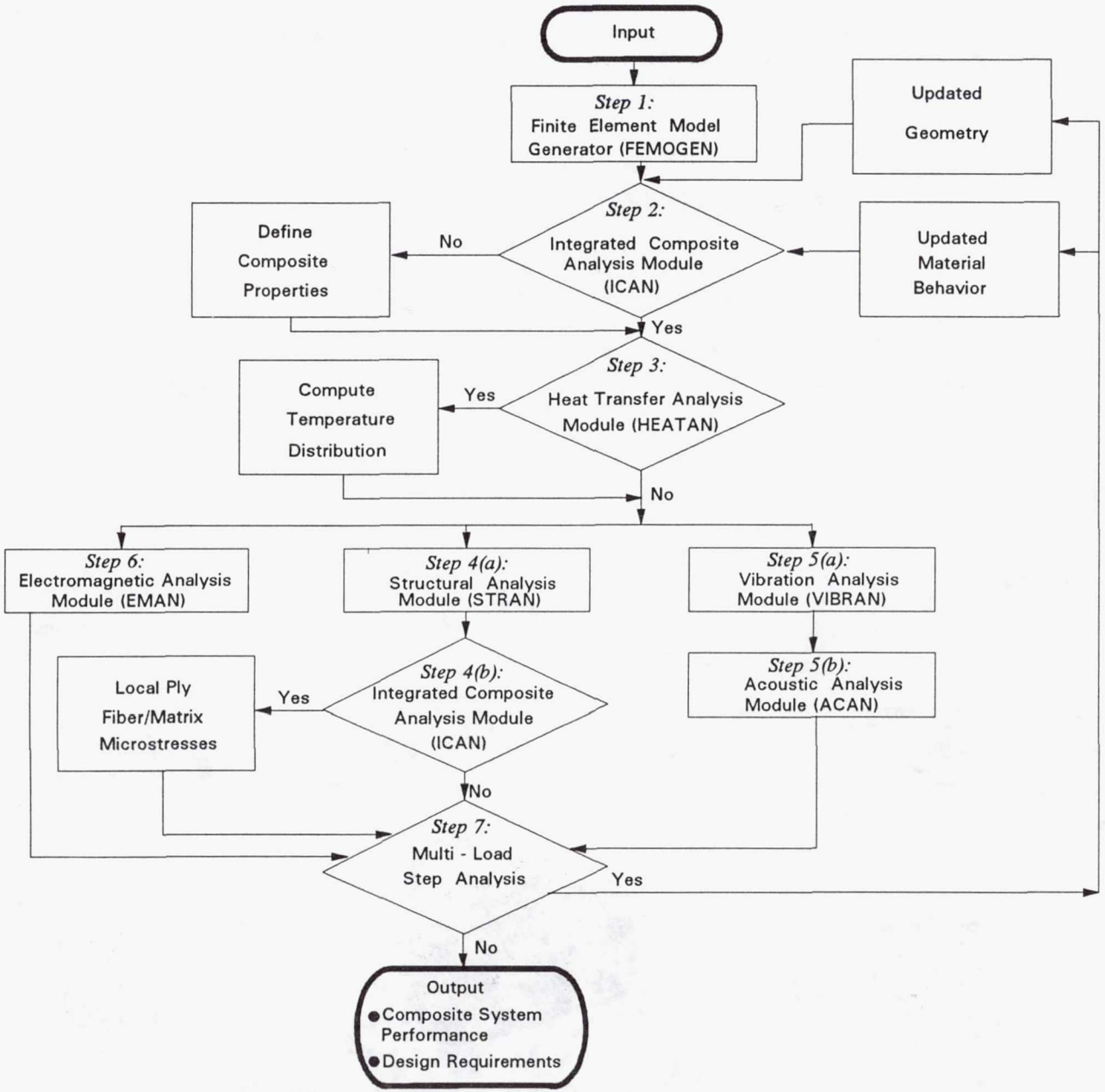


Figure 5: CSTEM Multi-disciplinary Computational Procedure

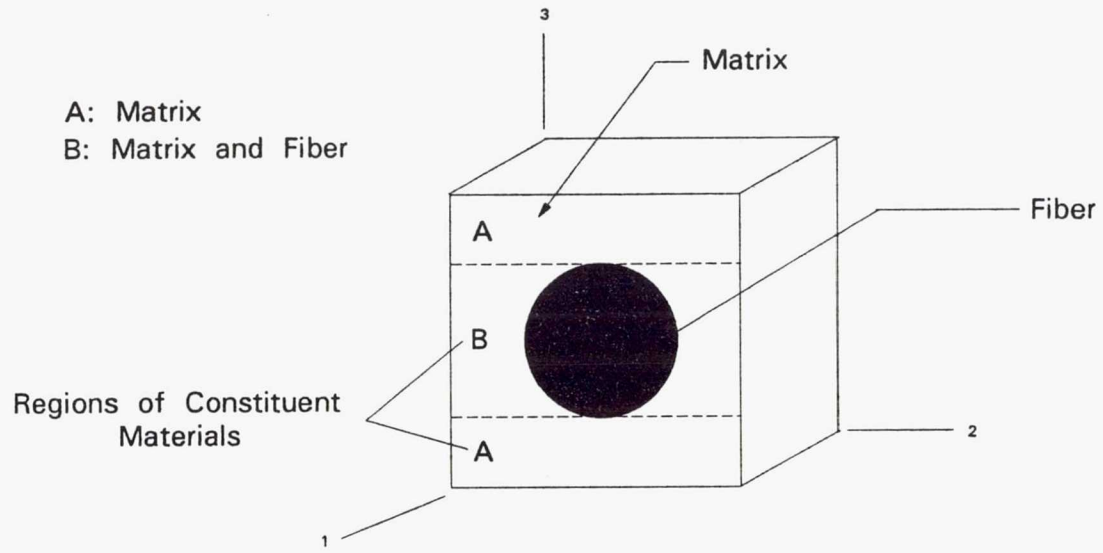


$$\frac{P_M}{P_{Mo}} = \left[ \frac{T_{GW} - T}{T_{GD} - T_o} \right]^{1/2}$$

$$T_{GW} = (0.005\,M^2 - 0.1\,M + 1)\,T_{GD}$$

$P_M$ = Matrix Property at Current Temp., T

$P_{Mo}$ = Matrix Property at Reference Temp., $T_o$

$T_{GW}$ = Wet Glass Transition Temp.

$T_{GD}$ = Dry Glass Transition Temp.

M = Moisture

Figure 6 : Regions of Constituent Materials and Nonlinear Material Characterization Model

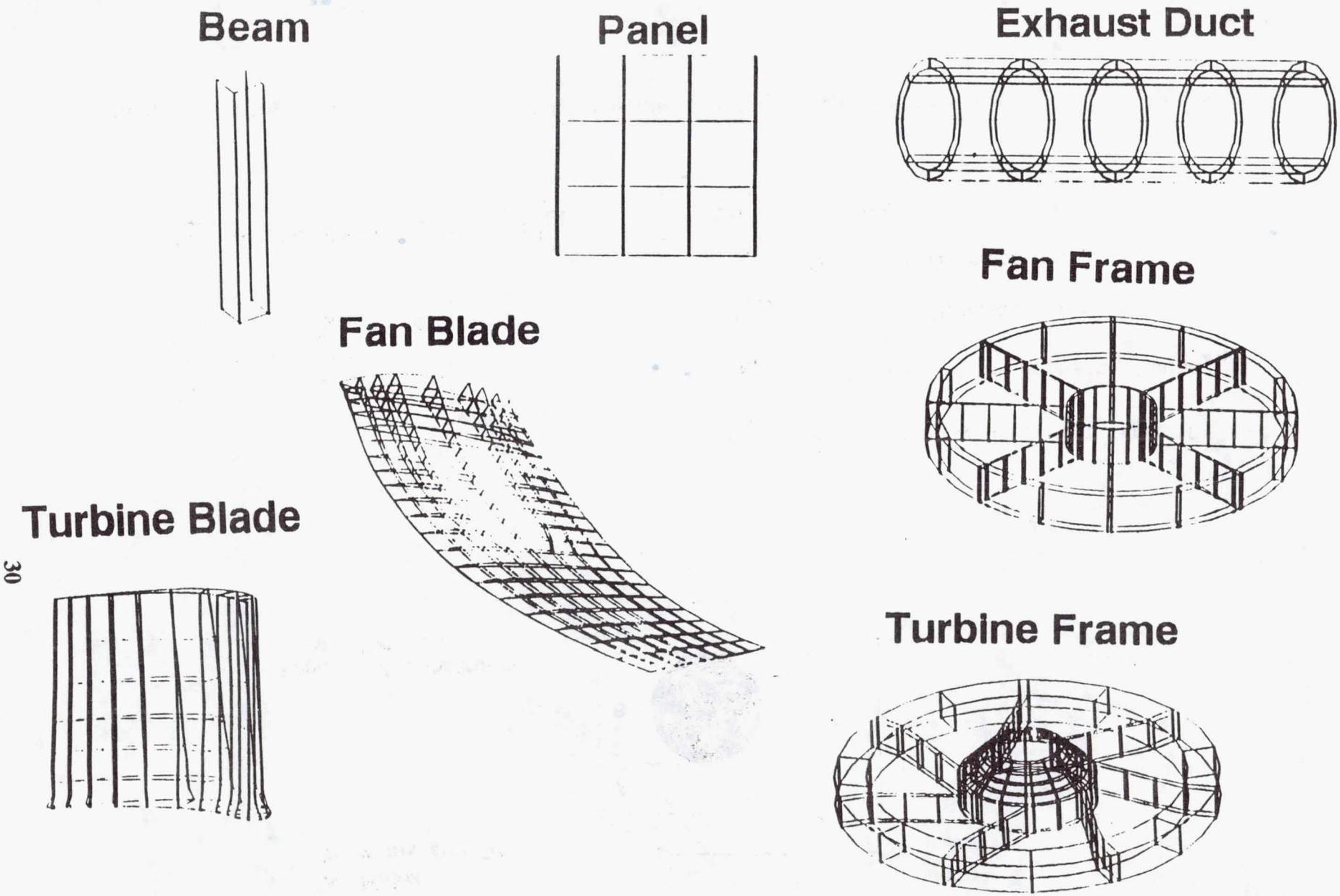




Figure 7: Geometry of Contractor-Supplied Sample Cases

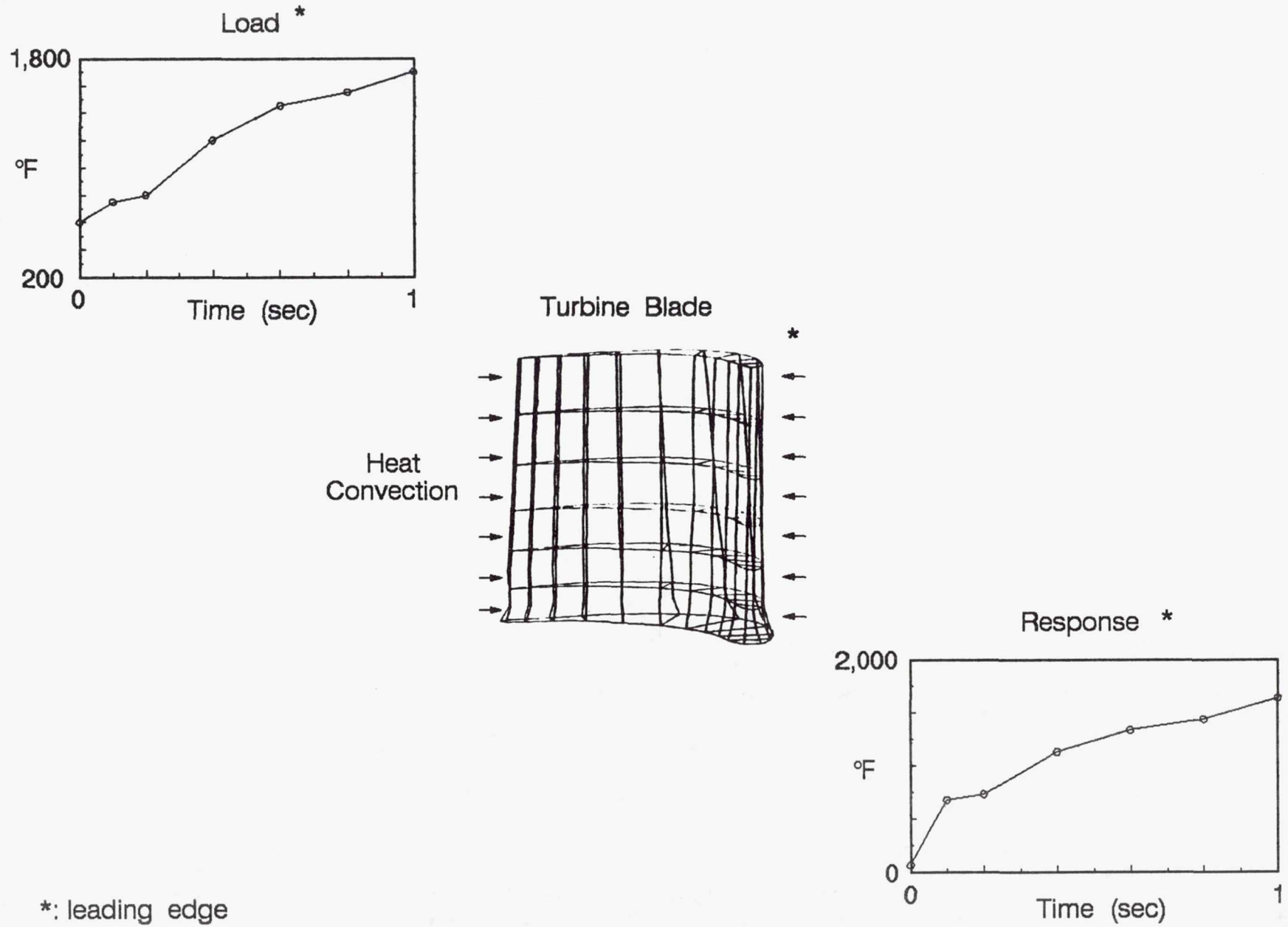


Figure 8: Transient Thermal Response of Turbine Blade

First Vibration Mode of Turbine Frame

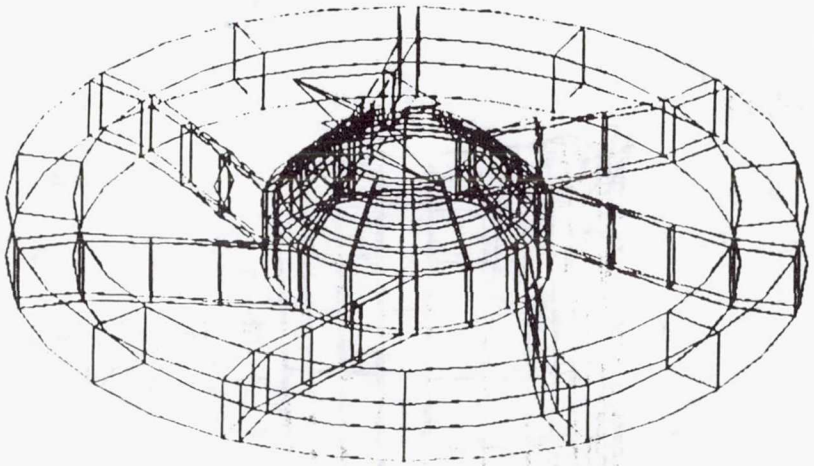

Frequency = 45.49 cps

Figure 9: Vibration of Composite Turbine Frame

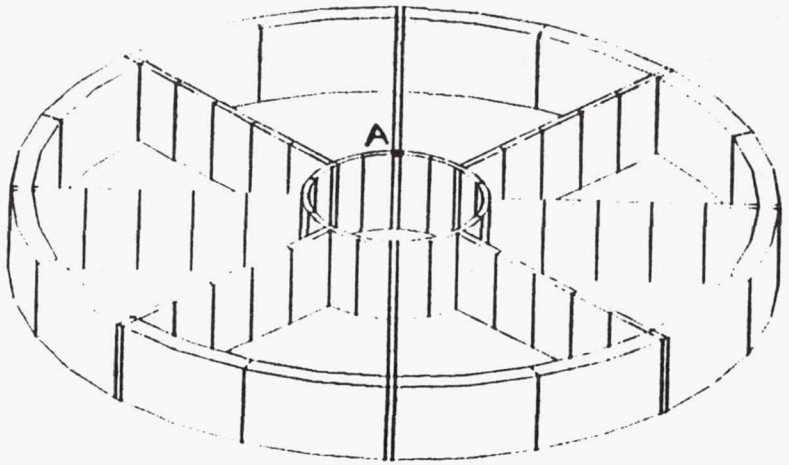


Acoustic Loading at Point A
10,000 lb (thickness direction)
Forcing Function (F) vs. Frequency ($\omega$)

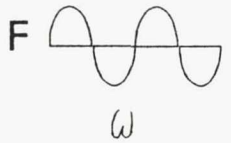


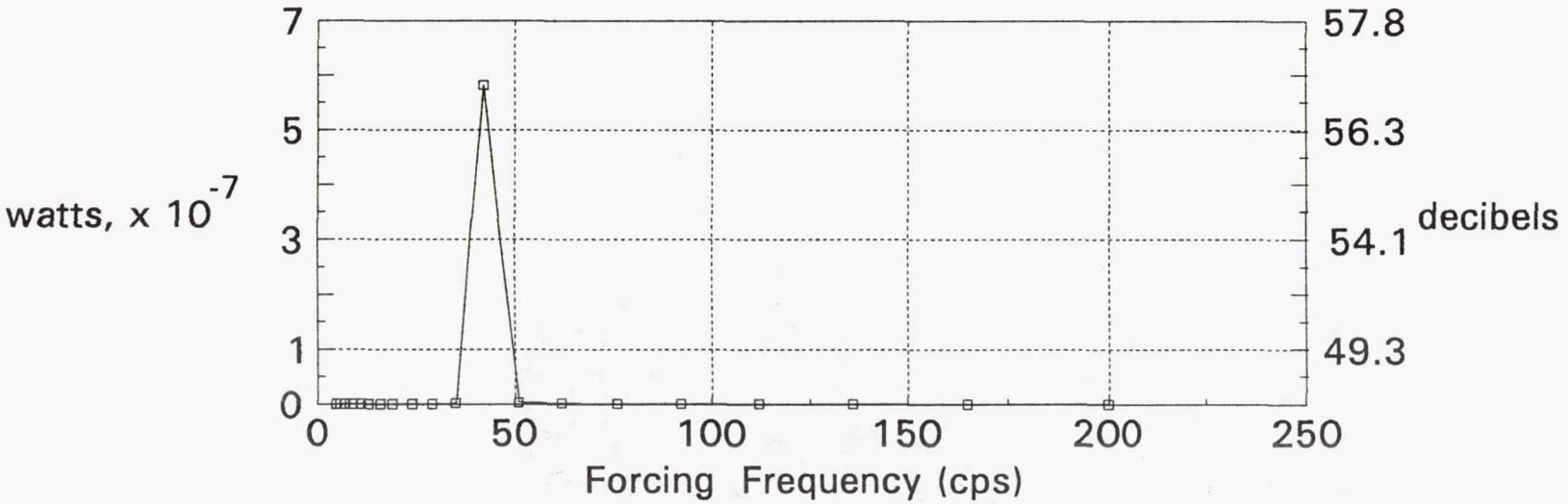


modal loss factor = $1 \times 10^{-5}$

Figure 10: Acoustic Noise from Composite Fan Frame

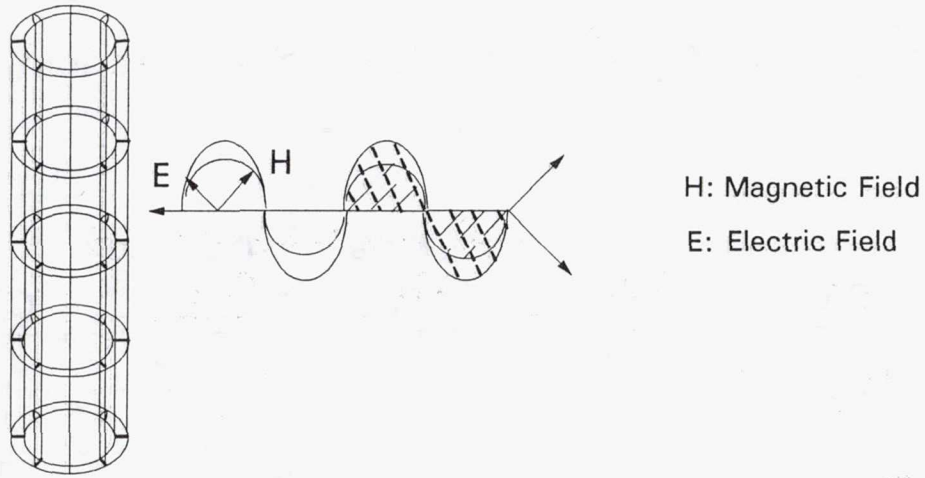


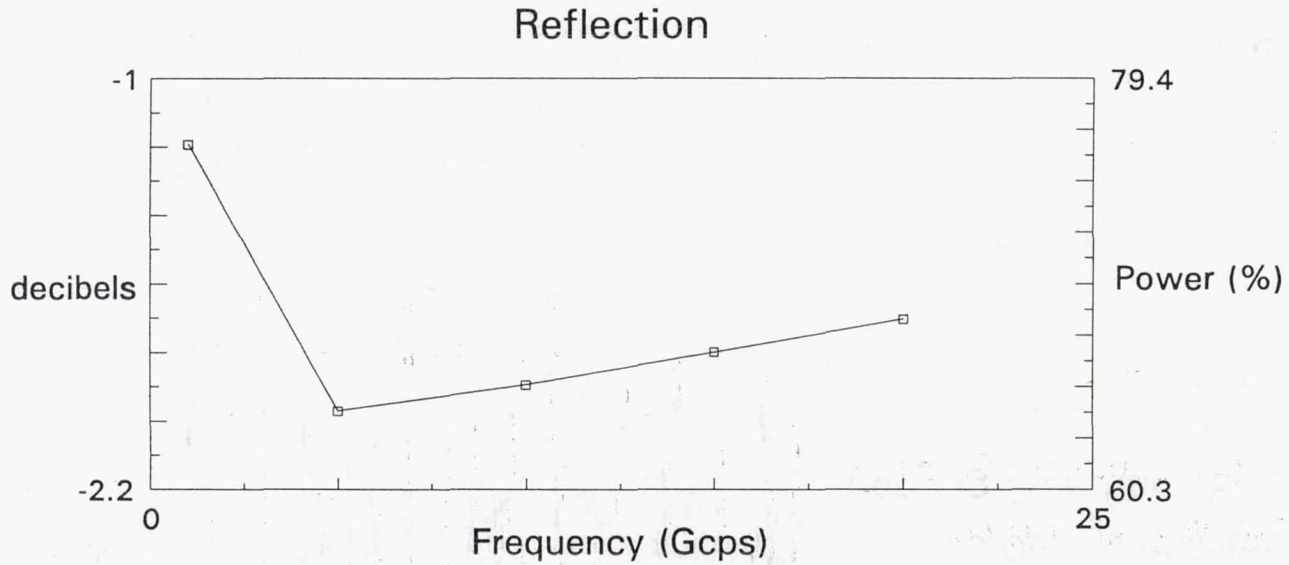


Figure 11: Electromagnetic Reflection from Composite Exhaust Duct

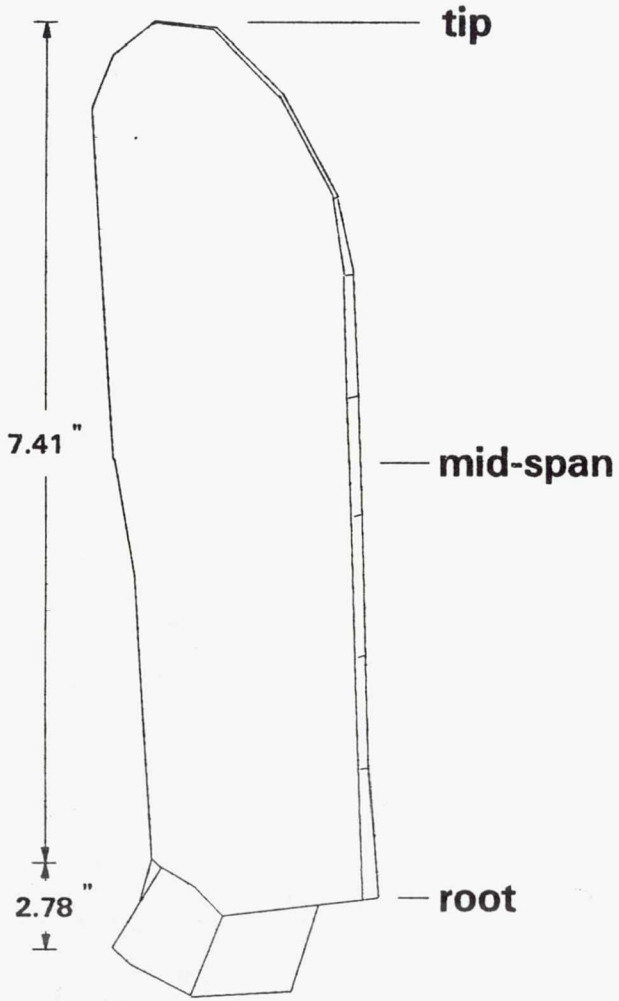


| Region | Dimension | | | |
|---|---|---|---|---|
| | Chord (inches) | Twist (deg. w.r.t. root) | Thickness (inches) | |
| | | | @ leading edge | @ trailing edge |
| tip | 1.22 | 39.8 | 0.01 | 0.007 |
| mid-span | 3.64 | 21.5 | 0.07 | 0.04 |
| root | 0.67 | 0.0 | 0.1 | 0.08 |

Figure 12: Geometry of the Fan Blade

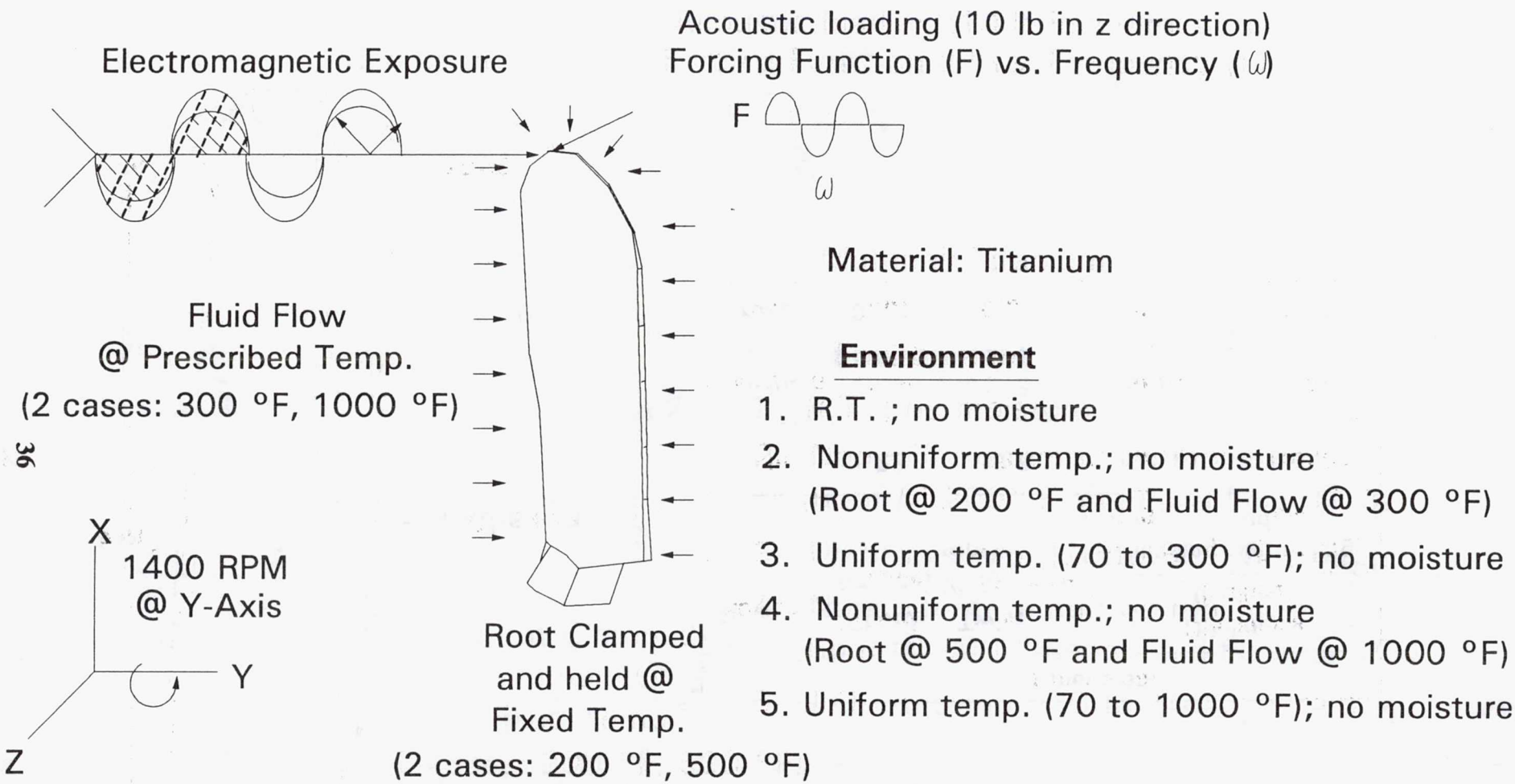




Figure 13: Thermal/Mechanical/Acoustic/Electromagnetic Loading for Metal Fan Blade

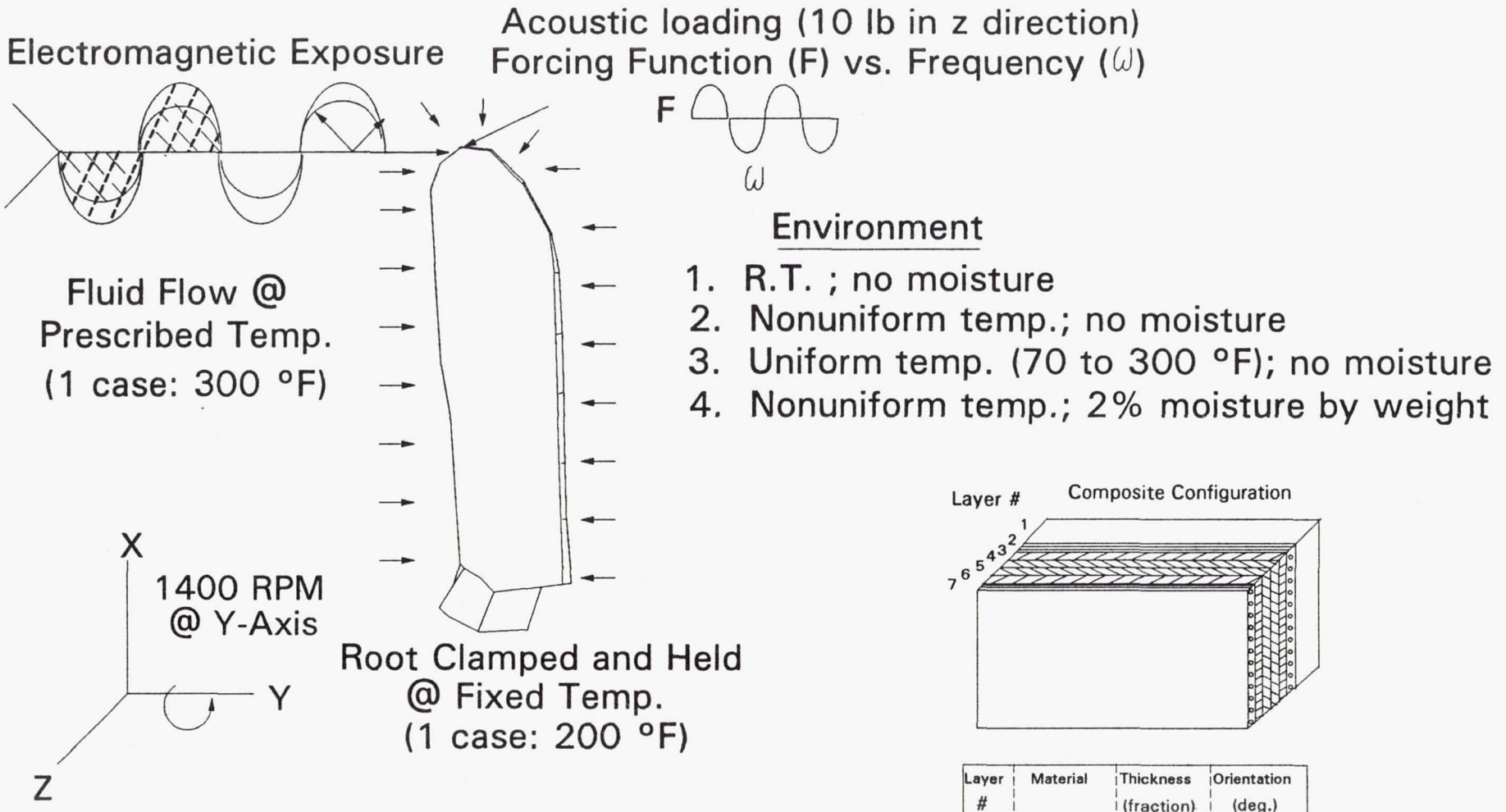


## Environment

1. R.T. ; no moisture
2. Nonuniform temp.; no moisture
3. Uniform temp. (70 to 300 °F); no moisture
4. Nonuniform temp.; 2% moisture by weight




| Layer # | Material | Thickness (fraction) | Orientation (deg.) |
|---|---|---|---|
| 1 | Titanium | 0.4 | — |
| 2 | T300/IMHS | 0.1 | 0 |
| 3 | T300/IMHS | 0.1 | 30 |
| 4 | T300/IMHS | 0.1 | -30 |
| 5 | T300/IMHS | 0.1 | -30 |
| 6 | T300/IMHS | 0.1 | 30 |
| 7 | T300/IMHS | 0.1 | 0 |

Material: 40% Titanium and 60% $(0/30\text{-}30)_S$

0.6 FVR T300/IMHS Composite

Figure 14: Thermal/Mechanical/Acoustic/Electromagnetic Loading for Multi-layered, Multi-material Composite Fan Blade

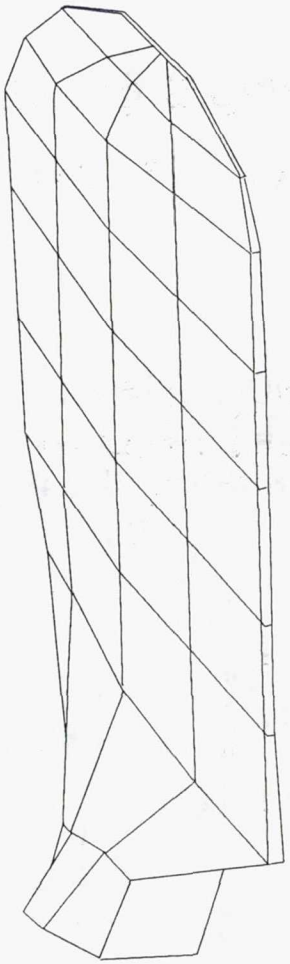

Fourty 20-noded (8 corner and 12 mid-sided)
Brick Elements and 110 nodes

Figure 15: Finite Element Model of Fan Blade

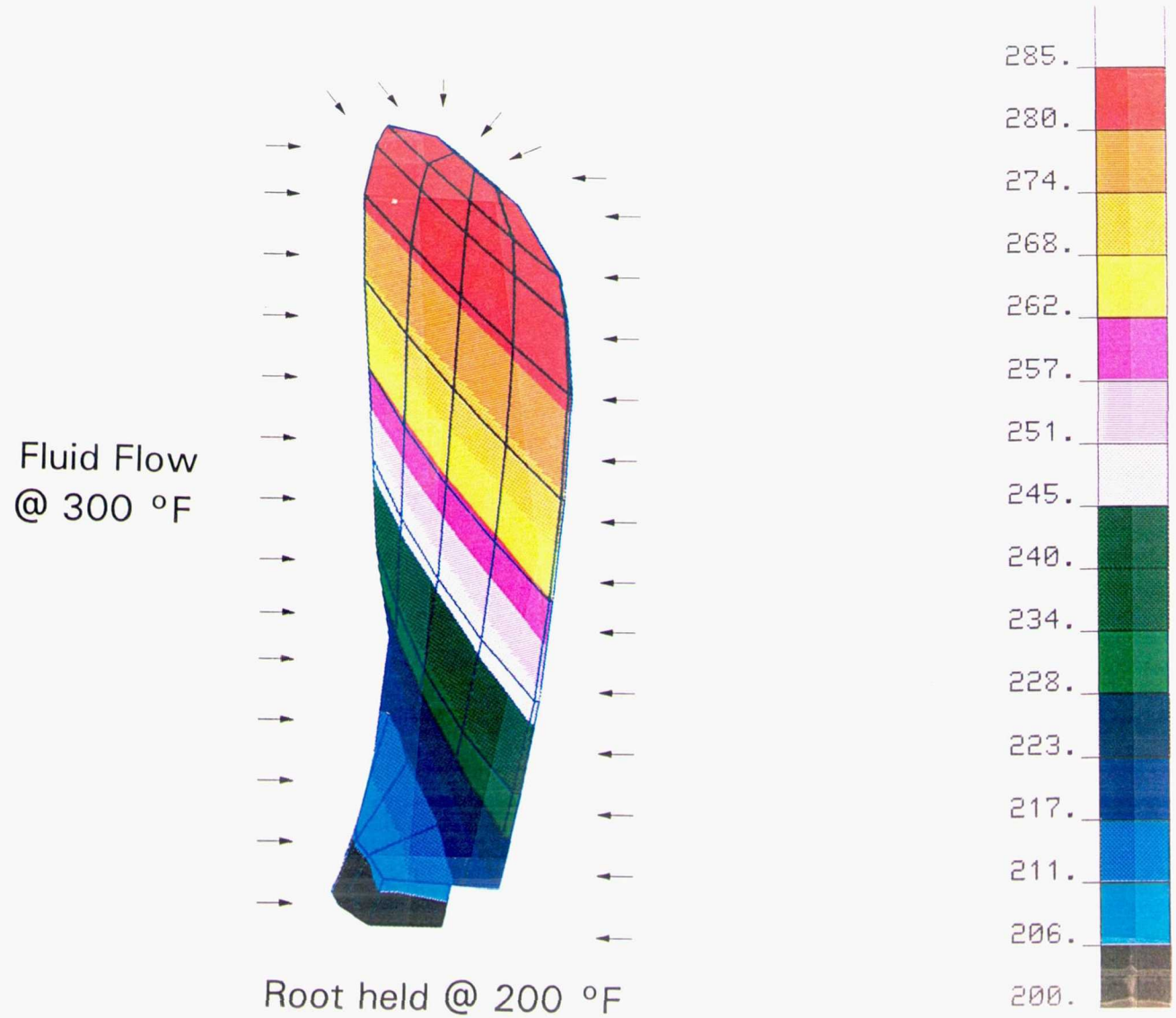


**Figure 16: Steady State-Nonlinear Thermal Response of Metal Fan Blade @ 300 °F**

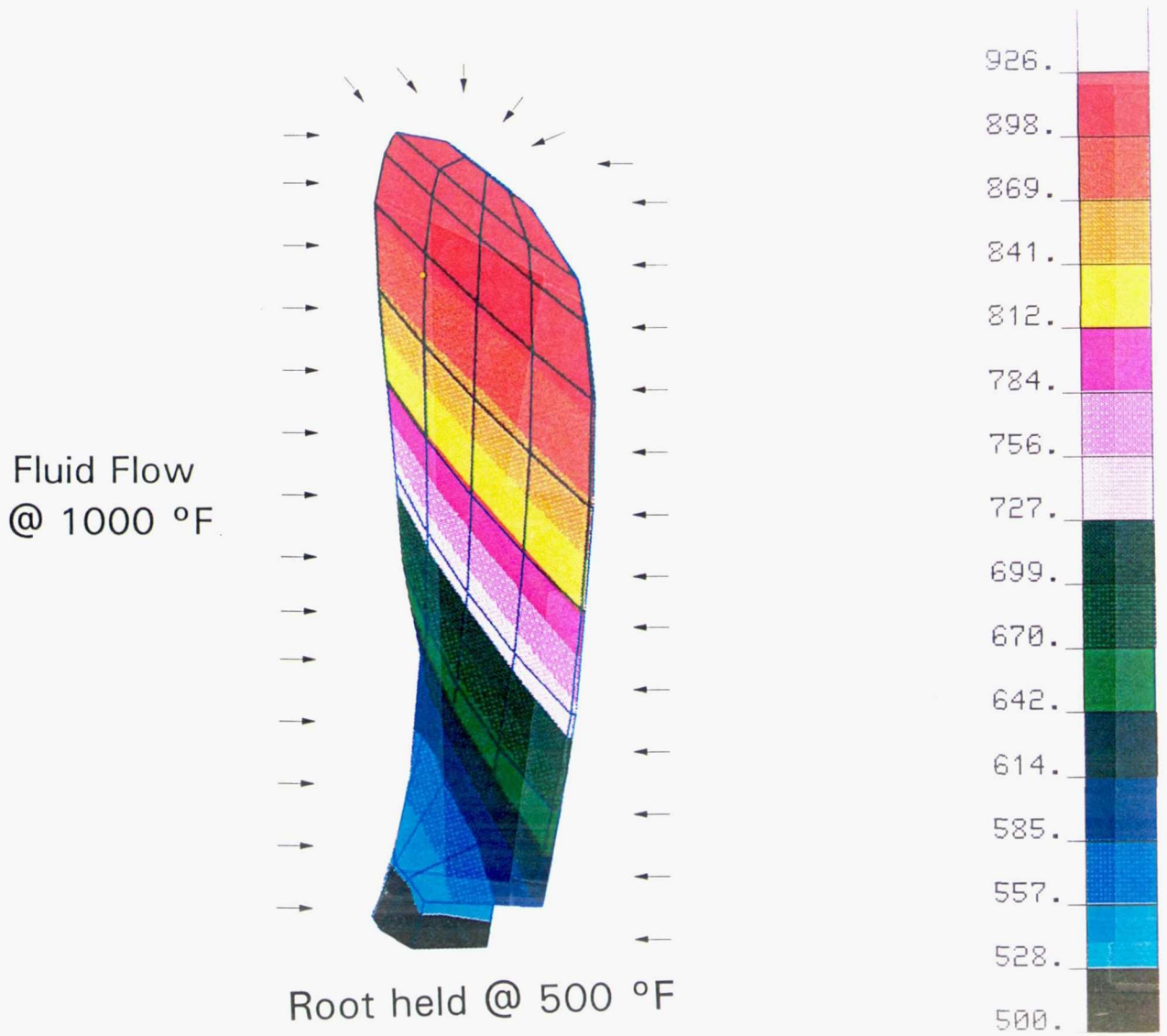


Figure 17: Steady State-Nonlinear Thermal Response of Metal Fan Blade @ 1000 °F

Temperature (°F) Contours via Coupled Composite-Mechanics/Heat-Transfer Analysis

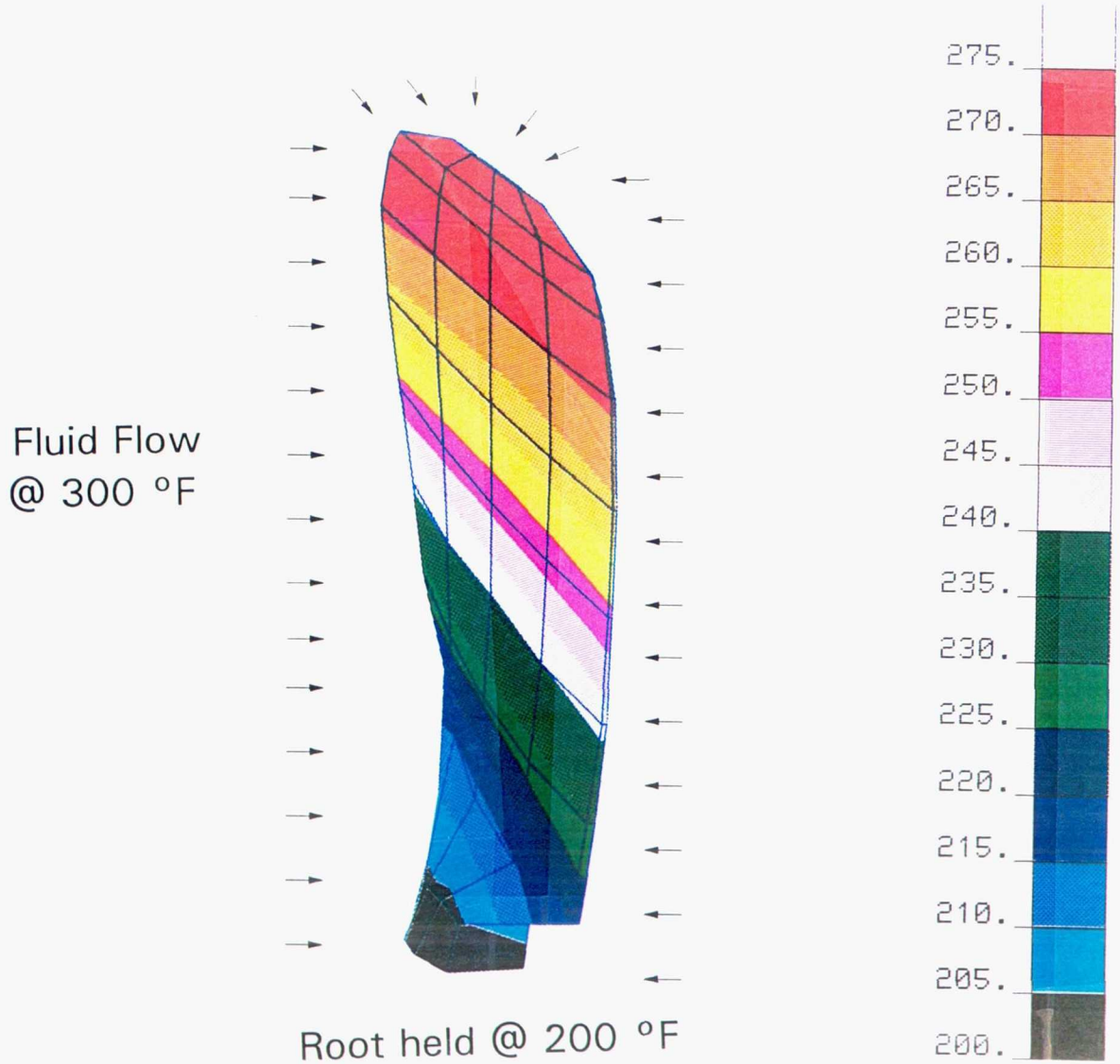


Figure 18: Steady State-Nonlinear Thermal Response of Composite Fan Blade @ 300 °F Fluid Flow

Temperature Distribution via Coupled Composite-Mechanics/Heat-Transfer Analysis
Effect of Material: Metal vs. Composite

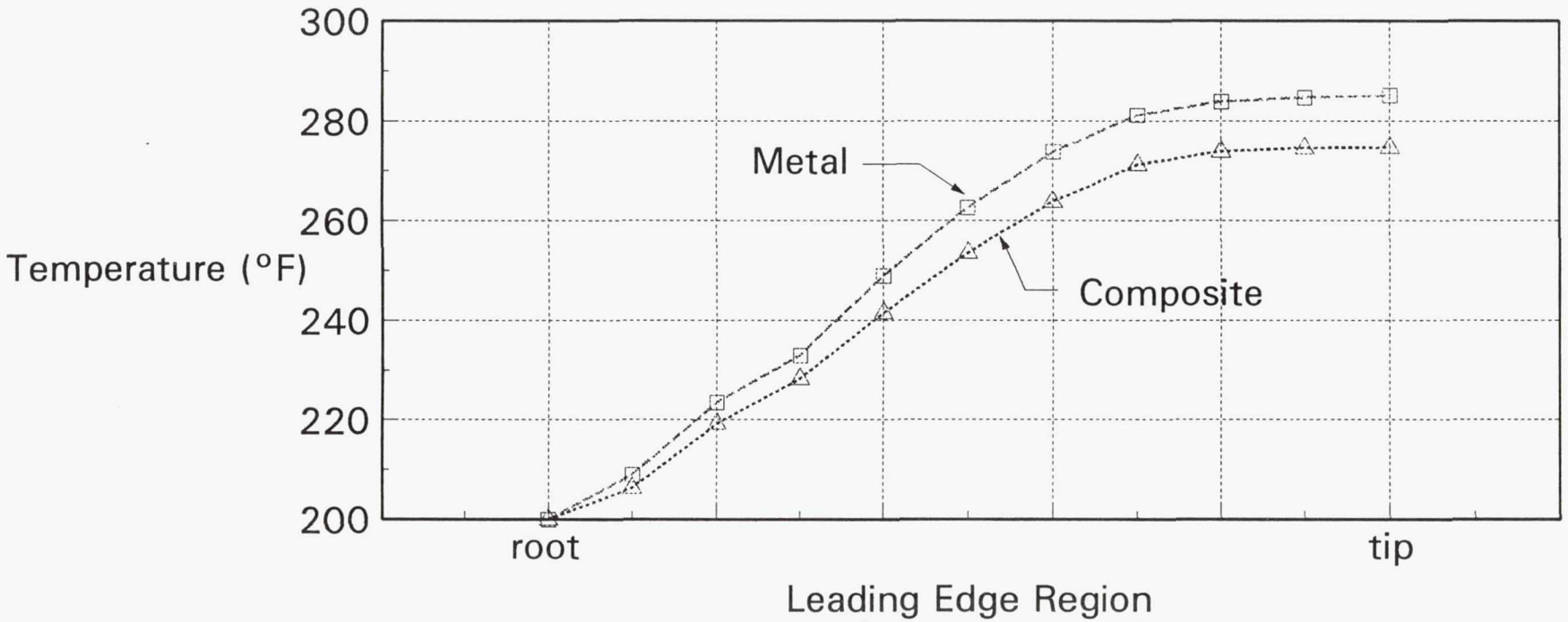


Figure 19: Steady State-Nonlinear Thermal Response of Fan Blade @ 300 °F Fluid Flow

Deformed Shape via Coupled Heat-Transfer/Structural Analysis

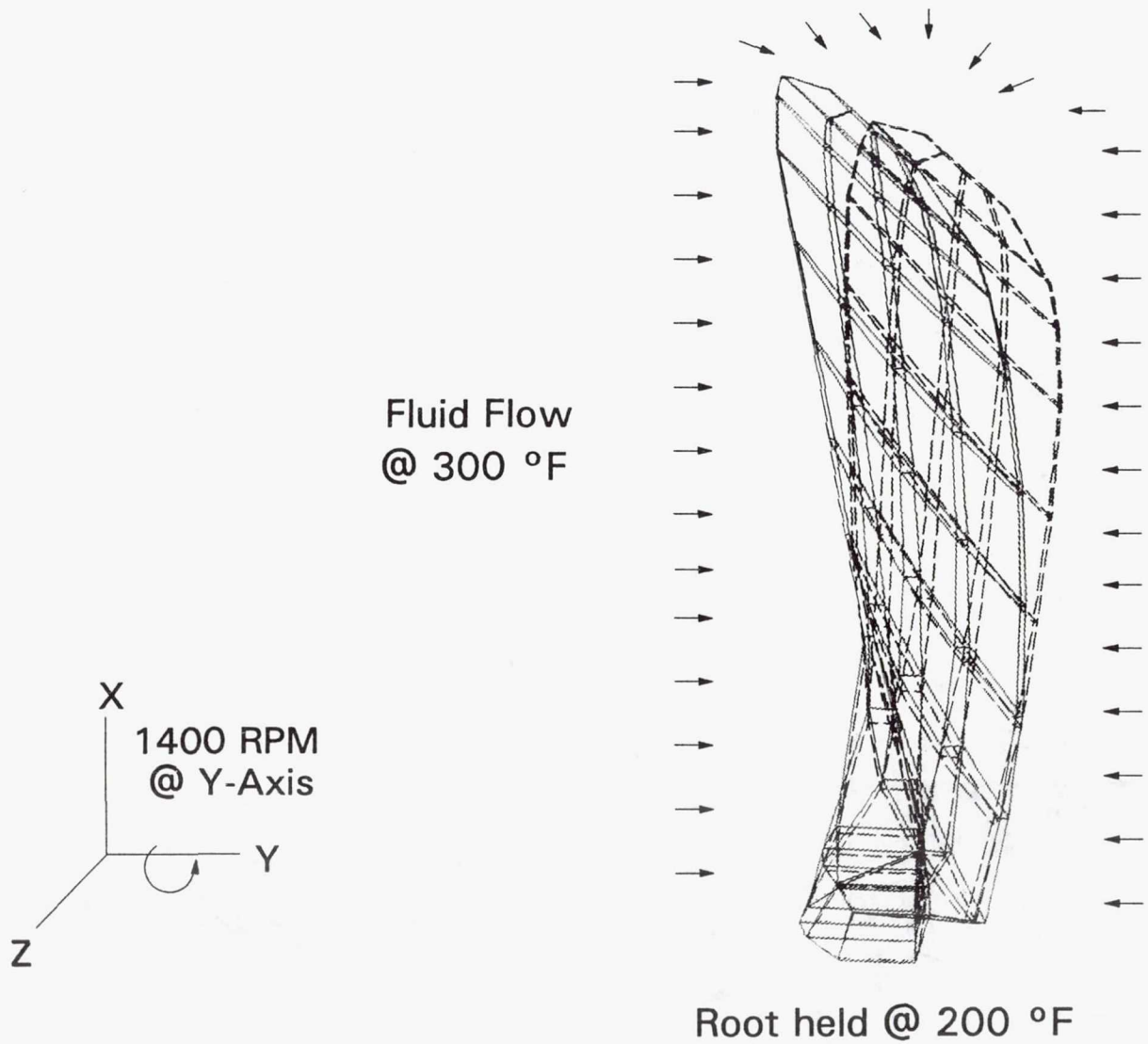


Figure 20: Structural Response of Metal Fan Blade @ 300 °F Fluid Flow

Deformed Shape via Coupled Heat-Transfer/Structural Analysis

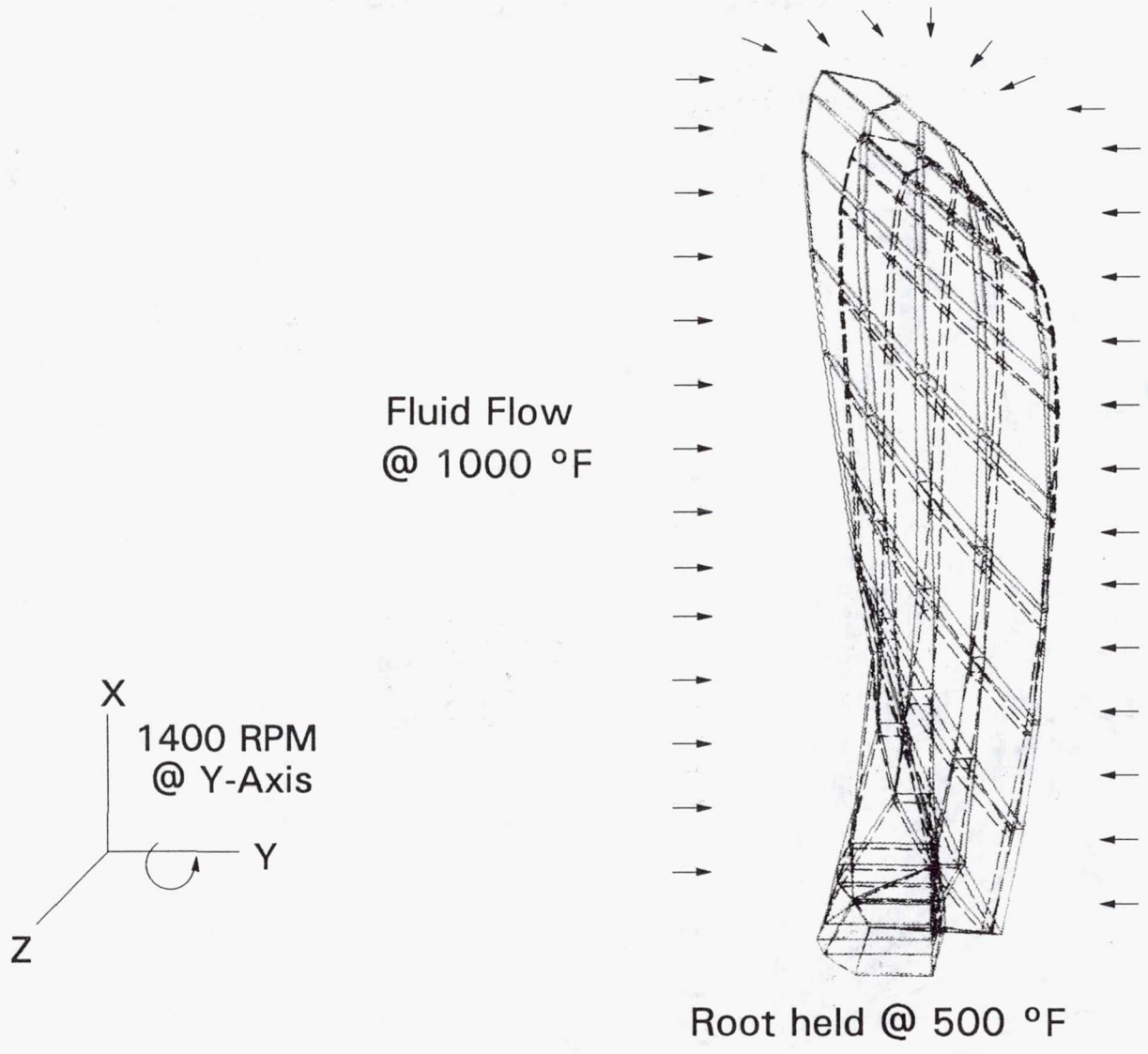


Figure 21: Structural Response of Metal Fan Blade @ 1000 °F Fluid Flow

Deformed Shape via Coupled Heat-Transfer/Structural Analysis

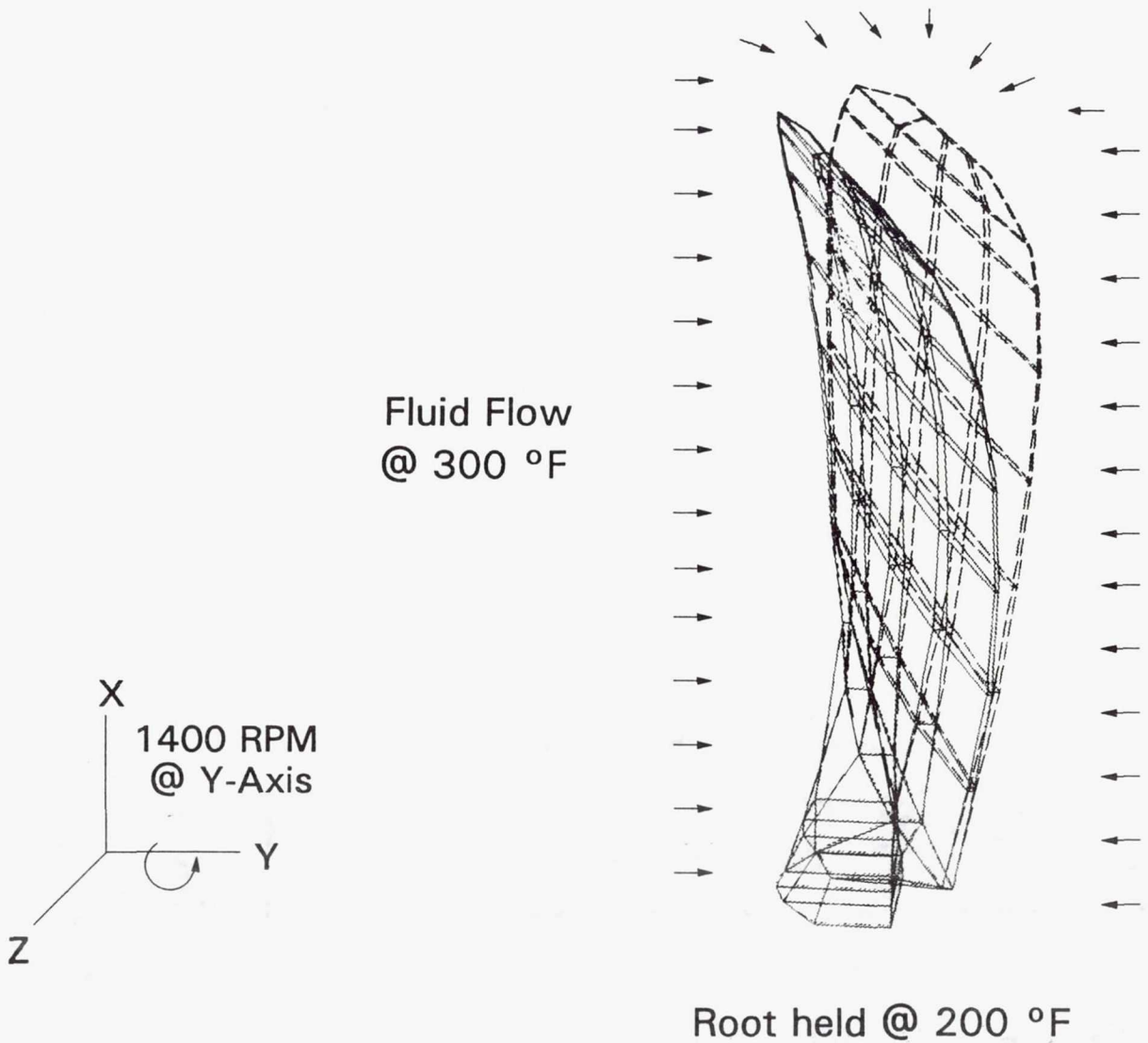


Figure 22: Structural Response of Composite Fan Blade @ 300 °F Fluid Flow

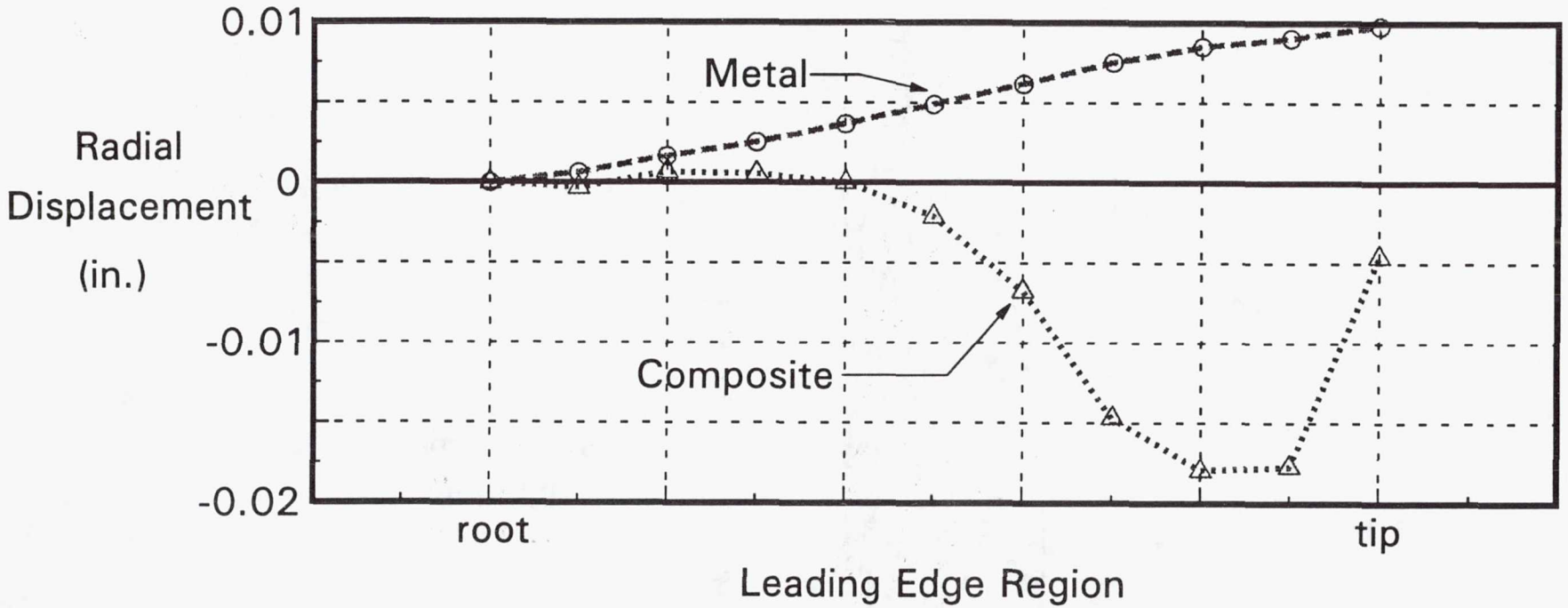


Figure 23: Structural Response of Fan Blade @ 300 °F Fluid Flow: Radial Displacement

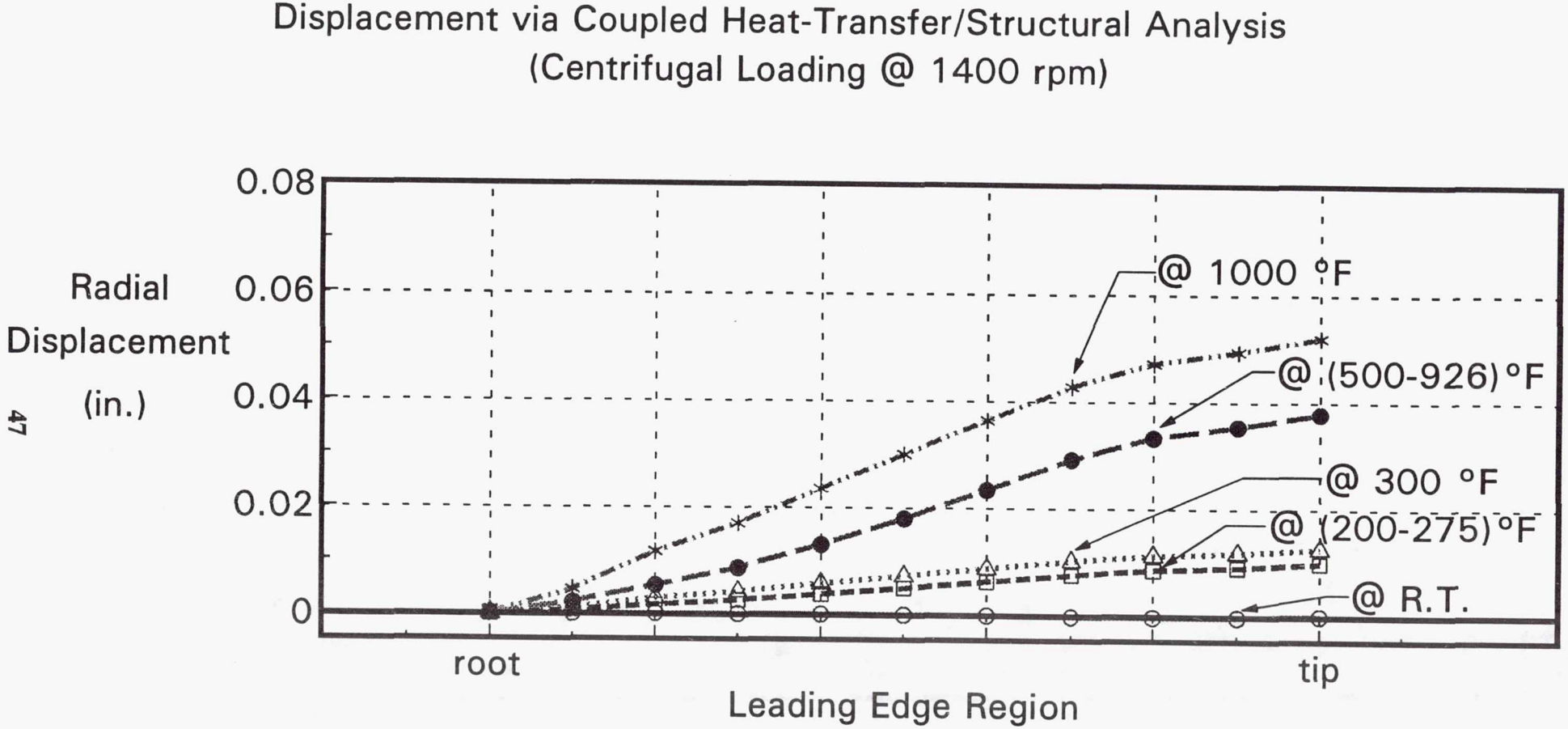


Figure 24: Structural Response of Metal Fan Blade - Displacement vs. Environment

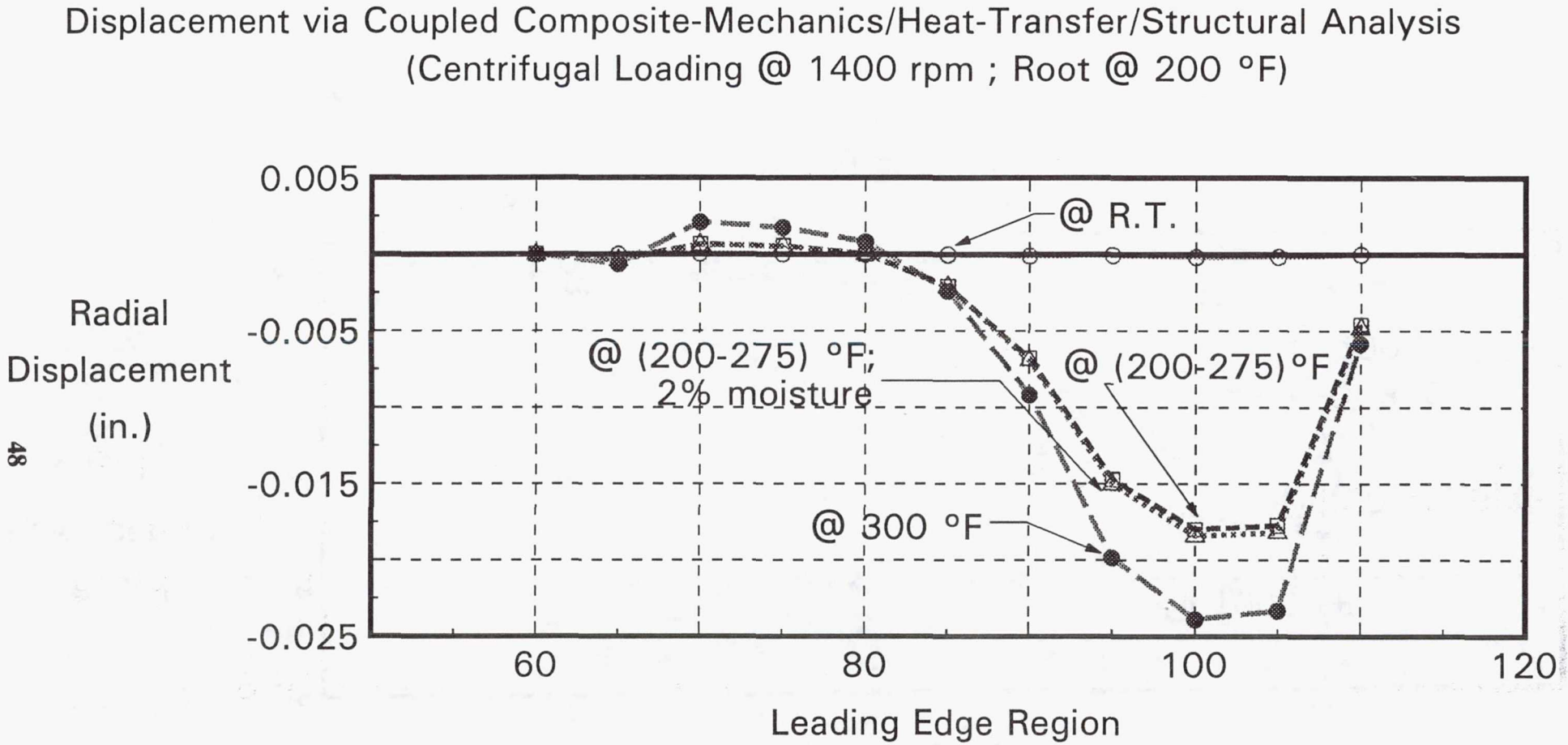


Figure 25: Structural Response of Composite Fan Blade - Displacement vs. Environment

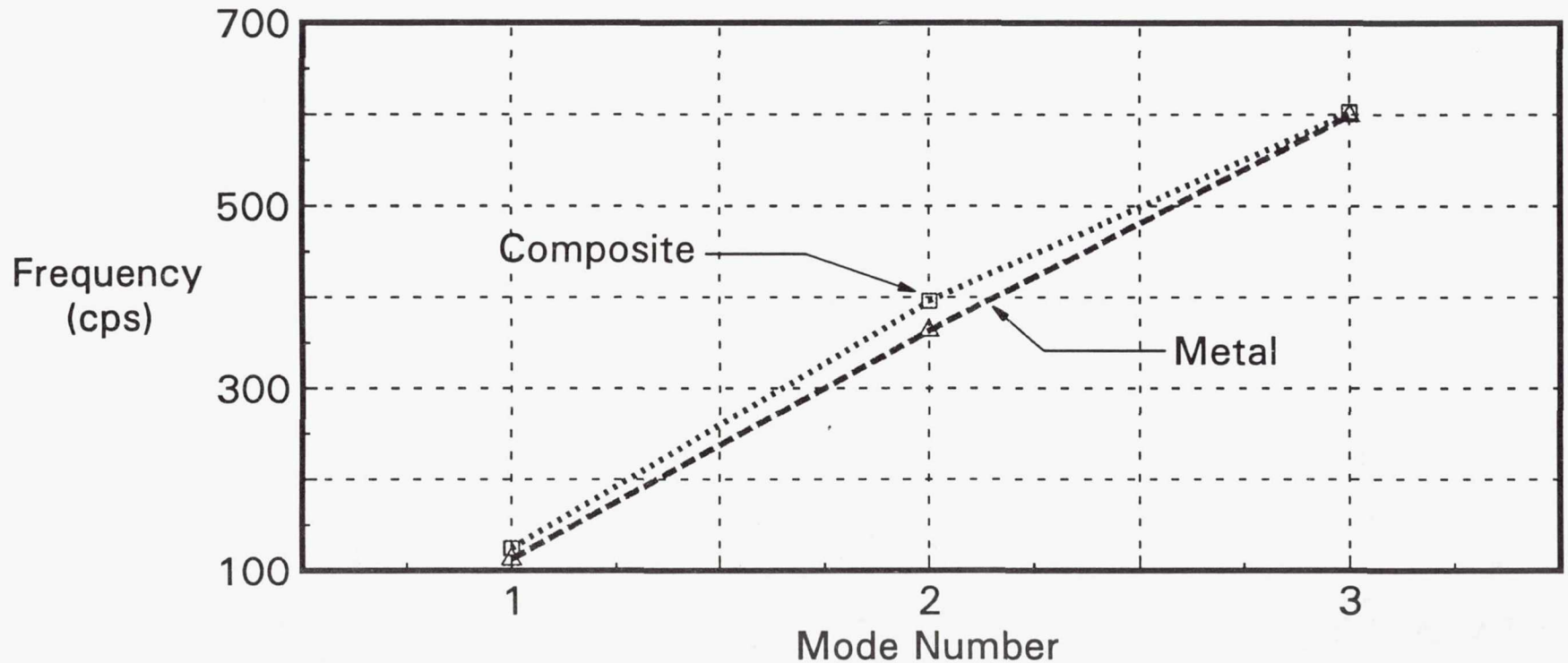


Figure 26: Vibration Response of Fan Blade - Frequencies

Vibration Modes via Coupled Heat-Transfer/Vibration Analysis
(Root @ 200 °F; Fluid Flow @ 300 °F)

**First Mode**

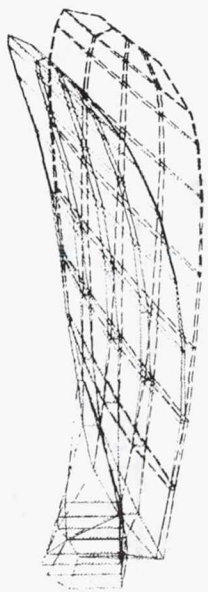

112.35 cps

**Second Mode**

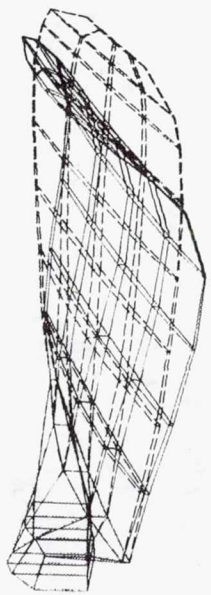

363.20 cps

**Third Mode**

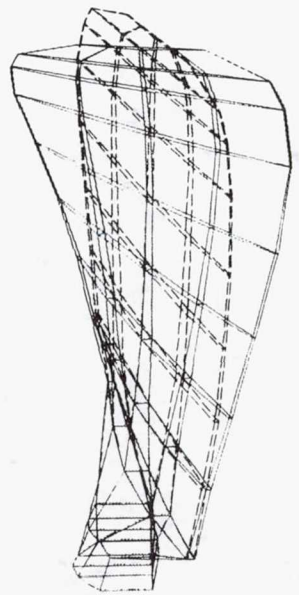

598.58 cps

Figure 27: Vibration Response of Metal Fan Blade - Mode Shapes

Vibration Modes via Coupled Composite-Mechanics Heat-Transfer/Vibration Analysis
(Root @ 200 °F; Fluid Flow @ 300 °F)

**First Mode**

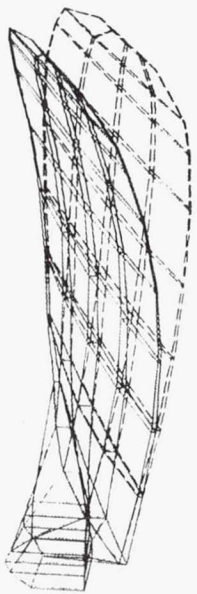

124.52 cps

**Second Mode**

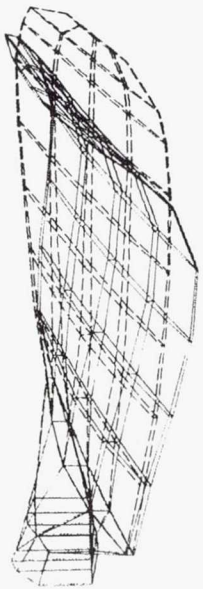

395.98 cps

**Third Mode**

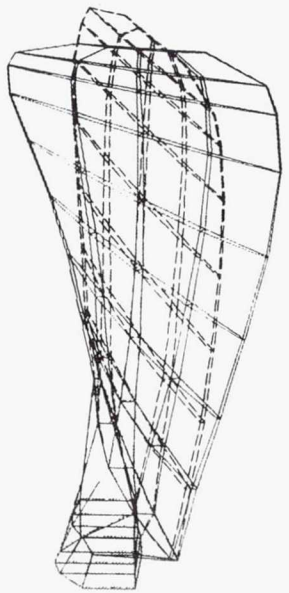

602.65 cps

Figure 28: Vibration Response of Composite Fan Blade - Mode Shapes

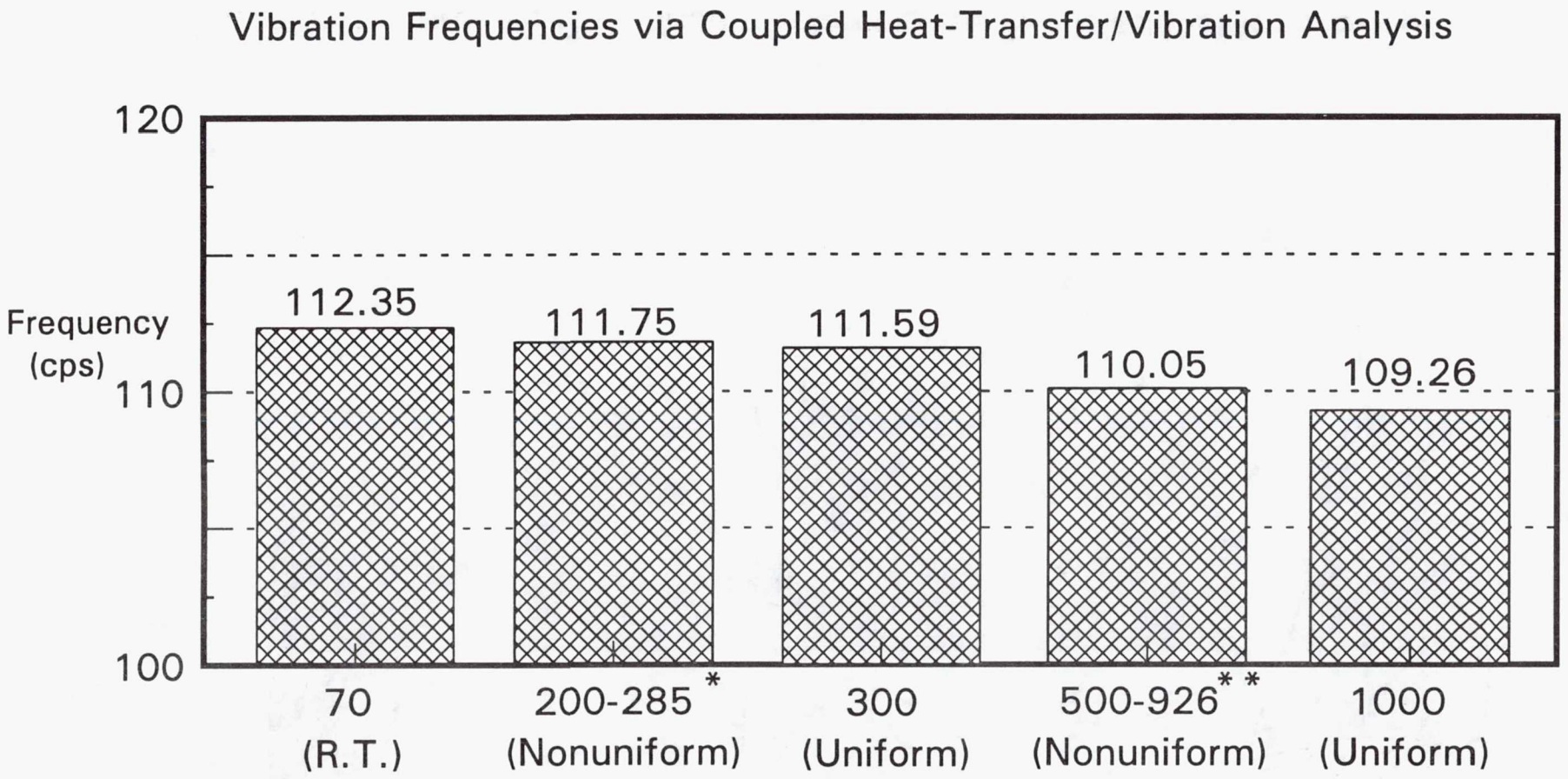


*: Root @ 200 °F; Fluid Flow @ 300 °F

**: Root @ 500 °F; Fluid Flow @ 1000 °F

Figure 29: Vibration Response of Metal Fan Blade - Fundamental Frequency vs. Environment

Vibration Frequencies via Coupled Composite-Mechanics/Heat-Transfer/Structural/ Vibration Analysis

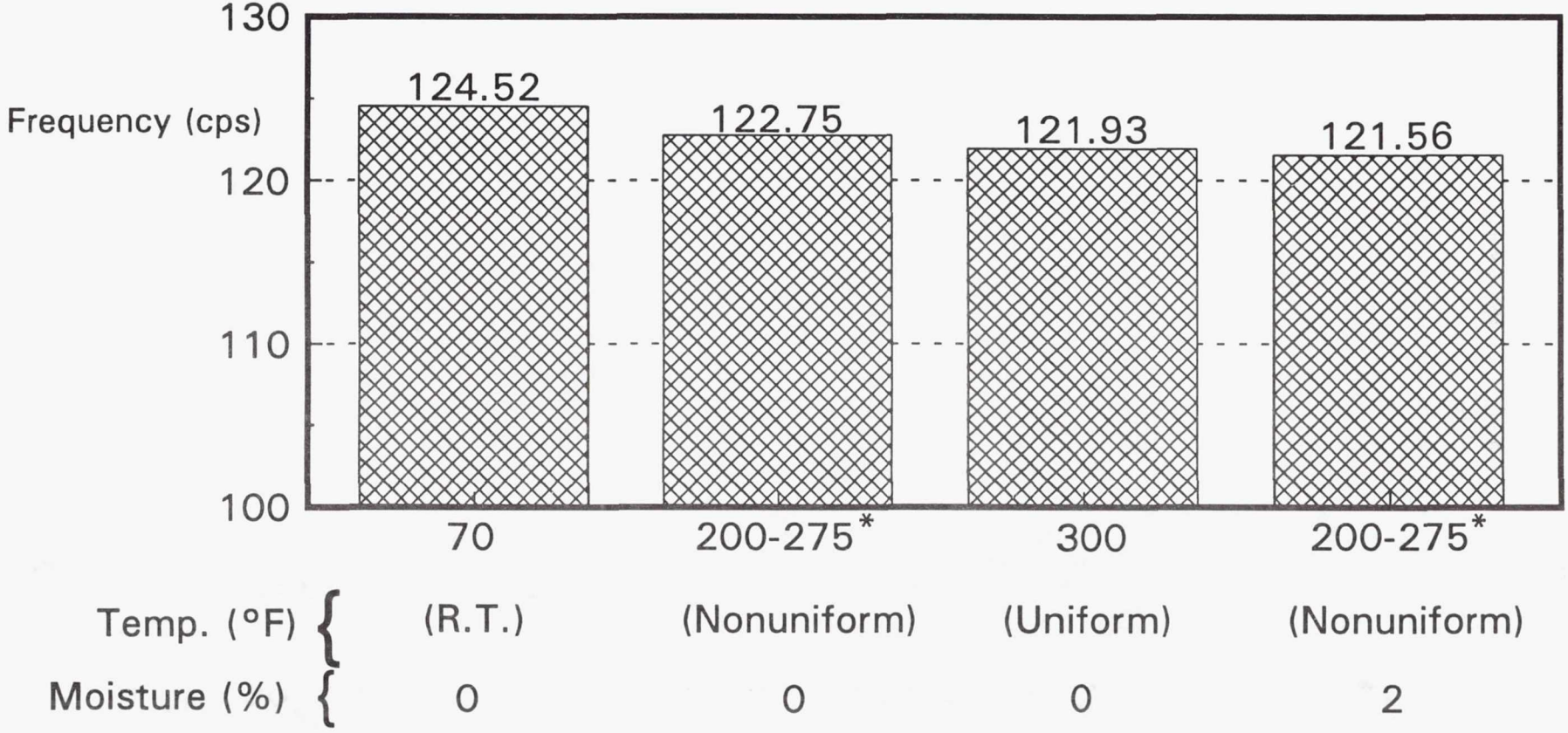


*: Root @ 200 °F; Fluid Flow @ 300 °F

Figure 30: Vibration Response of Composite Fan Blade - Fundamental Frequency vs. Environment

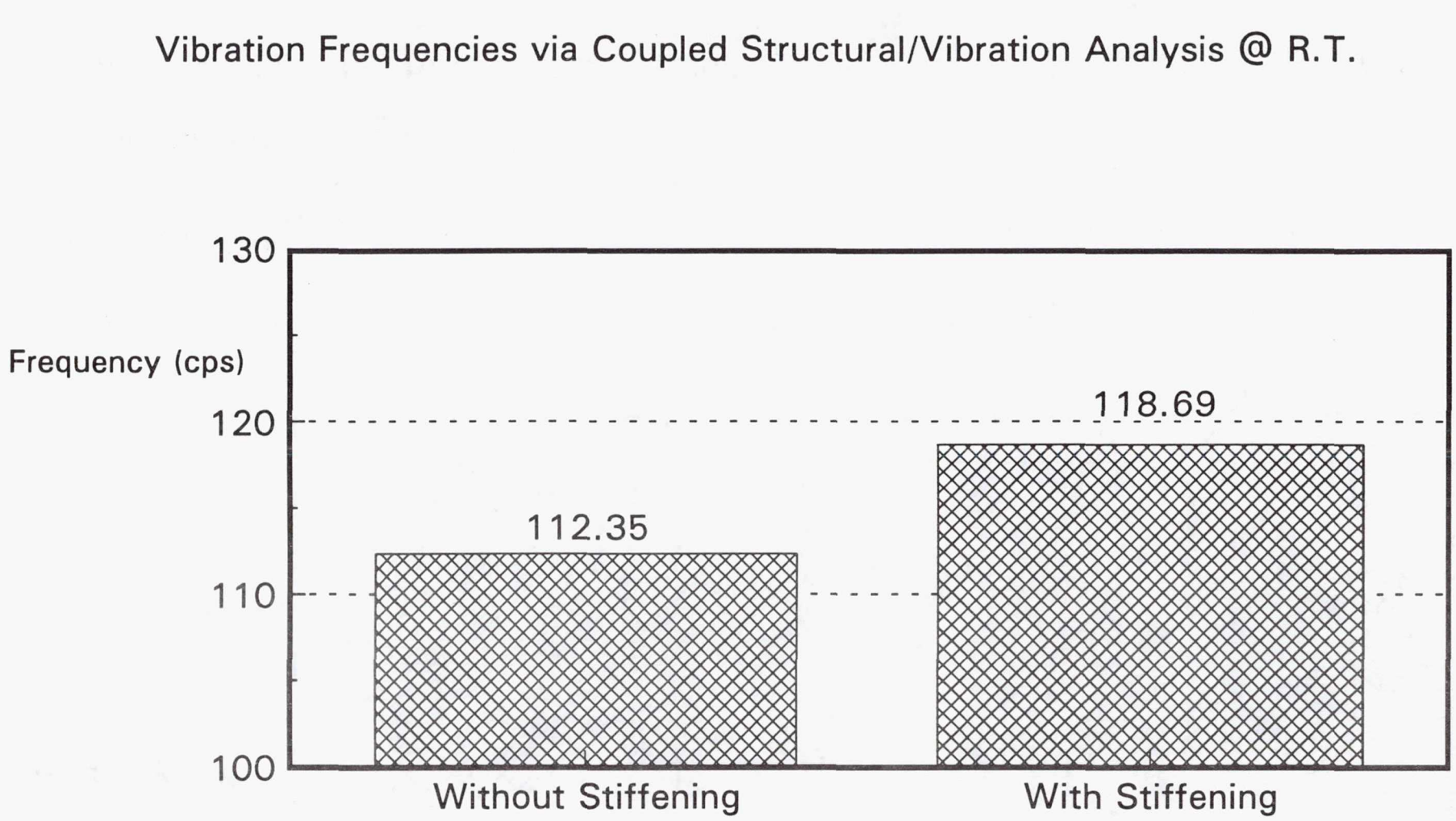


Figure 31: Vibration Response of Metal Fan Blade - Fundamental Frequency vs. Geometric Stiffening

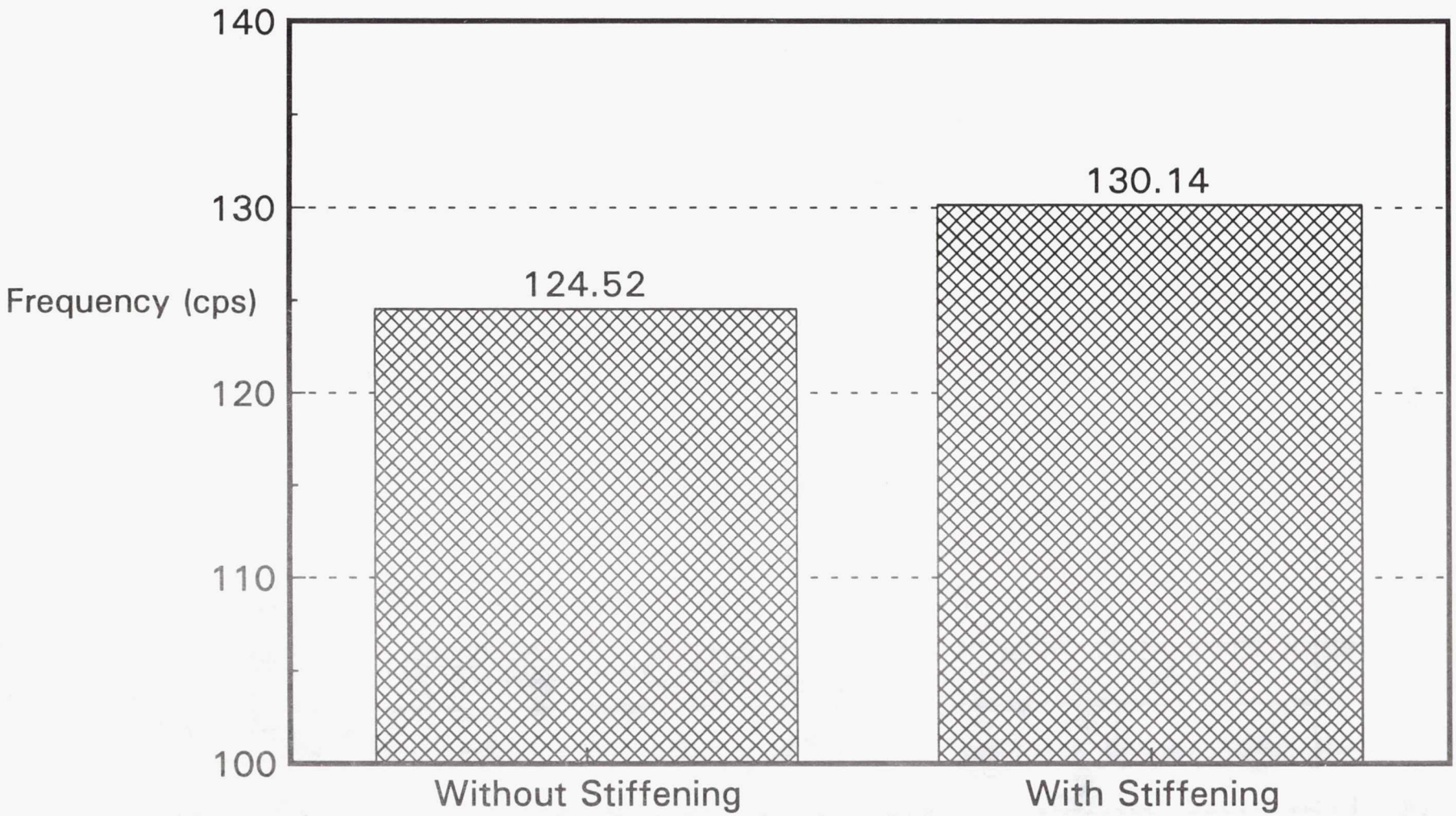


Figure 32: Vibration Response of Composite Fan Blade - Fundamental Frequency vs. Geometric Stiffening

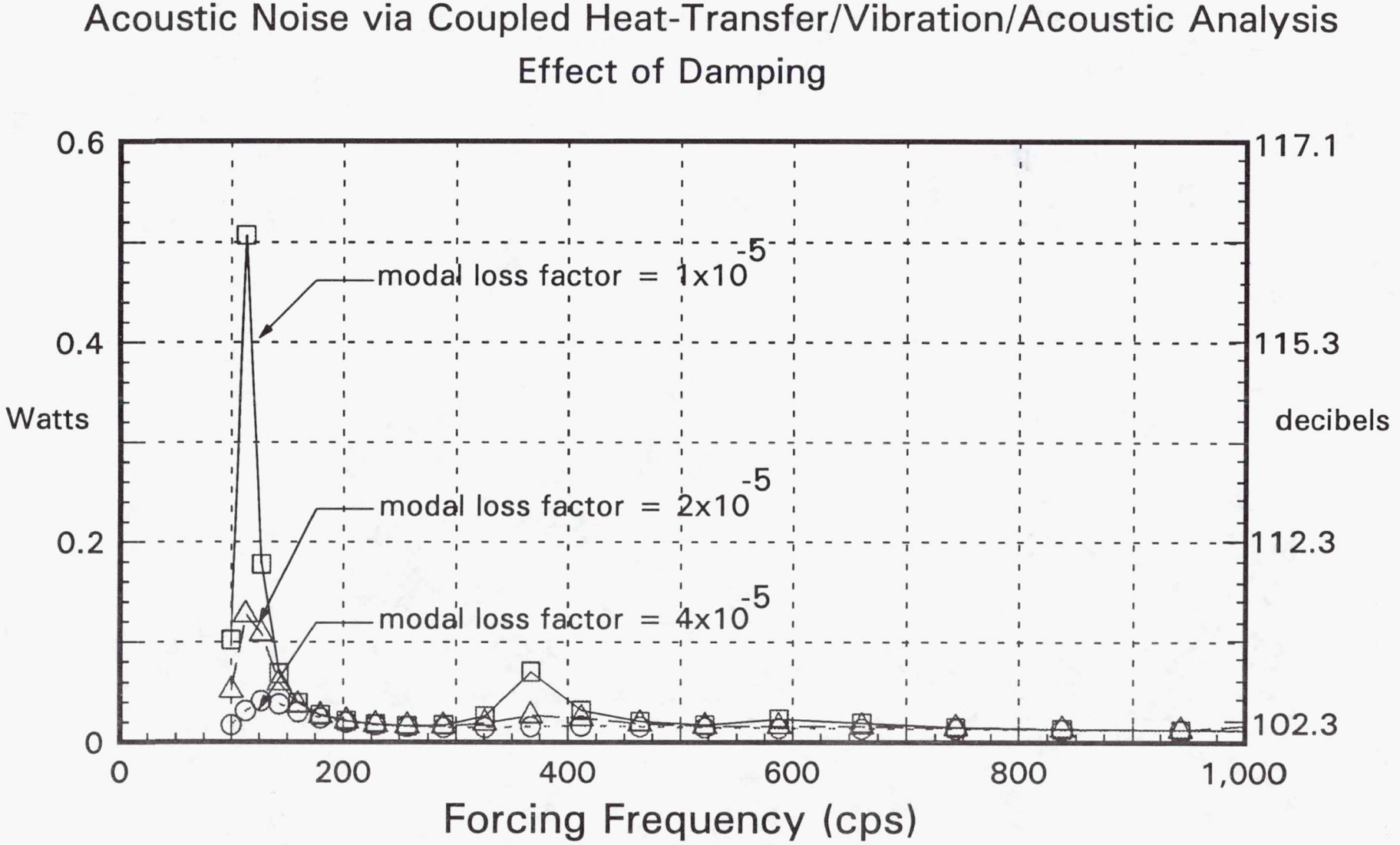


Figure 33: Acoustic Noise Emitted from Metal Fan Blade

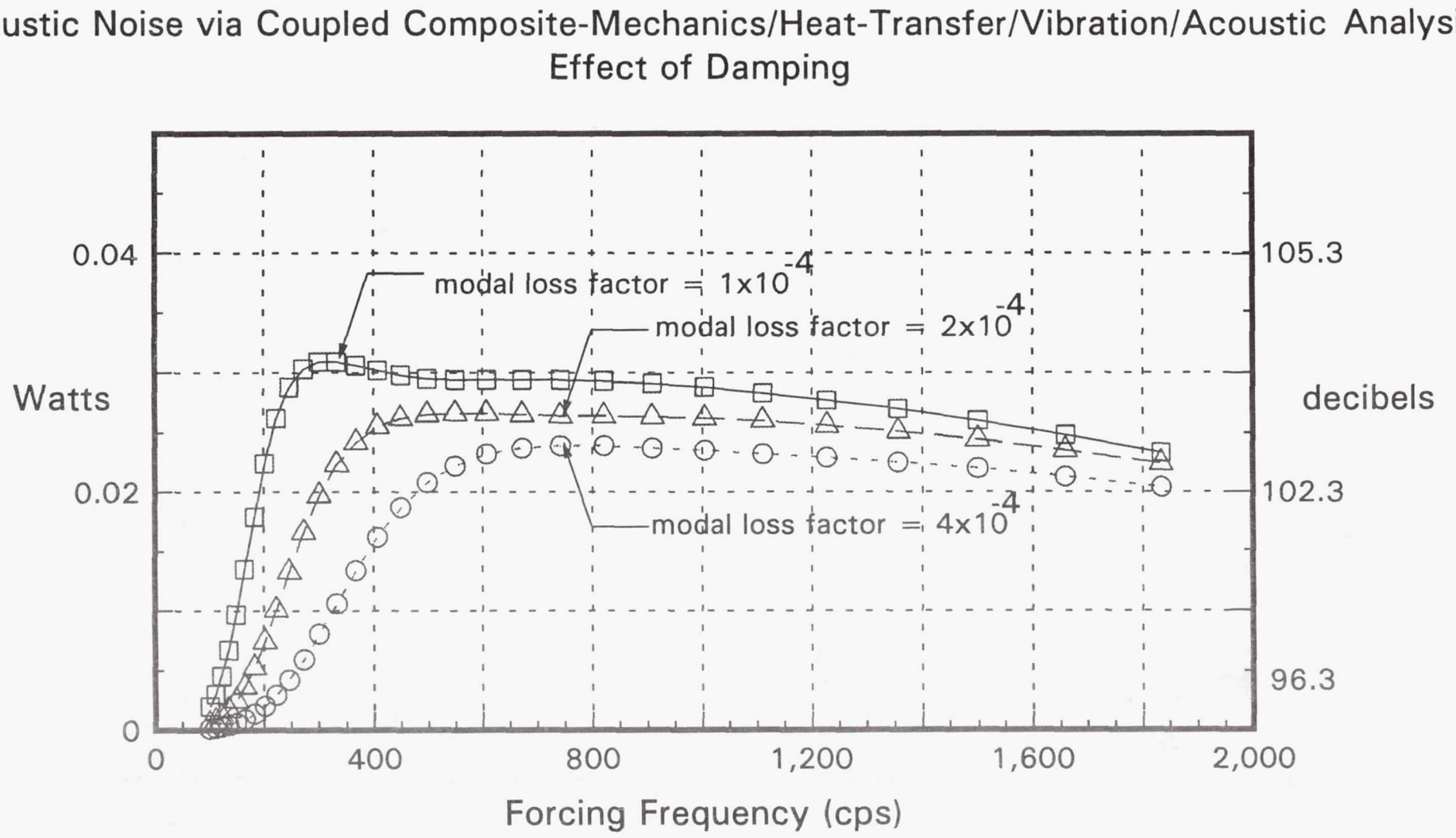


Figure 34: Acoustic Noise Emitted from Composite Fan Blade

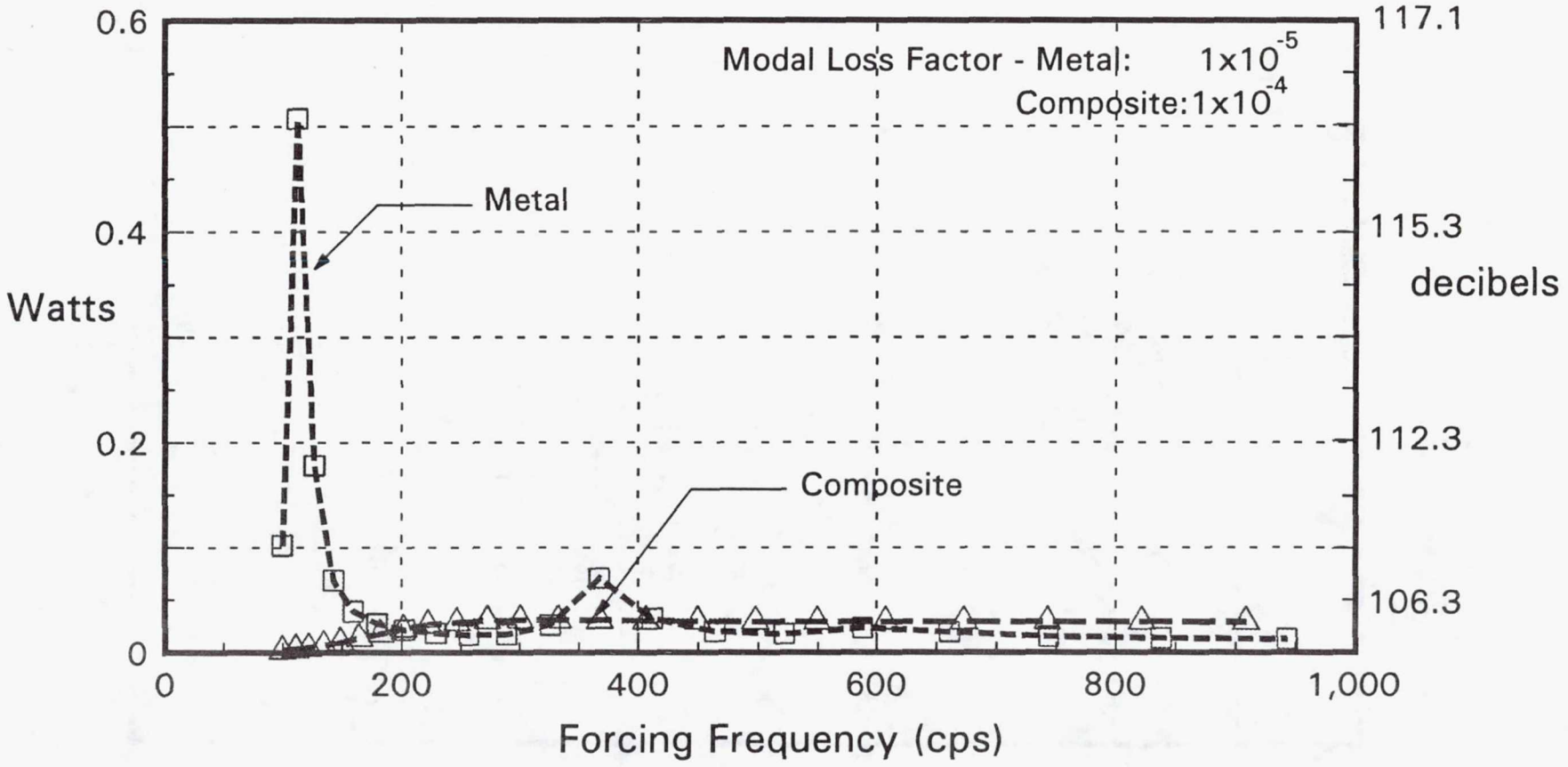


Figure 35: Acoustic Noise Emitted from Fan Blade

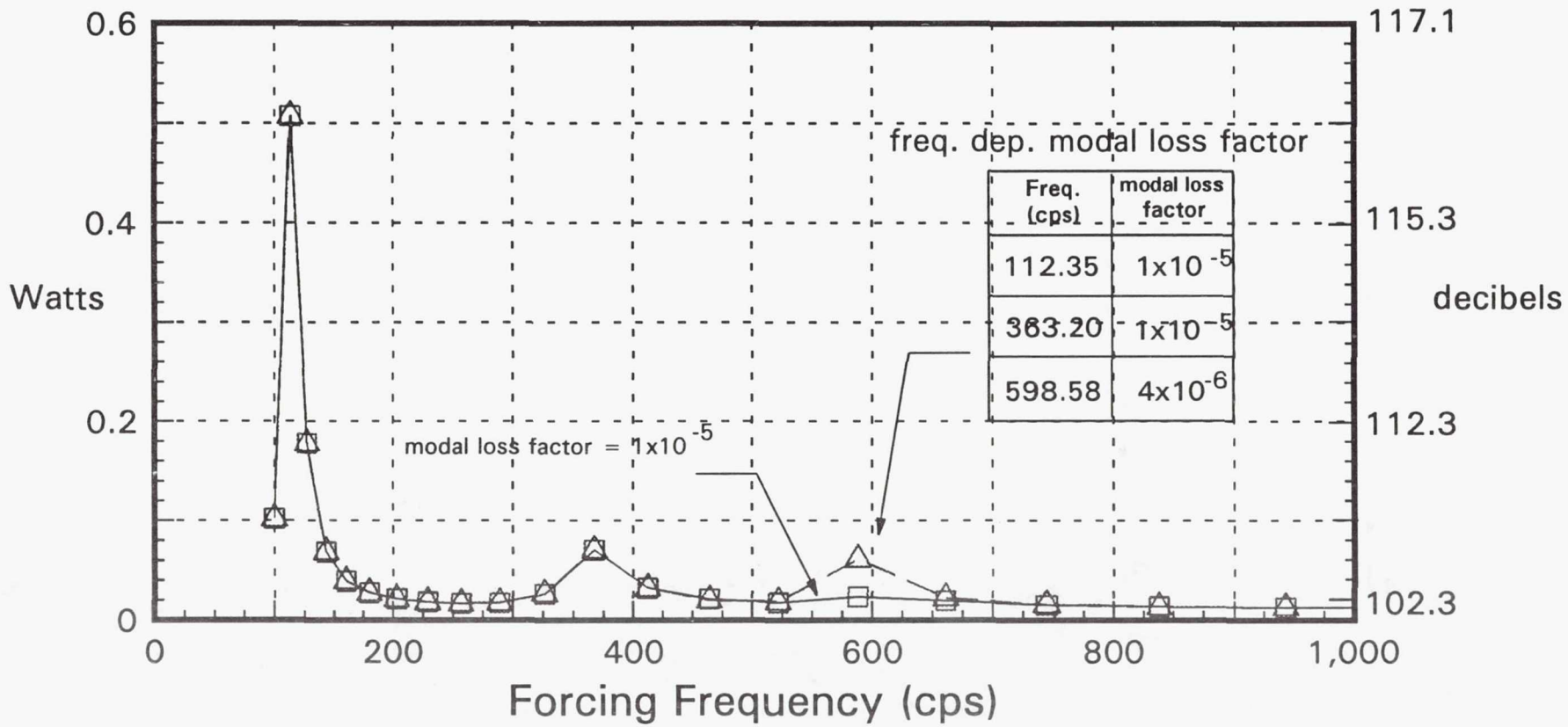


Figure 36: Acoustic Noise Emitted from Metal Fan Blade - Frequency Dependent Damping

Acoustic Noise via Coupled Composite-Mechanics/Heat-Transfer/Vibration/
Acoustic Analysis Effect of Frequency Dependent Damping

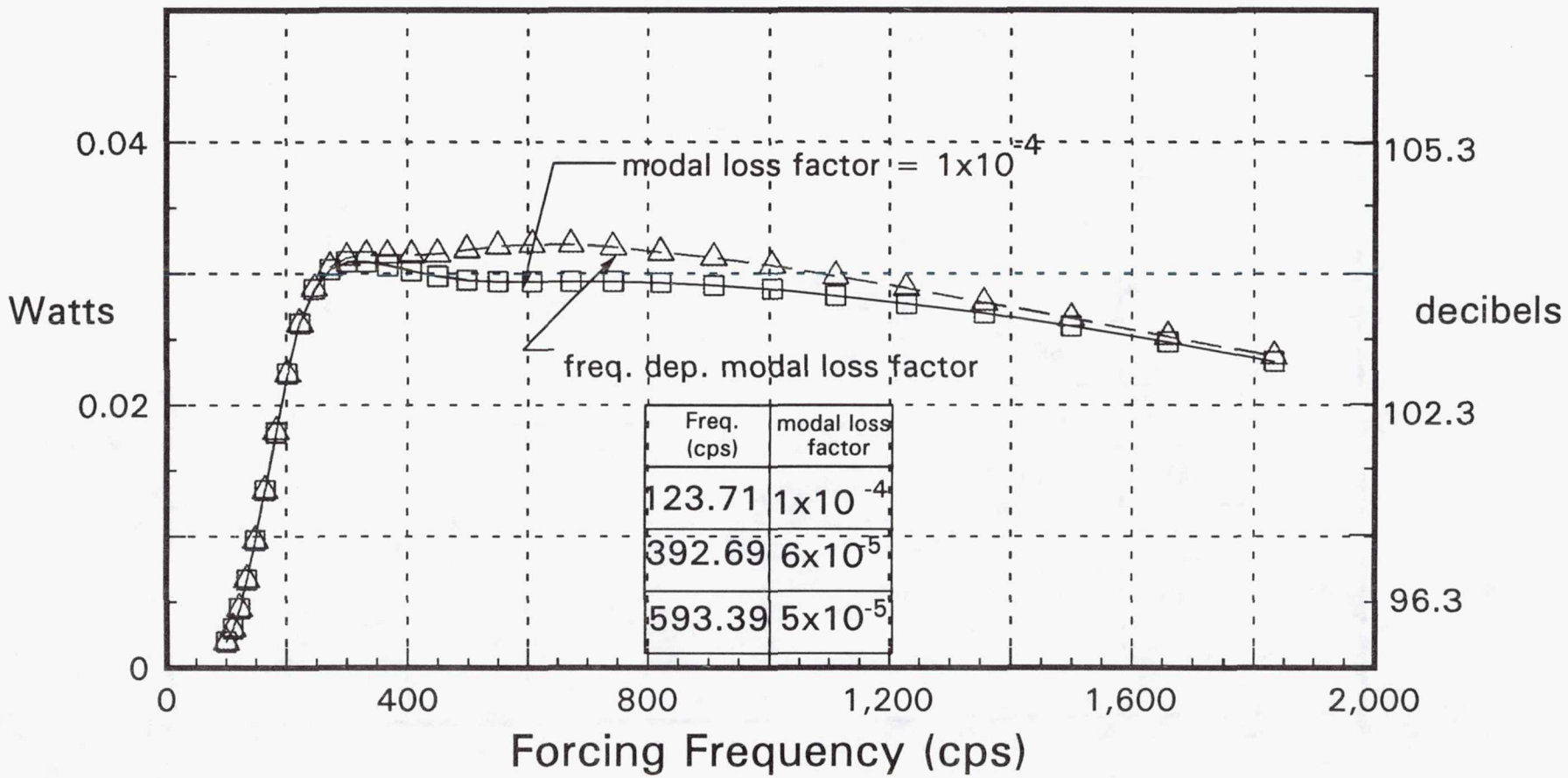


Figure 37: Acoustic Noise Emitted from Composite Fan Blade - Frequency Dependent Damping

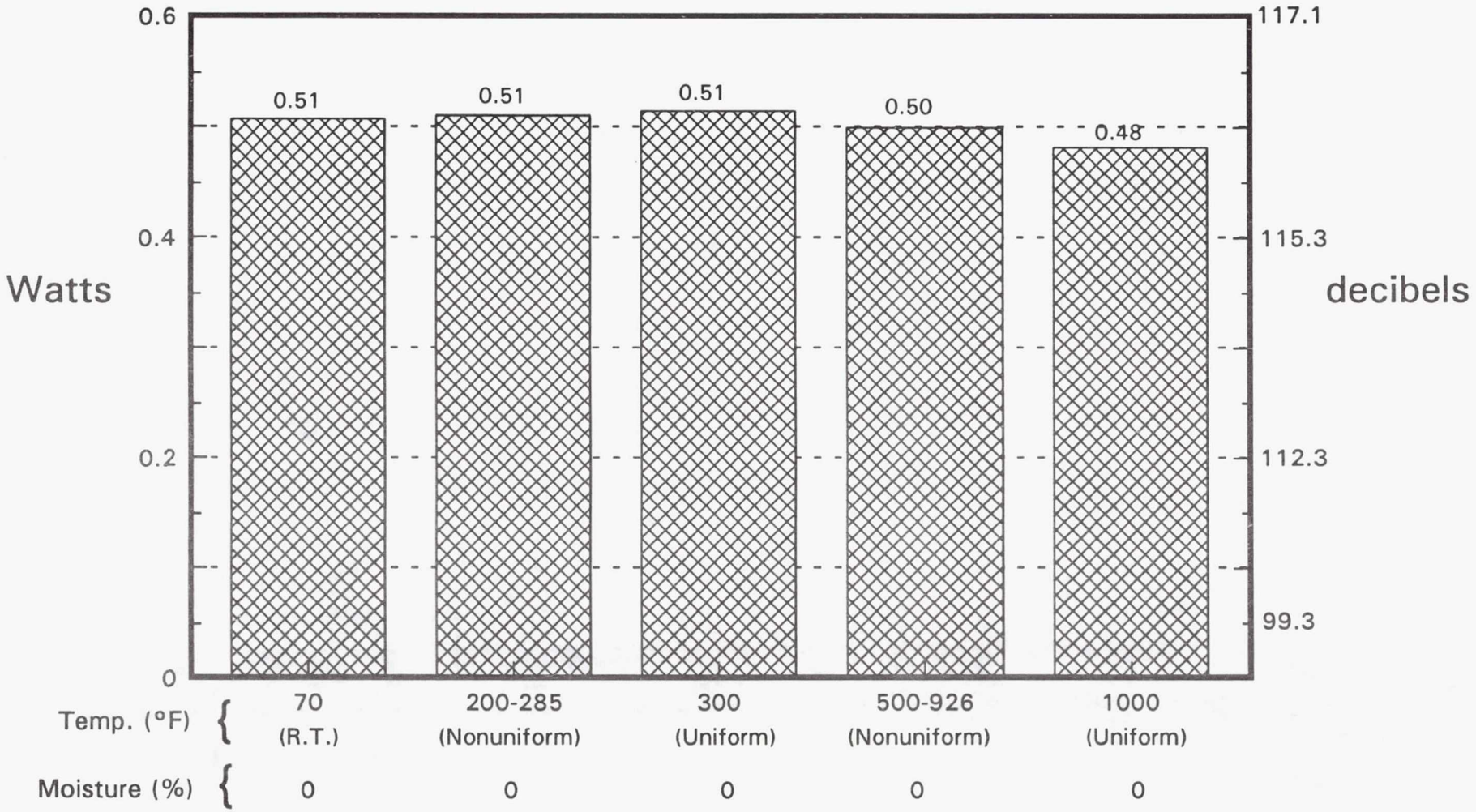


Figure 38: Environmental Effects on Acoustic Noise Emitted from Metal Fan Blade @ Specified Forcing Frequency

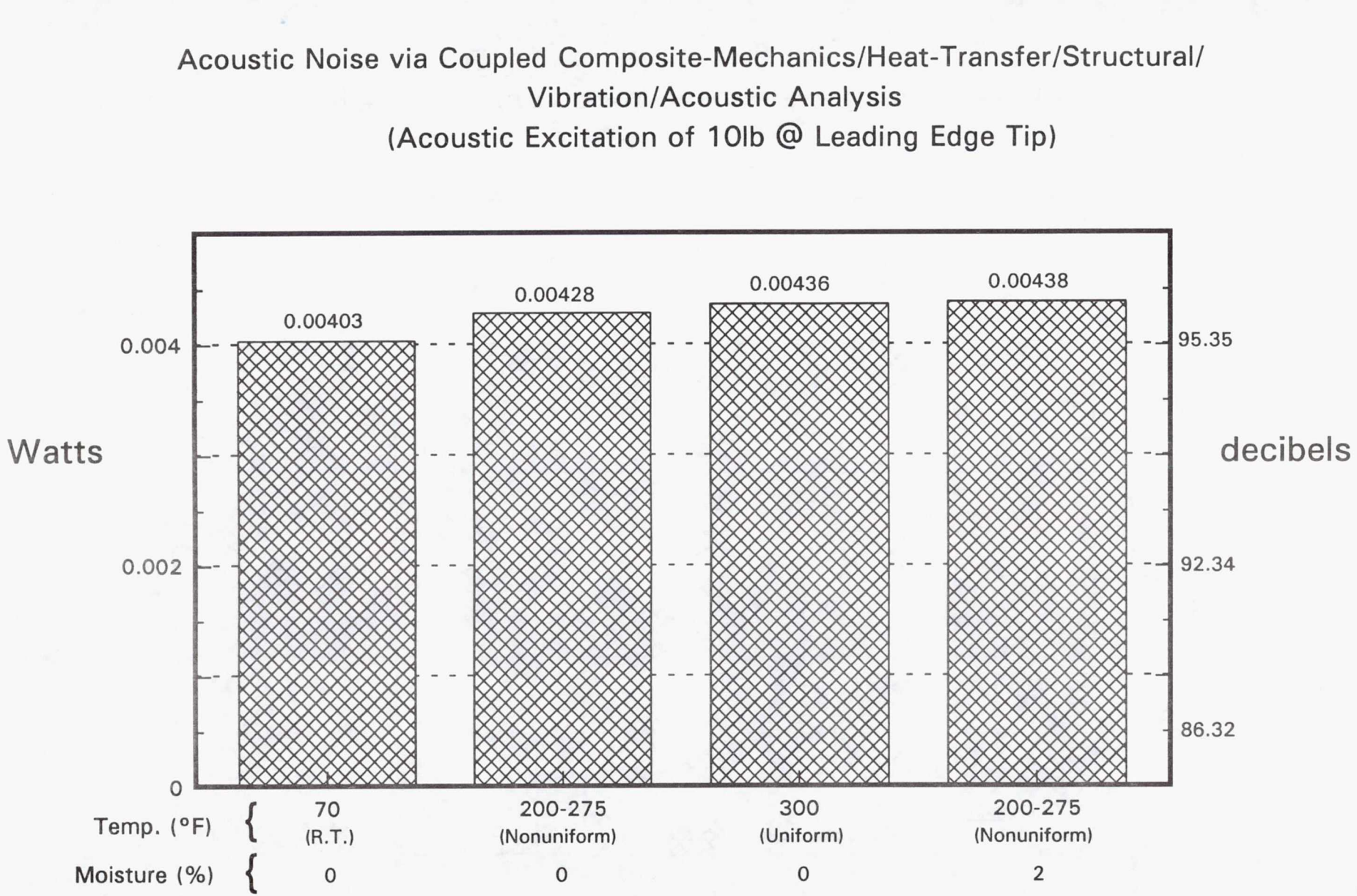


Figure 39: Environmental Effects on Acoustic Noise Emitted from Composite Fan Blade @ Specified Forcing Frequency

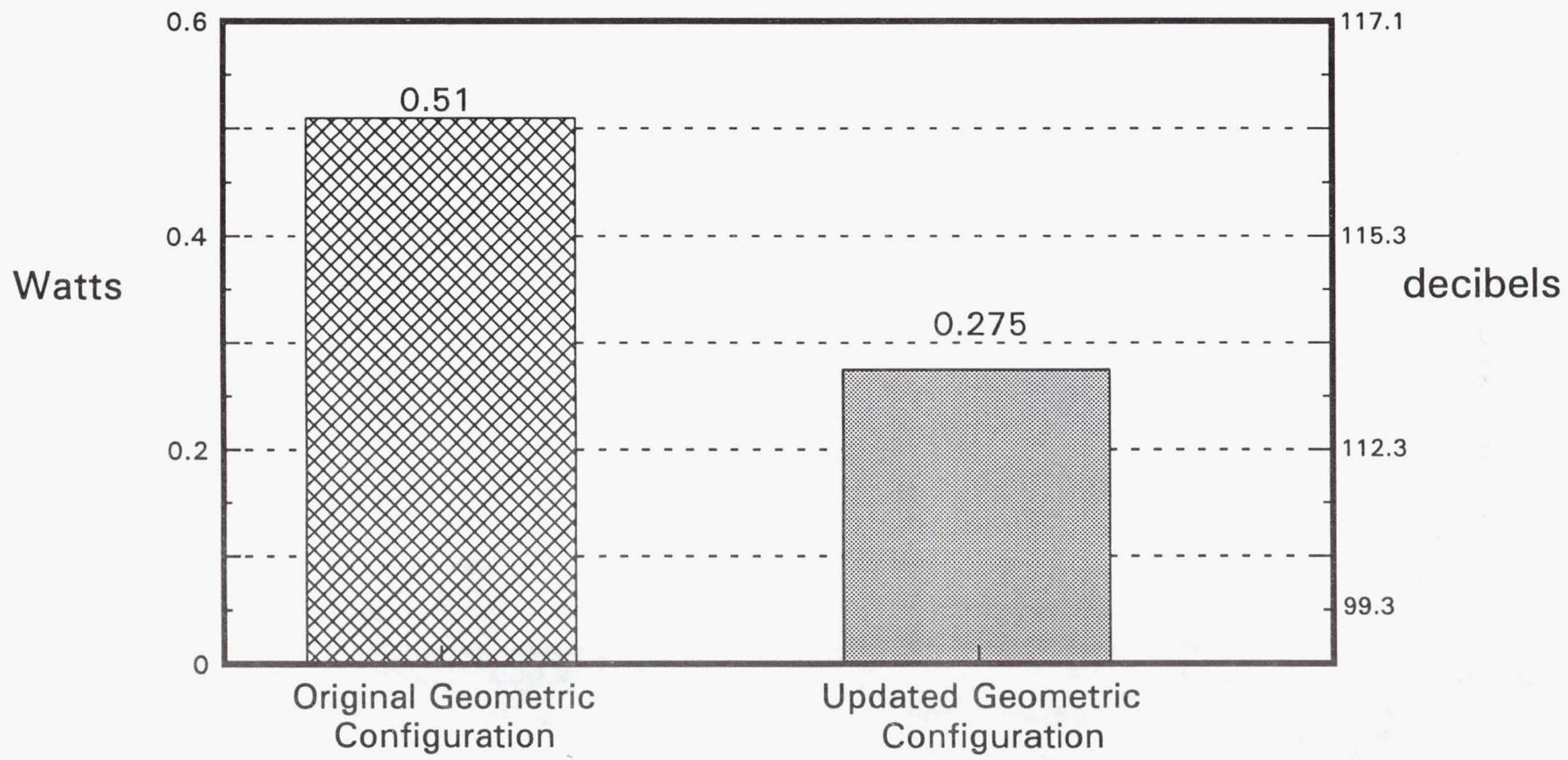


**Figure 40: Geometric Stiffening Effects on Acoustic Noise Emitted from Metal Fan Blade @ Specified Forcing Frequency**

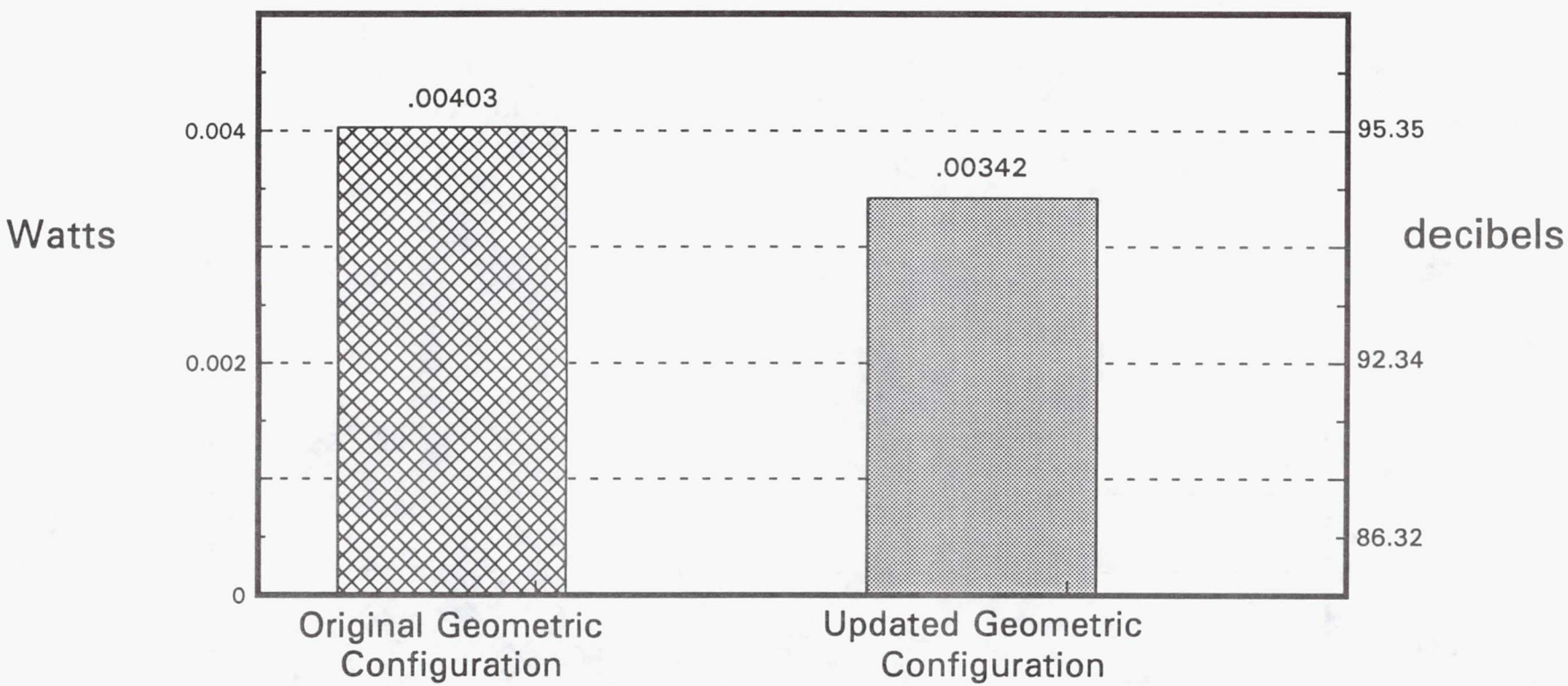


**Figure 41: Geometric Stiffening Effects on Acoustic Noise Emitted from Composite Fan Blade @ Specified Forcing Frequency**

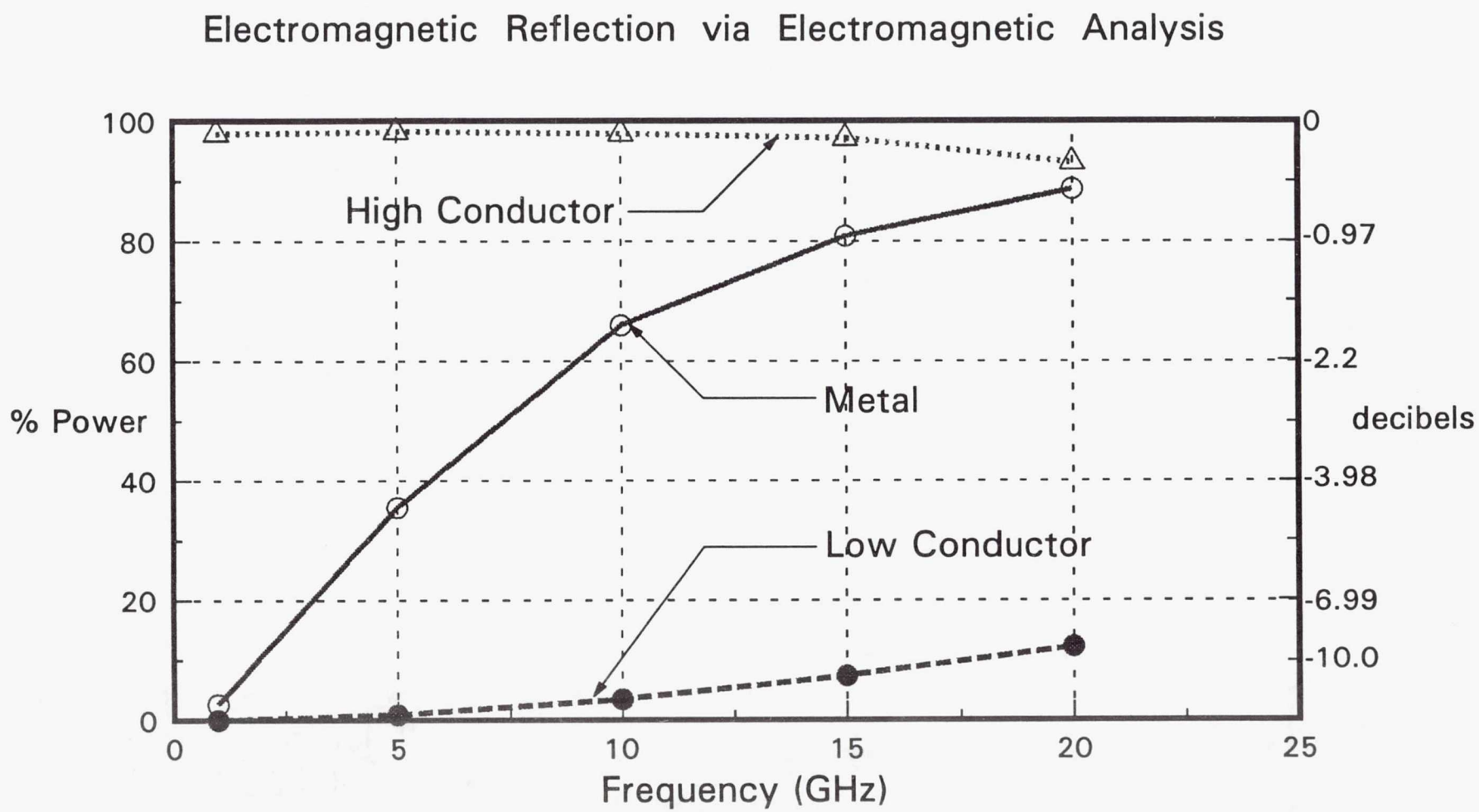


location: tip leading edge
global incidence angle: 0 deg.
local incidence angle: 39.45 deg.

Figure 42: Electromagnetic Response from Metal Fan Blade - Effect of Material

Electromagnetic Reflection via Coupled Composite-Mechanics/Electromagnetic Analysis

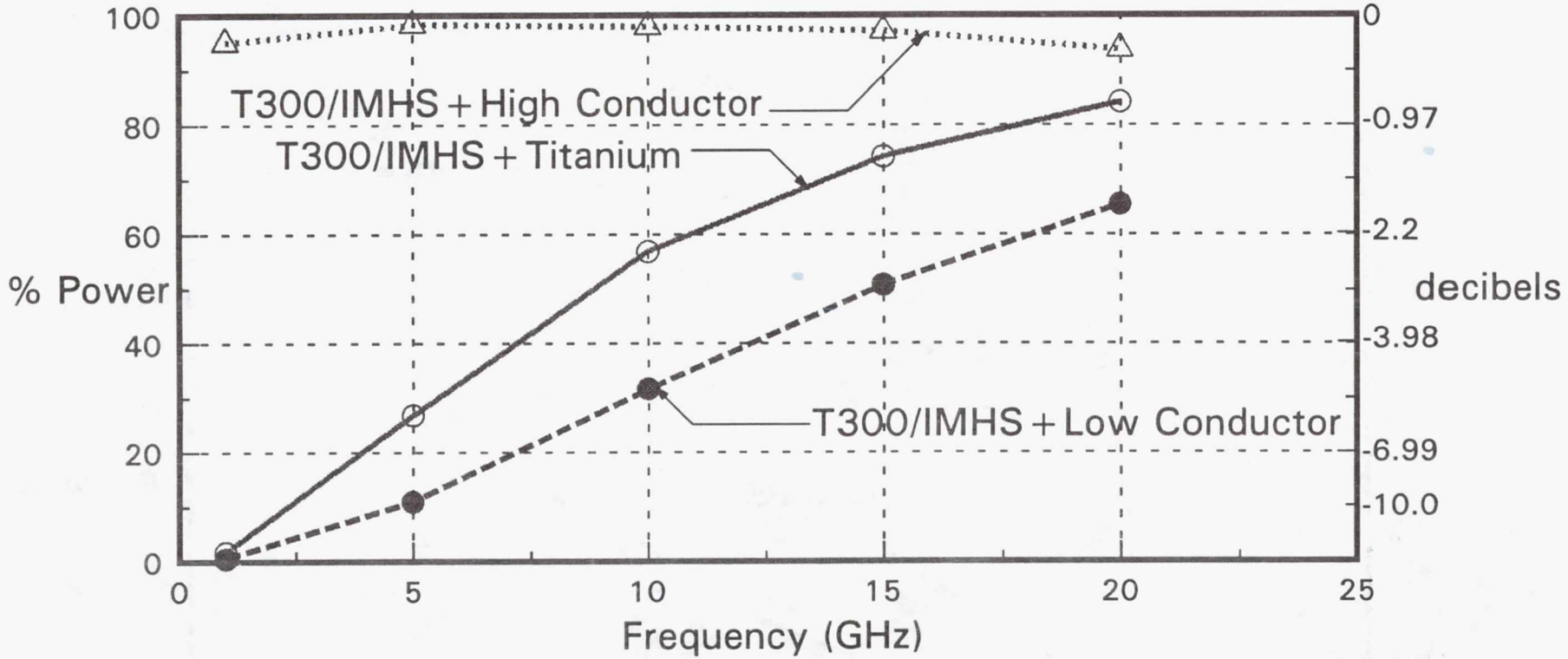


location: tip leading edge
global incidence angle: 0 deg.
local incidence angle: 39.45 deg. (first layer)

Figure 43: Electromagnetic Response from Composite Fan Blade-Effect of Material

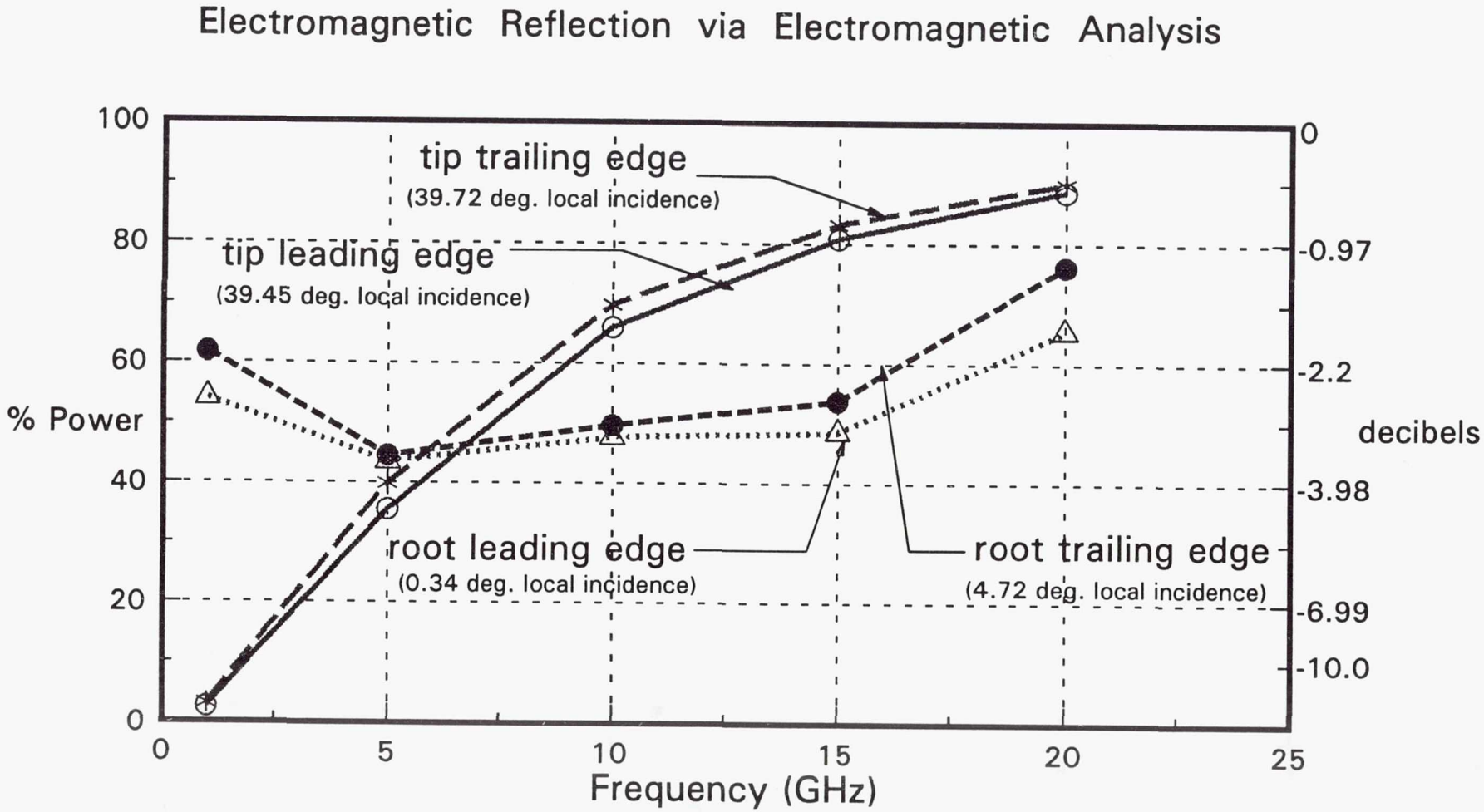


Figure 44: Geometric Effects on Electromagnetic Response from Metal Fan Blade

Electromagnetic Reflection via Coupled Composite-Mechanics/Electromagnetic Analysis

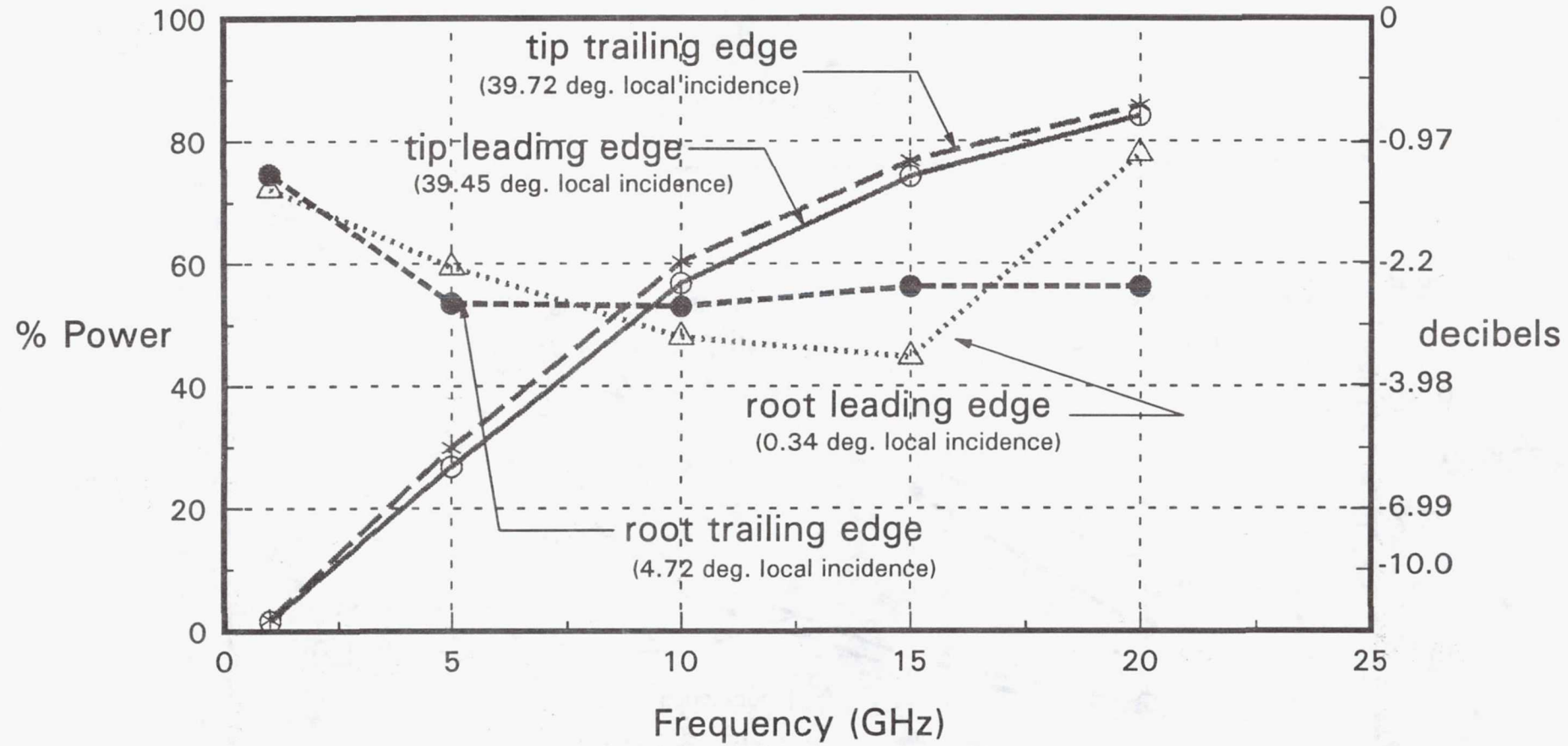


materials: T300/IMHS

global incidence angle: 0 deg.

Figure 45: Geometric Effects on Electromagnetic Response from Composite Fan Blade

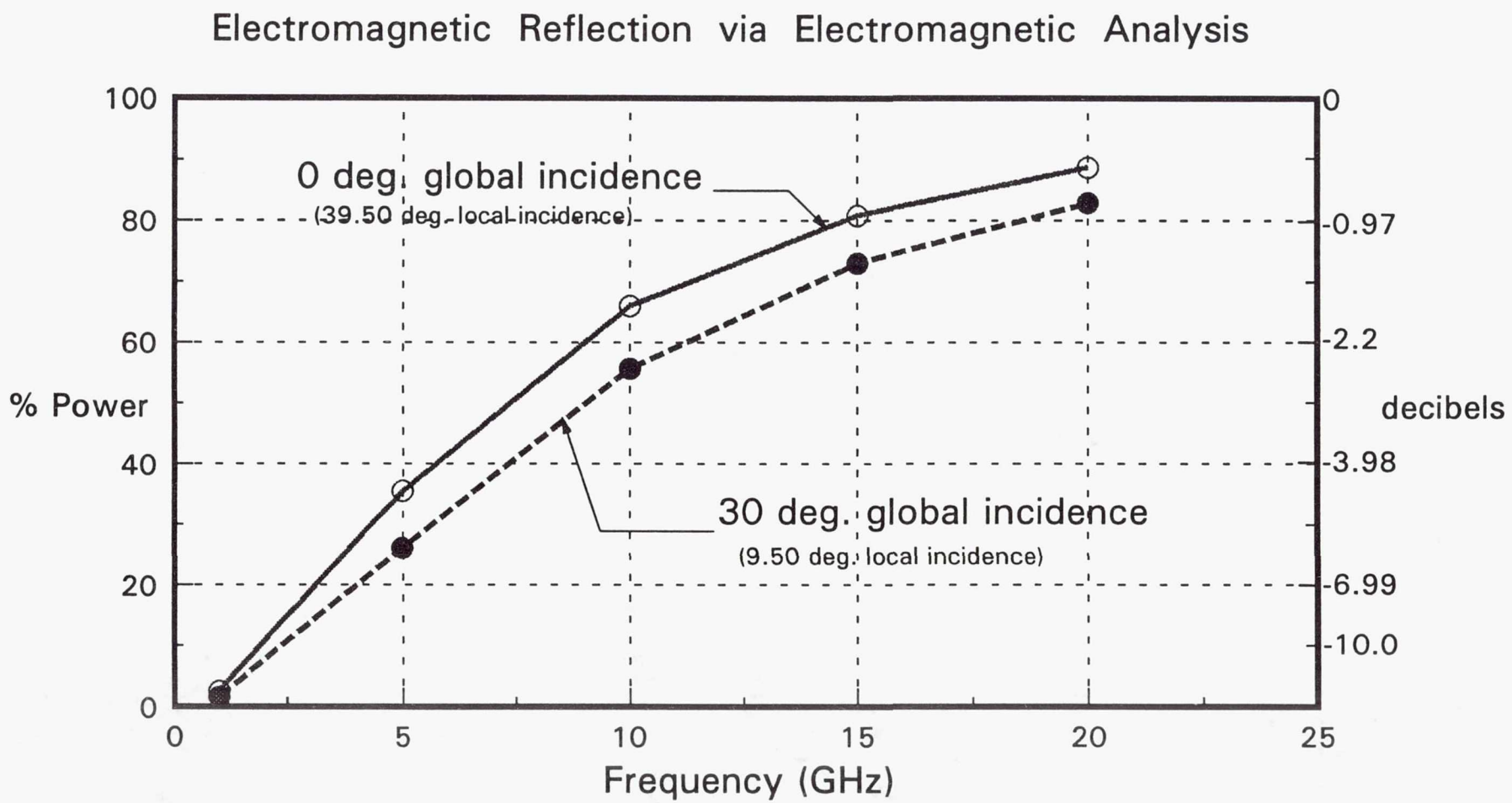


material: titanium
location: tip leading edge

Figure 46: Incidence Angle Effects on Electromagnetic Response from Metal Fan Blade

Electromagnetic Reflection via Coupled Composite-Mechanics/Electromagnetic Analysis

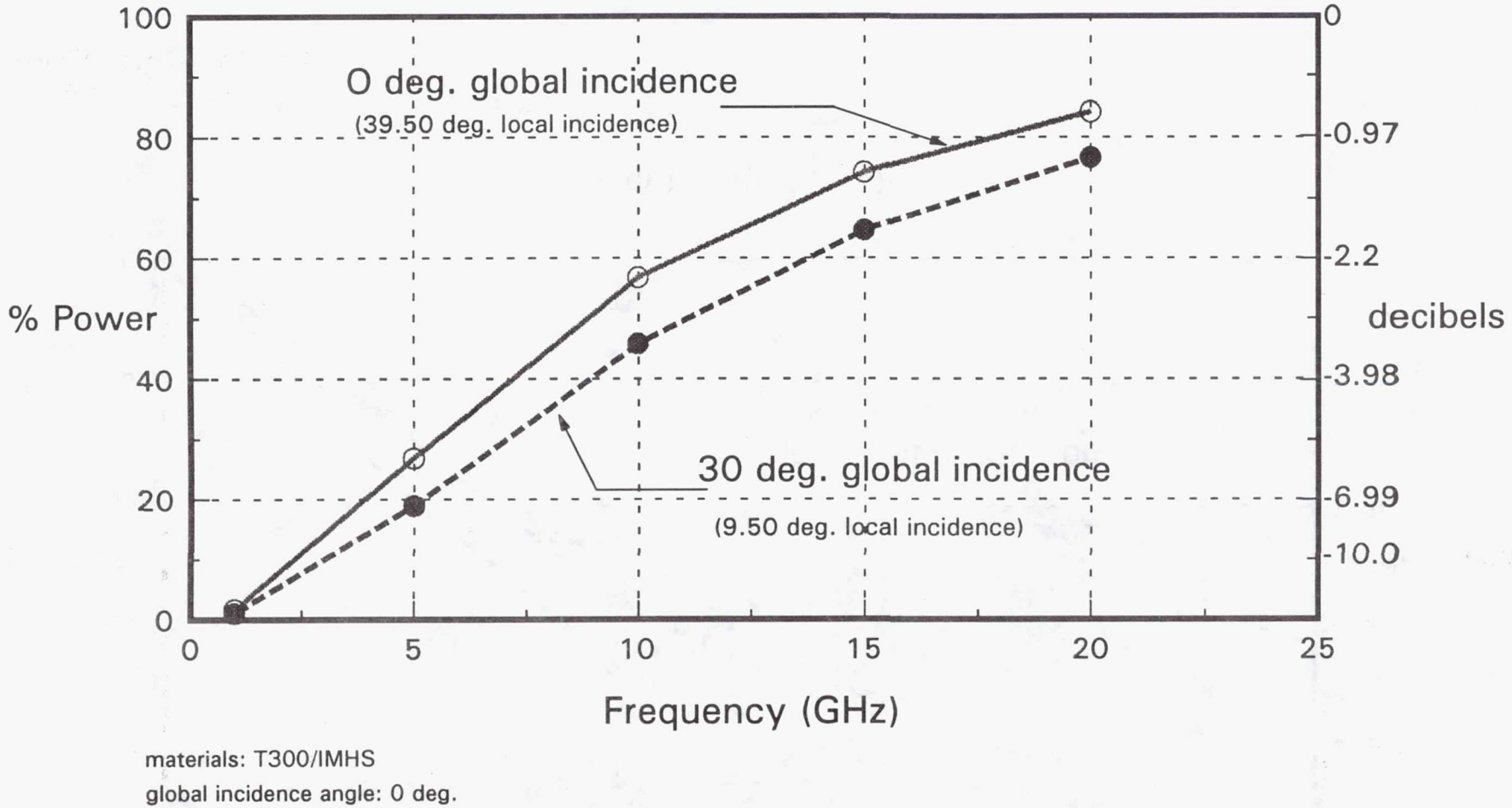


Figure 47: Incidence Angle Effects on Electromagnetic Response from Composite Fan Blade

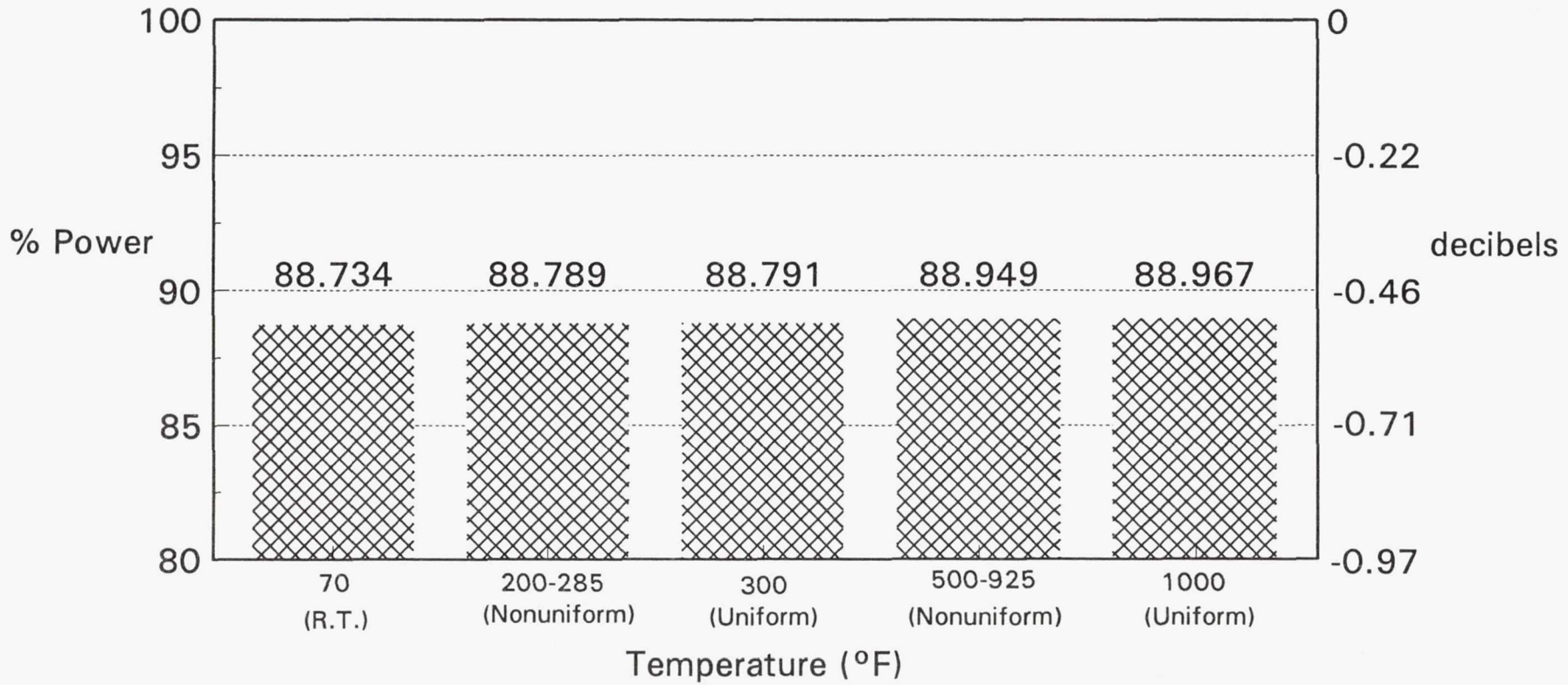


material: titanium
location: tip leading edge
global incidence angle: 0 deg.
local incidence angle: 39.45 deg.

Figure 48: Electromagnetic Response from Metal Fan Blade - Effect of Temperature @ 20 GHz

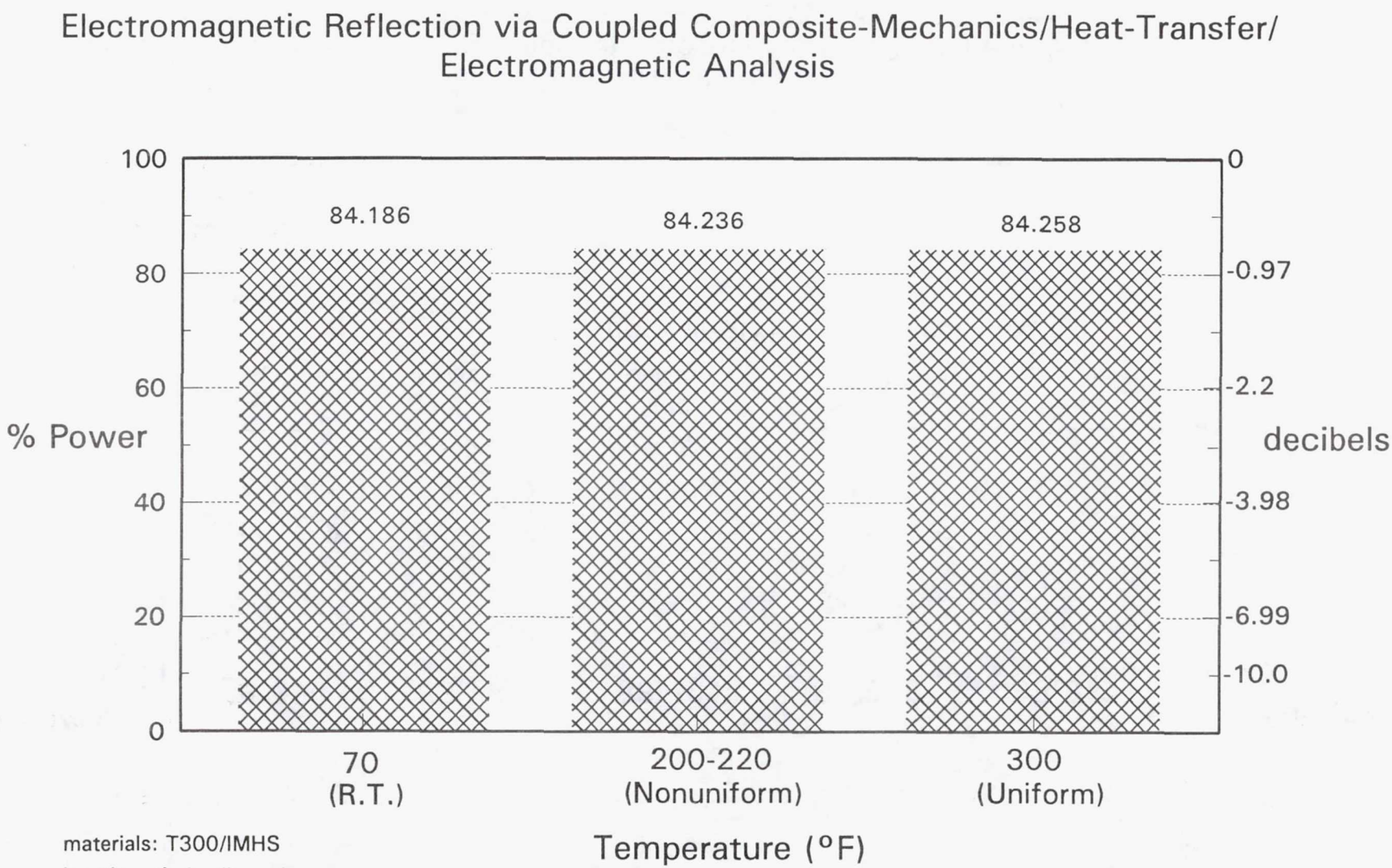


Figure 49: Electromagnetic Response from Composite Fan Blade - Effect of Temperature @ 20 GHz

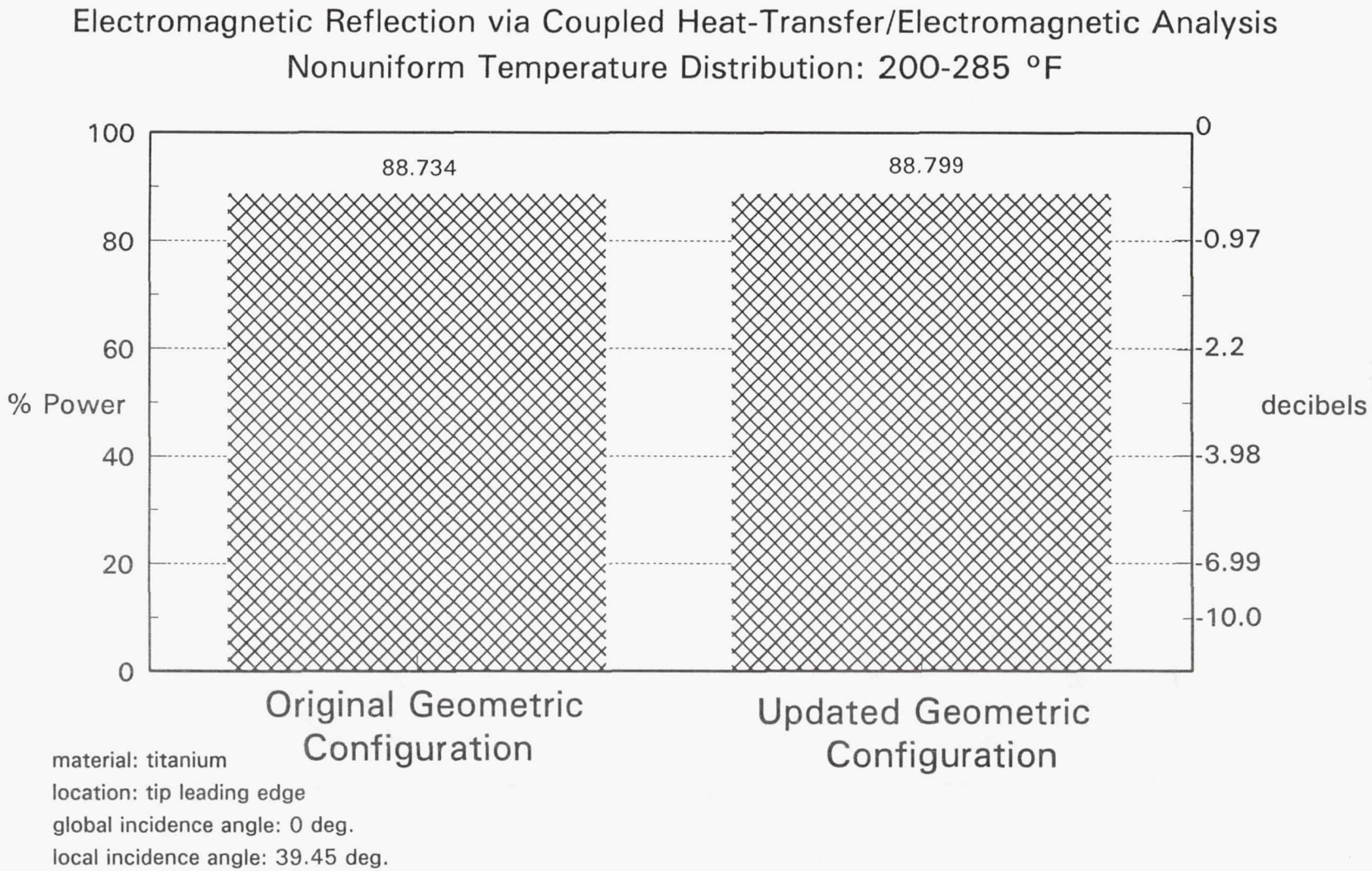


Figure 50: Electromagnetic Response from Metal Fan Blade -
Effect of Geometric Configuration due to Stiffening @ 20 GHz

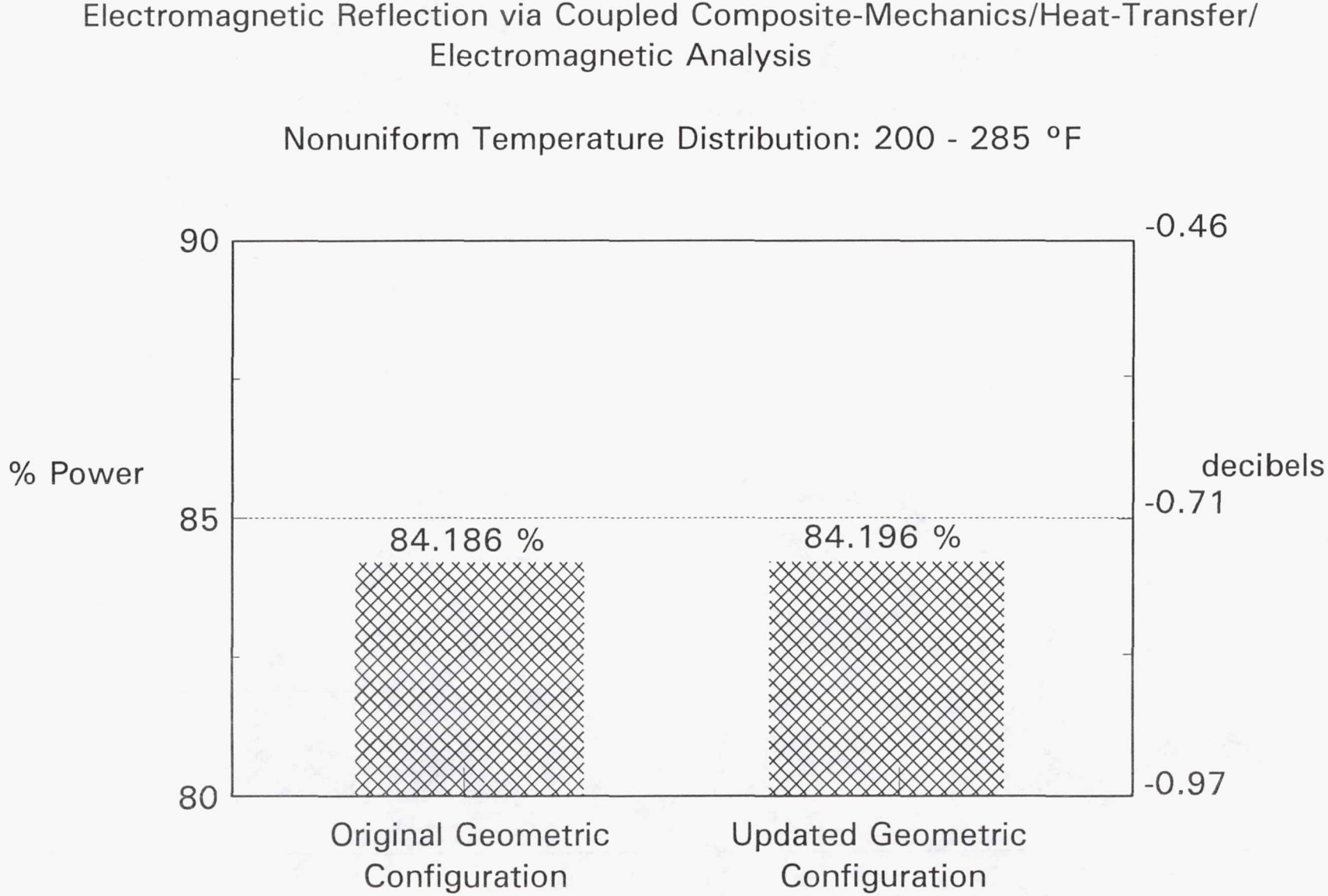


Figure 51: Electromagnetic Response from Composite Fan Blade -
Effect of Geometric Configuration due to Stiffening @ 20 GHz

# REPORT DOCUMENTATION PAGE

Form Approved
OMB No. 0704-0188



| 1. AGENCY USE ONLY (*Leave blank*) | 2. REPORT DATE | 3. REPORT TYPE AND DATES COVERED |
|---|---|---|
| | February 1993 | Technical Memorandum |

**4. TITLE AND SUBTITLE**

Coupled Multi-Disciplinary Composites Behavior Simulation

**5. FUNDING NUMBERS**

WU–505–63–53

**6. AUTHOR(S)**

Surendra N. Singhal, Pappu L.N. Murthy, and Christos C. Chamis

**7. PERFORMING ORGANIZATION NAME(S) AND ADDRESS(ES)**

Sverdrup Technology, Inc.
Lewis Research Center Group
2001 Aerospace Parkway
Brook Park, Ohio 44142

**8. PERFORMING ORGANIZATION REPORT NUMBER**

E–7565

**9. SPONSORING/MONITORING AGENCY NAMES(S) AND ADDRESS(ES)**

National Aeronautics and Space Administration
Lewis Research Center
Cleveland, Ohio 44135–3191

**10. SPONSORING/MONITORING AGENCY REPORT NUMBER**

NASA TM–106011

**11. SUPPLEMENTARY NOTES**

Surendra N. Singhal, Sverdrup Technology, Inc., Lewis Research Center Group, 2001 Aerospace Parkway, Brook Park, Ohio 44142 and Pappu L.N. Murthy and Christos C. Chamis, NASA Lewis Research Center. Responsible person, Pappu L.N. Murthy, (216) 433–3332.

**12a. DISTRIBUTION/AVAILABILITY STATEMENT**

Unclassified - Unlimited
Subject Category 39

**12b. DISTRIBUTION CODE**

**13. ABSTRACT** ***(Maximum 200 words)***

The capabilities of the computer code CSTEM (Coupled Structural/Thermal/Electro-Magnetic Analysis) are discussed and demonstrated. CSTEM computationally simulates the coupled response of layered multi-material composite structures subjected to simultaneous thermal, structural, vibration, acoustic, and electromagnetic loads and includes the effect of aggressive environments. The composite material behavior and structural response is determined at its various inherent scales: constituents (fiber/matrix), ply, laminate, and structural component. The thermal and mechanical properties of the constituents are considered to be nonlinearly dependent on various parameters such as temperature and moisture. The acoustic and electromagnetic properties also include dependence on vibration and electromagnetic wave frequencies, respectively. The simulation is based on a three dimensional finite element analysis in conjunction with composite mechanics and with structural tailoring codes, and with acoustic and electromagnetic analysis methods. An aircraft engine composite fan blade is selected as a typical structural component to demonstrate the CSTEM capabilities. Results of various coupled multi-disciplinary heat transfer, structural, vibration, acoustic, and electromagnetic analyses for temperature distribution, stress and displacement response, deformed shape, vibration frequencies, mode shapes, acoustic noise, and electromagnetic reflection from the fan blade are discussed for their coupled effects in hot and humid environments. Collectively, these results demonstrate the effectiveness of the CSTEM code in capturing the coupled effects on the various responses of composite structures subjected to simultaneous multiple real-life loads.

| 14. SUBJECT TERMS | 15. NUMBER OF PAGES |
|---|---|
| Absorption; Acoustic excitation; Acoustic noise; Composite fatigue; Composite materials; Composite structures; Composite mechanics; Computational simulation; Coupled analysis; Electromagnetic waves; Environment; Frequencies; Geometric stiffening; Heat transfer; Hygrothermo-mechanics; Large deformation; Modal response; Mode shapes; Moisture; Multi-disciplinary analysis; Optics; Permeability; Permittivity; Polymer matrix composites; Reflection; Refraction; Simulation; Sound; Structural analysis; Temperature; Thermal response; Transmission; Vibration; Waves | 76 |
| | 16. PRICE CODE A05 |

| 17. SECURITY CLASSIFICATION OF REPORT | 18. SECURITY CLASSIFICATION OF THIS PAGE | 19. SECURITY CLASSIFICATION OF ABSTRACT | 20. LIMITATION OF ABSTRACT |
|---|---|---|---|
| Unclassified | Unclassified | Unclassified | |